(12) INTERNATIONAL APPLICATION PUBLISHED UNDER THE PATENT COOPERATION TREATY (PCT)

(19) World Intellectual Property Organization
International Bureau

(43) International Publication Date
22 February 2001 (22.02.2001)

PCT

(10) International Publication Number
WO 01/12234 A1

(51) International Patent Classification[7]: A61K 48/00, 35/00, 49/00, 51/00

(21) International Application Number: PCT/US00/22456

(22) International Filing Date: 16 August 2000 (16.08.2000)

(25) Filing Language: English

(26) Publication Language: English

(30) Priority Data:
09/374,972 16 August 1999 (16.08.1999) US
09/585,194 1 June 2000 (01.06.2000) US

(71) Applicant: UAB RESEARCH FOUNDATION [US/US]; 701 South 20th Street, Suite 1120G/AB, Birmingham, AL 35294-0111 (US).

(72) Inventors: BUCHSBAUM, Donald, J.; 1013 32nd Street South, Birmingham, AL 35205 (US). CURIEL, David, T.; 824 Linwood Road, Birmingham, AL 35222 (US). ZINN, Kurt, R.; 405 Magnolia Trace Circle, Hoover, AL 35244 (US). ROGERS, Buck, E.; 1865 Southwood Road, Vestavia Hills, AL 35216 (US).

(74) Agent: ADLER, Benjamin, A.; McGregor & Adler, LLP, 8011 Candle Lane, Houston, TX 77071 (US).

(81) Designated States *(national)*: AU, CA, JP.

(84) Designated States *(regional)*: European patent (AT, BE, CH, CY, DE, DK, ES, FI, FR, GB, GR, IE, IT, LU, MC, NL, PT, SE).

Published:
— *With international search report.*
— *Before the expiration of the time limit for amending the claims and to be republished in the event of receipt of amendments.*

For two-letter codes and other abbreviations, refer to the "Guidance Notes on Codes and Abbreviations" appearing at the beginning of each regular issue of the PCT Gazette.

(54) Title: GENE TRANSFER IMAGING AND USES THEREOF

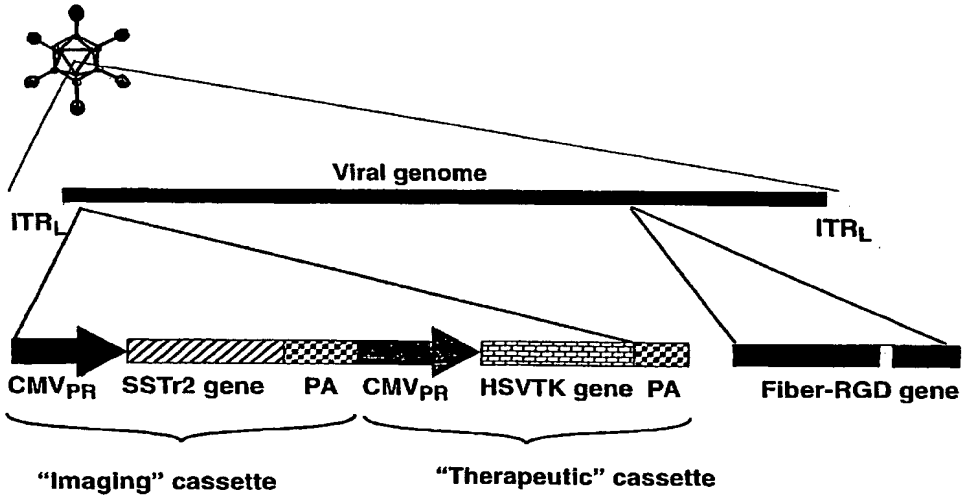

(57) Abstract: The present invention provides a method for monitoring therapeutic gene transfer and expression into a subject. Also provided is a recombinant adenoviral vector encoding at least one therapeutic gene and a gene for a membrane expressed targeting molecule including human somatostatin subtype (2) receptor. Such vector may be used for treating various tumors.

GENE TRANSFER IMAGING AND USES THEREOF

BACKGROUND OF THE INVENTION

Cross-Reference to Related Application

This patent application is a continuation-in-part of U.S. application Serial Number 09/374,972, filed August 16, 1999, which is a continuation-in-part of U.S. application Serial Number 08/948,132, filed October 9, 1997, which is a continuation-in-part of U.S. application Serial Number 08/739,826, filed February 11, 1997, now U.S. Patent Number 5,902,583, issued May 11, 1999.

Field of the Invention

The present invention relates generally to the fields of radioimmunobiology, gene therapy and nuclear medicine. More specifically, the present invention relates to a method for monitoring gene transfer and expression into a subject.

Description of the Related Art

The paradigm of radioimmunotherapy (RAIT) has been based upon the premise that a targeting molecule (*e.g.* an antibody) carrying a radionuclide has the potential of selectively delivering radiation to tumor sites. Considerable clinical experience with this strategy has been accomplished over the past decade, with success limited primarily to malignant lymphomas (1,2). This limited efficacy reflects fundamental problems in achieving adequate tumor localization of radiolabeled antibodies, which may be due either to inadequate intratumoral expression of the target antigen or to biodistribution problems associated with the use of intact antibody as the targeting moiety (3-6). A variety of strategies have thus been developed as alternatives to radiolabeled intact mouse monoclonal antibodies (MAbs) to enhance tumor localization of an injected radiolabeled ligand, including the employment of second generation high affinity antibodies, humanized antibodies, genetically engineered antibody fragments, peptides, and pretargeting of unlabeled antibody followed by radiolabeled haptens.

"Targeted" radiation therapy is an important cancer research strategy. The use of external beam radiation therapy has produced curative treatment programs for several tumor types. However, this technique has practical limitations in regards to limited field of therapy, normal tissue toxicity, and radioresistance mechanisms. Considerable research efforts have been directed at ways to "target" radioactive isotopes to sites of malignant disease. Currently, the use of monoclonal antibodies directed to "tumor-associated" antigens on cancer cells represents

one approach to this problem which has had success in various animal model systems (5-9) and is the subject of considerable current phase I and II trials in man (10-14). Such a strategy provides the ability to localize radioactive isotopes to multiple sites of disease with hopefully adequate amounts of radiation to produce an antitumor effect and/or radioimmune imaging for diagnostic purposes.

A second emerging strategy is to use radioactively labeled peptides able to bind to receptor positive tumor cells (*e.g.* octreotide to somatostatin receptors in malignant carcinoid) (15,16). Research efforts which provide better radioactive isotope delivery systems and/or targeting strategies will enhance the ability to apply targeted radiation therapy.

Radiolabeled monoclonal antibodies (single-step radioimmunotherapy) have serious limitations in treating human cancer. Successful application of radiolabeled monoclonal antibodies in a single-step protocol for radioimmunodetection and radioimmunotherapy of tumors has been hindered in man by problems related to the low percentage uptake of injected radioactivity in tumors (0.001 to 0.1% ID/g), the slow penetration of relatively large (160 kD) intact antibodies into tumors and heterogeneous distribution, their long persistence times in normal tissues leading to high background radioactivity and bone marrow suppression, and the development of human anti-mouse antibody (HAMA) responses.

To overcome these problems, several groups have considered the use of antibody fragments and single chain antibodies (17-22), regional administration (23-25), the use of

various radionuclides (5), the use of more stable (26) or enzymatically cleavable chelating agents (27), the use of cytokines to upregulate tumor-associated antigen expression (28, 29), irradiation of the tumor to increase vascular permeability (14, 30-32), the use of cytokines to protect against bone marrow suppression (33, 34), and the use of autologous bone marrow transplantation (2, 35). Despite these efforts, the results of clinical radioimmunotherapy of solid tumors have been disappointing. In spite of these shortcomings, antitumor efficacy has been demonstrated in clinical trials for therapy of the radiosensitive lymphoma types of tumors.

The prior art is deficient in the lack of effective means of monitoring gene transfer and expression into a subject to further improve the efficacy of gene therapy. The present invention fulfills this long-standing need and desire in the art.

SUMMARY OF THE INVENTION

The present invention is directed to a method for monitoring gene transfer and expression into a subject. One method of the present invention includes administering to the subject a genetic vector encoding at least one selected therapeutic gene to be expressed in the subject and a gene for human somatostatin receptor subtype 2 wherein the vector and the genes are capable of being expressed in the subject. A somatostatin analogue having a detectable radioisotope label attached thereto is administered to the subject and the subject is imaged to determine if the labeled somatostatin analogue has bound to

human somatostatin receptor subtype 2 expressed in the subject. No attempt is being made to distinguish the actual binding to the membrane receptor, and subsequent events that allow for imaging. These subsequent events include internalization of the radiolabeled peptide to the inside of the cell, therefore it is no longer surface bound. Also, the clearance of the non-bound peptide from the blood to decrease background is part of the process that allows for imaging. The imaging depends on surface binding, however, by the time the positive image is possible, it is likely that the radiolabeled peptide is no longer surface bound.

In another embodiment of the present invention, there is provided a method for monitoring reporter and/or therapeutic gene transfer and expression into a subject, comprising the steps of administering to the subject a vector encoding at least one therapeutic gene and a reporter gene for a membrane expressed targeting molecule, wherein both genes are capable of expressing in the subject; administering a radiolabeled ligand to the subject, wherein the ligand has a high affinity for the membrane expressed targeting molecule; and then imaging the subject by detecting the binding of the radiolabeled ligand with the membrane expressed targeting molecule, wherein the binding is directly proportional to the transfer and expression of the therapeutic gene into the subject. Preferably, the membrane expressed targeting molecule is human somatostatin subtype 2 receptor.

In another embodiment of the present invention, there is provided a method to control the expression of a reporter gene

and/or therapeutic gene that have been transferred to target cells in the host.

In still another embodiment of the present invention, there is provided a recombinant adenoviral vector encoding at least one therapeutic gene and a gene for a membrane expressed targeting molecule. Preferably, membrane expressed targeting molecule is human somatostatin subtype 2 receptor.

In still another embodiment of the present invention, there is provided a method of treating an individual having a tumor by administering the recombinant adenoviral vector disclosed herein to the individual. Preferably, the recombinant adenoviral vector may be administered with 5-fluorocytosine (5-FC), ganciclovir (GCV) or a radiolabeled peptide.

Other and further aspects, features, and advantages of the present invention will be apparent from the following description of the presently preferred embodiments of the invention given for the purpose of disclosure.

BRIEF DESCRIPTION OF THE DRAWINGS

So that the matter in which the above-recited features, advantages and objects of the invention, as well as others which will become clear, are attained and can be understood in detail, more particular descriptions of the invention briefly summarized above may be had by reference to certain embodiments thereof which are illustrated in the appended drawings. These drawings form a part of the specification. It is to be noted, however, that the appended drawings illustrate preferred embodiments of the

invention and therefore are not to be considered limiting in their scope.

Figure 1 shows recombinant adenovirus vector with expanded tissue tropism expressing HSV-TK and SSTR2.

Figures 2A and **2B** show conversion of tritiated 5-FC to 5-FU and binding of ^{125}I-somatostatin in SK-OV-3.ip1 cell lysates and membrane preparations, respectively. SK-OV-3.ip1 cells were co-infected at 10, 100, and 300 moi with AdCMVSSTr2, AdCMVCD, or both. Two days later the cells were harvested to prepare lysates for the conversion assay or membrane preparations for the binding assay. **Figure 2A** shows the percentage of tritiated 5-FC converted to 5-FU and **Figure 2B** shows the amount of ^{125}I-somatostatin bound as a percentage of the total radioactivity added. Note that assay for AdCMVSSTr2-infected cells at 300 moi was not performed.

Figures 3A and **3B** show gamma camera images of a 24-well plate containing mixtures of AdSSTr2-infected and uninfected cells during incubation with [^{111}In]-DTPA-D-Phe^1-octreotide (**Figure 3A**) and after 1 h and an acid wash (**Figure 3B**). The percentages of SSTr2 positive cells are indicated on the right. The last 3 columns had excess unlabeled octreotide added as an inhibitor. **Figure 3C** shows the percentage dose internally bound per mg protein. After imaging, the cells were harvested, counted in a gamma counter and the percentages of internally bound radioactivity standardized for the total amount of protein.

Figures 4A-4D show representative gamma camera images of mice injected with [^{111}In]-DTPA-D-Phe^1-octreotide. Mice bearing *s.c.* A-427 tumors were administered a single intratumoral

injection (**Figures 4A** and **4B**) or two intratumoral injections (**Figures 4C** and **4D**) of AdSSTr2 (right solid circles) and AdTRHr (left dashed circles). [^{111}In]-DTPA-D-Phe^1-octreotide was administered *i.v.* 48 h (**Figures 4A** and **4C**) and 96 h (**Figures 4B** and **4D**) after adenoviral injection and the mice imaged 5.5 h later. The squares show the clearance of the radioactivity through the bladder.

Figure 5A shows region of interest analysis of tumors in mice injected with [^{111}In]-DTPA-D-Phe^1-octreotide and imaged with a gamma camera. Data are presented as the % ID per g ± SD (n =4-5). The % ID per g was calculated based on the tumor weight at the time the animals were sacrificed after the imaging session. **Figure 5B** shows biodistribution of [^{111}In]-DTPA-D-Phe^1-octreotide after the animals were imaged. The animals were killed and the tissues were collected, weighed, and counted in a gamma counter. Biodistribution data are presented as the % ID per g of tissue ± SD (n = 4-5).

Figure 6A shows growth of A-427 tumors following intratumoral injection of AdSSTr2 and *i.v.* injection of [^{90}Y]-SMT 487. Groups of mice (n = 10) received a total of two AdSSTr2 injections and four injections of either 400 μCi or 500 μCi [^{90}Y]-SMT 487. Untreated controls or no adenovirus plus 500 μCi [^{90}Y]-SMT 487 controls are also shown. Data represent the median change in tumor surface area for surviving mice in each group (n ≥ 7) relative to the tumor surface area at the time of the first AdSSTr2 injection (Day 0). **Figure 6B** shows proportion of mice with tumors that quadrupled in size from time of first AdSSTr2 injection (Day 0). Solid arrows represent AdSSTr2 injections and

dashed arrows represent [^{90}Y]-SMT 487 injections. The no treatment (_), AdSSTr2 + 400 μCi [^{90}Y]-SMT 487 (_), AdSSTr2 + 500 μCi [^{90}Y]-SMT 487 (_), and no virus + 500 μCi [^{90}Y]-SMT 487 (_) are shown.

Figures 7A and 7B show the imaging of SSTr2 and TK gene expression following *i.t.* injection of 5 x 10^8 pfu AdSSTr2 (left tumor) or AdTKSSTr2 (right tumor) (**Figure 7A**) or 5 x 10^8 pfu AdTK (left tumor) or 5 x 10^8 pfu AdTKSSTr2 (right tumor) (**Figure 7B**) into *s.c.* A427 tumor xenografts at 5 h after *i.v.* injection of ^{99m}Tc-P2049 and ^{131}I-FIAU.

Figures 8A and 8B show immunohistochemistry of adenovirus-injected tumor xenografts. Stained frozen sections (x 200) are from Ad5-CMVhSSTr2-injected tumor, which shows cells expressing somatostatin receptors along apparent injection tract (**Figure 8A**, arrows) (necrosis is at apparent end of tract, upper and lower arrows) and Ad5-CMVTRHr-injkected tumor from same mouse as in Figure 7A showing only scattered macrophage staining (**Figure 8B**).

Figure 9A shows the images in two mice of gastrin releasing peptide receptor (GRPr) expression using a ^{99m}Tc-labeled BBN analogue. In the two Experiments, male CD1 mice were injected in the rear footpad with either an adenoviral vector encoding GRPr (Ad-CMVGRPr) or a negative control adenoviral vector encoding β-galactosidase (AdLacZ). **Figure 9B** shows tissue biodistribution of ^{99m}Tc-labeled BBN analogue in the two Experiments. It demonstrates significant ($p<0.05$) and specific retention of the ^{99m}Tc-labeled BBN analogue in the footpad of mice injected with AdGRPr (Experiment 1: 1.3 ± 0.2% dose/g;

Experiment 2: 0.9 ± 0.1% dose/g) compared to mice injected with AdLacZ (Experiment 1: 0.5 ± 0.1% dose/g, Experiment 2: 0.5 ± 0.1% dose/g).

Figure 10 shows binding of ^{64}Cu-TETA-octreotide to A427 and SKOV3.ip1 membrane preparations from cells which were either uninfected or infected with 10 or 100 pfu/cell of AdSSTR2. A427 cells were infected with 10 pfu/cell, while SKOV3.ip1 cells were infected with 100 pfu/cell. Binding to infected cells was blocked using a 1,000-fold molar excess of unlabeled octreotide. Each bar represents the mean amount of ^{64}Cu-TETA-octreotide bound as a percentage of total radioactivity added ± SD ($n \geq 6$).

Figure 11 shows biodistribution of ^{64}Cu-TETA-octreotide in nude mice inoculated with 2 x 10^7 SKOV3.ip1 human ovarian cancer cells *i.p.* Five days after tumor cell inoculation, AdSSTR2 or AdLacZ was injected *i.p.*, followed by *i.p.* administration of ^{64}Cu-TETA-octreotide 2 days later. Four hours after radioligand injection, groups of mice were killed and the organs harvested and counted in a gamma counter. BL = blood; LU = lung; LI = liver; SI = small intestine; SP = spleen; KI = kidney; BO = bone; PL = peritoneal lining; UT = uterus; PA = pancreas; TU = tumor. Each bar represents the median tissue concentration from a group of 5 animals with a range from the 25th percentile to the 75th percentile.

Figure 12 shows biodistribution of ^{64}Cu-TETA-octreotide in nude mice inoculated with 2 x 10^7 SKOV3.ip1 human ovarian cancer cells *i.p.* Five days after tumor cell inoculation, AdSSTR2 was injected *i.p.*, followed by *i.p.* administration of ^{64}Cu-

TETA-octreotide 2 or 4 days later. Four hours after radioligand injection, groups of mice were killed and the organs harvested and counted in a gamma counter. Each bar represents the median tissue concentration from a group of 5 animals with a range from the 25th percentile to the 75th percentile. Abbreviations are defined in Figure 11.

Figure 13 shows biodistribution of ^{64}Cu-TETA-octreotide in nude mice inoculated with 2 x 10^7 SKOV3.ip1 human ovarian cancer cells *i.p.* Five days after tumor cell inoculation, AdSSTR2 was injected *i.p.*, followed by *i.p.* administration of ^{64}Cu-TETA-octreotide 2 days later. 4 and 18 hours after radioligand injection, groups of mice were killed and the organs harvested and counted in a gamma counter. Each bar represents the median tissue concentration from a group of 5 to 15 animals with a range from the 25th percentile to the 75th percentile. Abbreviations are defined in Figure 11.

Figure 14 shows surviving proportion of athymic nude mice that were injected *i.p.* with 3 x 10^7 SKOV3.ip1 cells. One group of 5 animals received 1 x 10^9 pfu AdSSTr2 intratumorally on Day 5 followed by 1.4 mCi ^{64}Cu-TETA-octreotide *i.p.* on Day 7. Another group of 5 animals received 1 x 10^9 pfu AdSSTr2 on Days 5 and 19, and received 1.4 and 0.7 mCi ^{64}Cu-TETA-octreotide *i.p.* on Days 7 and 21, respectively. Another group of 5 animals received 1 x 10^9 pfu AdSSTr2 on Day 5 and 2.0 mCi ^{64}Cu-TETA-octreotide on Day 7. An unrelated group of 5 animals served as a control.

Figure 15 shows schema for generation of recombinant GRPr encoding adenovirus under the control of the

DF3 promoter element. The GRPr gene was subcloned into the sites of pACDF3pLpARS(+) to form the plasmid pACDF3GRPrpLpARS(+). The GRPr expression shuttle vector and the adenoviral packaging plasmid pJM17 were cotransfected into 293 cells to generate the recombinant GRPr encoding adenovirus under the control of the DF3 promoter element.

Figures 16A-C show analysis of the GRPr encoding recombinant adenoviral vectors, AdDF3GRPr and AderbGRPr, under the control of the DF3 and erbB-2 promoters, respectively. **Figure 16A** is a structural map of AdDF3GRPr genomic DNA demonstrating localization of GRPr expression cassette at the site of E1 deletion. Restriction endonuclease sites are indicated. The genome is subdivided into 0-100 map units (m.u.). ITR indicates adenoviral inverted terminal repeats of genomic termini. **Figure 16B** shows PCR validation of the AdDF3GRPr and AderbGRPr adenoviral vectors. **Figure 16C** shows restriction analysis of the AdDF3GRPr (lanes 1-6) and AderbGRPr (lanes 8-13) adenoviral vector genomic DNA using the following restriction enzymes. Lanes 1, 8: EcoR1; lanes 2, 9: ClaI; lanes 3, 10: HindIII; lanes 4, 11: KpnI; lane 5, 12: BamHI; lanes 6, 13: XbaI; lane 7: 1 kb ladder. Products of the digestion were analyzed by electrophoresis on 1% agarose gel and ethidium bromide staining.

Figure 17 shows binding of ^{125}I-BBN to breast cancer cells infected with adenoviral vectors encoding the GRPr under the control of the CMV (AdCMVGRPr) or the erbB-2 (AderbGRPr) promoter at an MOI of 50, 200, and 500 pfu/ cell. The cells were harvested 48 hours later and assayed for ^{125}I-BBN binding employing an *in vitro* live-cell binding assay. Uninfected and

AdCMVlacZ cells served as controls. As a positive control the murine fibroblast cell line, BNR-11, stably transfected to express the GRPr gene was used. The cells were counted in a well-type gamma scintillation counter. A representative experiment for each cell line done in triplicate is shown.

Figure 18 shows binding of ^{125}I-BBN to breast cancer cells infected with adenoviral vectors encoding the GRPr under the control of the CMV (AdCMVGRPr) or the DF3 (AdDF3GRPr) promoter at an MOI of 50, 200, and 500 pfu/cell. The cells were harvested 48 hours later and assayed for ^{125}I-BBN binding employing an *in vitro* live-cell binding assay. Uninfected and AdCMVlacZ infected cells served as controls. As a positive control the murine fibroblast cell line, BNR-11, stably transfected to express the GRPr gene was used. The cells were counted in a well-type gamma scintillation counter. A representative experiment for each cell line done in triplicate is shown.

Figure 19 shows binding of ^{125}I-BBN to pancreatic and cholangiocarcinoma cancer cells infected with adenoviral vectors encoding the GRPr under the control of the CMV (AdCMVGRPr) or the DF3 (AdDF3GRPr) promoter at an MOI of 50, 200, and 500 pfu/cell. The cells were harvested 48 hours later and assayed for ^{125}I-BBN binding employing an *in vitro* live-cell binding assay. Uninfected and AdCMVlacZ infected cells served as controls. As a positive control the murine fibroblast cell line, BNR-11, stably transfected to express the GRPr gene was used. The cells were counted in a well-type gamma scintillation counter. A representative experiment for each cell line done in triplicate is shown.

Figure 20 demonstrates the expression in 4 cell lines of MUC1 (A Panels) and broad spectrum cytokeratins (B Panels). All photographs are at 400 X magnification. The cell lines are 1: SK-ChA-1; 2: MDA-MB-231; 3: SK-BR-3; 4: Oz.

Figure 21 demonstrates the expression in 3 cell lines of MUC1 (A Panels) and broad spectrum cytokeratins (B Panels). All photographs are 400 X magnification. The cell lines are 1: BXPC-3; 2: ZR-75-1; 3: ASPC-1.

Figure 22 shows production of adenoviral vectors encoding gene of choice. The recombinant shuttle plasmid containing the gene of choice and parts of the adenovirus genome are co-transfected using a transfection reagent into 293 cells with a rescue plasmid containing the majority of the adenovirus genome with deletions in the E1 and E3 regions. The 293 cells contain the E1 region deleted in the rescue plasmid and thus allow for adenoviral production by homologous recombination between the gene of choice and the rescue plasmid through the Ad5 genome sequences flanking the gene of choice. Areas of adenoviral production appear as cytopathic effect plaques in the 293 cell monolayer. These plaques are picked and screened for the gene of choice and the positive plaques are used for large scale production of adenovirus.

Figure 23 shows partial E1-defective adenovirus strategy for increasing the expression of hSSTr2 throughout the tumor volume.

Figures 24A and **24B** show initial internalization imaging of different Ad vectors monitored by ^{99m}Tc-P2045 (**Figure 24A**) and ^{125}I-FIAU (**Figure 24B**), respectively. SKOV3

cells were infected with different vectors (Ad-TK, Ad-TK-hSSTr2, Ad-TK-hSSTr2 (RGD) and Ad-hSSTr2), and then imaged with the injection of the radiotracer ^{99m}Tc-P2045 or ^{125}I-FIAU.

Figures 25A and **25B** show internalization imaging of different Ad vectors monitored by ^{99m}Tc-P2045 (**Figure 25A**) and ^{125}I-FIAU (**Figure 25B**), respectively, wherein the imaging was obtained 20 minutes after the injection of the radiotracer.

Figures 26A and **26B** show internalization imaging of different Ad vectors monitored by ^{99m}Tc-P2045 (**Figure 26A**) and ^{125}I-FIAU (**Figure 26B**), respectively, wherein the imaging was obtained 60 minutes after the injection of the radiotracer.

Figures 27A and **27B** show internalization imaging of different Ad vectors monitored by ^{99m}Tc-P2045 (**Figure 27A**) and ^{125}I-FIAU (**Figure 27B**), respectively, wherein the imaging was obtained 90 minutes after the injection of the radiotracer.

Figures 28A and **28B** show internalization imaging of different Ad vectors monitored by ^{99m}Tc-P2045 (**Figure 28A**) and ^{125}I-FIAU (**Figure 28B**), respectively, wherein the imaging was obtained 120 minutes after the injection of the radiotracer.

Figures 29A and **29B** show the comparison of percentage dose internally bound per μg protein (^{99m}Tc-P2045/μg protein) between the cells infected with Ad-TK-SSTr2 (**Figure 29A**) and with Ad-TK-SSTr2-RGD (**Figure 29B**).

Figure 30 shows the schema of a reporter system to image gene transfer, wherein SSTr2 receptor/^{99m}Tc-labeled peptide were used.

Figure 31 shows imaging of the gene transfer to subcutaneous A427 tumors. Nude mice were injected with control

Ad on left flank and Ad-hSSTr2 on right flank. 48 hours later, a radiotracer was injected into the mice (^{111}In-octreotide, ^{99m}Tc-P829 and ^{99m}Tc-P2045). Images were obtained 5 h after the injection.

Figures 32A and 32B show the imaging of the gene transfer to *i.p.* ovarian tumors. Three mice having SKOV3.ip1 tumors were injected with Ad-hSSTr2 vector 48 hours before the injection of a radiotracer, while three others received no Ad vector. Both groups were imaged 5 h after injection of the radiotracer, (*e.g.* ^{99m}Tc-P2045). **Figure 32A** shows the imaging obtained on the non-Ad group, while **Figure 32B** shows the Ad-treated group.

Figure 33A shows the initial images of ^{125}I-FIAU in both MKN-28 and KATO-3 cells. **Figure 33B** shows the final images of ^{125}I-FIAU in both MKN-28 and KATO-3 cells, which were taken after 1 hr incubation.

Figures 34A and 34B show imaging of hSSTr2 reporter gene transfer to A427 cells using the herpes simplex virus. **Figure 34A** shows the initial images of P2045, while **Figure 33B** shows the final images, which were taken after 1 hr incubation.

Figures 35A and 35B show imaging of hSSTr2 reporter gene transfer to A427 cells using Ad-hSSTr2 and ^{188}Re-P2045. **Figure 35A** shows the initial images of P2045, while **Figure 35B** shows the final images, which were taken after 1 hr incubation.

DETAILED DESCRIPTION OF THE INVENTION

The methods of the present invention induce normal or cancerous cells to synthesize a membrane expressed targeting molecule (an antigen, a receptor or a modification thereof) which will have a high affinity for infused radioisotopic ligands (including antibodies, peptides, drugs, growth factors, hormones, vitamins and proteins). The use of gene therapy technology to induce expression of high affinity membrane molecules/receptors can be used to image gene transfer of reporter and/or therapeutic genes. A bicistronic adenoviral vector encoding both the cytosine deaminase (CD) gene and the human somatostatin subtype 2 receptor gene were produced. A bicistronic vector encoding the herpes simplex virus-thymidine kinase (HSV-TK) gene and the human somatostatin receptor subtype 2 gene has also begun to be constructed. These vectors are used to demonstrate imaging of reporter and/or therapeutic gene transfer.

The present invention provides a method for monitoring gene transfer and expression into a subject by administering to the subject a genetic vector encoding at least one therapeutic gene (*e.g.* HSV-TK, CD, p53) to be expressed in the subject and a gene for human somatostatin receptor subtype 2 with the genes being capable of expression in the subject. A somatostatin analogue (or other molecule with affinity for the receptor) having a detectable radioisotope attached thereto is administered to the subject and the subject is then imaged in order to determine if the radiolabeled somatostatin analogue has bound to the human somatostatin subtype 2 receptor expressed in

the subject. The detection of specific binding of the radiolabeled somatostatin analogue with the human somatostatin subtype 2 receptor indicates the transfer and expression of the genes transferred into the subject. Such method could be universally used to image gene transfer following the administration of any genetic vector encoding a therapeutic gene and the human somatostatin receptor subtype 2 gene.

In one embodiment of the present invention, there is provided a method for monitoring therapeutic gene transfer and expression into a subject, comprising the steps of administering to the subject a vector encoding at least one therapeutic gene and a reporter gene for a membrane expressed targeting molecule, wherein both genes are capable of expressing in the subject; administering a radiolabeled ligand to the subject, wherein the ligand has a high affinity for the membrane expressed targeting molecule; and then imaging the subject by detecting the binding of the radiolabeled ligand with the membrane expressed targeting molecule, wherein the binding is directly proportional to the transfer and expression of the reporter and therapeutic gene into the subject. Preferably, the membrane expressed targeting molecule is an antigen or a receptor or a modification thereof, selected from the group consisting of the human somatostatin subtype 2 receptor, the gastrin releasing peptide receptor, the vasoactive intestinal peptide receptor and the dopamine receptor, and the ligand is an antibody, a peptide, a drug, a growth factor, a hormone, a vitamin or a protein for binding the respective receptor. Representative therapeutic genes include herpes simplex virus-thymidine kinase, cytosine deaminase, p53, p16,

bax, tumor antigens, antiangiogenesis molecules, pro-angiogenesis molecules, pro-apoptosis molecules, anti-apoptosis molecules, platelet factor-4, soluble Flt-1, angiopoietin-2, thrombospondin-1, angiostatin, endostatin, Fas, FasLigand, cytokines, GM-CSF, IL-2, IL-4, IL-6, IL-7, IL-12, TNF-α and interferon. Representative vectors include an adenoviral vector, a retroviral vector, an adeno-associated viral vector, herpes simplex viral vector, vaccinia virus vector, a liposome, plasmid DNA and a synthetic vector. Representative radioisotopes used for labeling the ligand include ^{99m}Tc, ^{111}In, ^{124}I, ^{18}F, ^{64}Cu, ^{123}I, ^{11}C, ^{131}I, ^{67}Cu, ^{211}At, ^{177}Lu, ^{186}Re, ^{212}Bi, ^{47}Sc, ^{105}Rh, ^{109}Pd, ^{153}Sm, ^{188}Re, ^{198}Au, ^{199}Au, ^{75}Br, ^{76}Br, ^{77}Br, ^{13}N, ^{34m}Cl, ^{38}Cl, ^{52m}Mn, ^{55}Co, ^{62}Cu, ^{68}Ga, ^{72}As, ^{76}As, ^{72}Se, ^{73}Se, ^{75}Se and ^{94m}Tc.

In another embodiment of the present invention, there is provided a recombinant adenoviral vector encoding at least one therapeutic gene and a gene for a membrane expressed targeting molecule. Preferably, the membrane expressed targeting molecule is human somatostatin subtype 2 receptor, wherein the gene for the receptor is tagged with the HA sequence of 9 amino acids (YPYDVPDYA, SEQ ID No. 1) at the N-terminus. In addition, the adenoviral vector may be further tropism-modified by incorporating the tumor cell targeting motifs in the HI loop of adenovirus fiber protein. Representative therapeutic genes include herpes simplex virus-thymidine kinase, cytosine deaminase, p53, p16, bax, tumor antigens, antiangiogenesis molecules, pro-angiogenesis molecules, pro-apoptosis molecules, anti-apoptosis molecules, platelet factor-4, soluble Flt-1, angiopoietin-2, thrombospondin-1, angiostatin, endostatin, Fas,

FasLigand, cytokines, GM-CSF, IL-2, IL-4, IL-6, IL-7, IL-12, TNF-α and interferon.

In still another embodiment of the present invention, there is provided a method of treating an individual having a tumor by administering the above claimed recombinant adenoviral vector to the individual and further administering 5-fluorocytosine (5-FC), ganciclovir (GCV) or a radiolabeled peptide to the individual, wherein the peptide has a high affinity for a membrane expressed targeting molecule. Preferably, the tumor is selected from the group consisting of ovarian tumor, colon tumor, lung tumor, pancreatic tumor, prostate tumor, breast tumor, head and neck tumor, and glioma tumor. Still preferably, the vector is administered systemically or locally by direct injection or via intraperitoneal injection. The peptide may be labeled by an radioisotope, *e.g.*, ^{32}P, ^{90}Y, ^{125}I, ^{212}Pb, ^{213}Bi, ^{111}In, ^{64}Cu, ^{123}I, ^{131}I, ^{67}Cu, ^{211}At, ^{177}Lu, ^{186}Re, ^{212}Bi, ^{47}Sc, ^{105}Rh, ^{109}Pd, ^{153}Sm, ^{188}Re, ^{198}Au, ^{199}Au, ^{77}Br and ^{175}Yb.

In still another embodiment of the present invention, there is provided a method to control the expression of a reporter gene and/or a therapeutic gene that have been transferred to target cells in the host. Such control is afforded by two separate mechanisms, which may also be used in combination. The first is dependent on placing the reporter and therapeutic gene under control of a tissue-specific promoter. Examples of tissue specific promoters include the insulin promoter, which is functional only in insulin-producing cells; oligodendrocyte-specific myelin basic protein (MBP) gene promoter, which is functional only in oligodendrocytes, and tumor specific promoters, which are active

only in cancerous cells, or at least significantly more active in these cells (for example a prostate specific antigen or a carcinoembryonic antigen). Other examples of tissue specific promoters are erbB-2 promoter, MUC1 promoter, alpha fetoprotein promoter, Cox-2 promoter, E2F promoter and myosin light chain 2 promoter. A second mechanism for control of gene expression is provided by inducible promoters or fragments thereof, wherein the fragments are cis-acting control sequences. The expression of genes under control of such promoters or fragments is afforded by addition of an exogeneous compound. An example of an inducible promoter is the tetracycline-inducible promoter which becomes active in a subject following administration of tetracycline or doxycycline, a tetracycline derivative. Another example of an inducible promoter is the multidrug resistance gene (mdr1) promoter, which is induced by mdr1 activating drugs.

The following examples are given for the purpose of illustrating various embodiments of the invention and are not meant to limit the present invention in any fashion.

EXAMPLE 1

Reporter Gene Construct

Modifications to the human type 2 somatostatin receptor gene were included in the adenovirus vector and thereby functioned as the reporter construct for imaging gene transfer. New "gutless" vector technology that is currently available in the laboratory allows for construction of vectors with two or more

inserted genes (38). Therefore, inclusion of the reporter gene will not interfere with inclusion of the therapeutic gene.

A modification was made to the somatostatin receptor gene to facilitate identification of the somatostatin receptor that results from gene transfer. This modification at the N-terminus is an "HA" tag of 9 amino acids (YPYDVPDYA, SEQ ID No. 1) derived from the influenza virus hemaglutinin. When expressed as a protein product, this epitope is recognized by a commercially available antibody. The HA sequence has been successfully inserted into both the N-terminal and C-terminal ends of recombinant proteins as a means of protein tagging (39).

Methods for HA-SSTR2 adenovirus generation: The expression plasmid used to HA-tag hSSTR2 was provided by Kerry J. Koller, Affymax Research Institute, Palo Alto, CA. Briefly, _+12CA5-KH contains the nine amino acid tag sequence YPYDVPDYA (SEQ ID No. 1) immediately following a starting methionine (39). The presence of unique EcoRI and NotI sites after this sequence enables the insertion of hSSTR2, which was released from the plasmid pAChSSTR2 using the same restriction enzymes.

To release the HA-hSSTR2 fragment from _+12CA5-KH and to create compatible restriction enzyme sites, it was digested with MluI, blunt-ended, and digested with NotI. This insert was ligated into the shuttle vector pAdTrack-CMV, which was previously digested with BglII, blunt-ended and cut with NotI. pAdTrack-CMV is used in the AdEasy system of recombinant adenovirus generation, which takes advantage of homologous recombination in bacteria rather than in eukaryotic cells (40).

This system was provided by Bert Vogelstein, Johns Hopkins Oncology Center. Briefly, HA-hSSTR2-pAdTrack-CMV was linearized with PmeI and purified using Wizard DNA clean-up purification resin (Promega, Madison, WI). To 40 µl of electrocompetent *E. coli* BJ5183 cells, 1 _g of linearized HA-hSSTR2-pAdTrack-CMV and 0.1 _g of the supercoiled adenoviral plasmid pAdEasy-1 were added. Electroporation was performed in 0.1 mm cuvettes at 1800V in an Eppendorf electroporator 2510, with a time constant between 4-5 sec. The cells were immediately resuspended in 1 ml SOC medium and grown at 37°C for 1 hour. The bacteria were then pelleted, resuspended in a smaller volume and plated onto kanamycin resistant plates. Smaller colonies, thought to represent the recombinants, were picked and grown overnight in L-Broth containing 50 _g/ml kanamycin.

Clones were first screened by comparing their supercoiled DNA sizes on agarose gels to pAdEasy-1, and possible recombinants were further subjected to PCR analysis using primers for hSSTR2 (forward: 5' TGG ATC CTT GGC CTC CAG 3' (SEQ ID No. 2), reverse: 5' ATT CTA GAA GCC AGG TGT GAG 3' (SEQ ID No. 3)), and Ad5 (forward: 5' TGT CGT TTC TCA GCA GCT GT 3' (SEQ ID No. 4), reverse: 5' TCT GAA CTC AAA GCG TGG GA 3' (SEQ ID No. 5)). Those which were positive for both hSSTR2 and Ad5 were electroporated into ElectroMAX DH10B cells (Gibco BRL Life Technologies) as described above and further analyzed by restriction enzyme digestion. Chosen clones were digested with Pac I, transfected into 293 cells (Microbix Biosystems Inc., Toronto, Ontario) and plaque purified according to standard

protocols. Purified plaques were also validated by PCR as described above, and used in a second round of purification in 293 cells. Plaques were again PCR validated and used to make seed stock of the adenovirus.

Results for HA-hSSTR2 adenovirus generation: Approximately 100 colonies of electroporated BJ5183 cells were obtained from a third of the total cell suspension. Of these, thirty-six extremely small colonies were picked, and the supercoiled DNA sizes were analyzed. One clone which did not appear to contain AdEasy-1, but a slightly larger entity was further determined to contain the hSSTR2 and Ad genes, but not the E1A gene; indicating recombination. Individual digestions with BamHI, SpeI, PacI, NotI and HindIII produced different banding patterns than that produced with the digestion of AdEasy-1 with the same enzymes. A double digestion with EcoRI and NotI produced the 1.7 kb hSSTR2 fragment which was originally inserted into the _+12CA5-KH expression plasmid. This indicates that successful recombination has been achieved.

From this recombinant, twelve plaques were purified after transfection into 293 cells and PCR validated. From these, two plaques were subjected to a second round of plaque purification at several different dilutions (10^{-4}-10^{-7}). In both cases, optimal results were obtained with the most concentrated dilution tested as determined by PCR. One of these was further chosen to make seed stock and purified adenovirus according to standard protocols. In particular, the HA sequence has been inserted on the N-terminal end of the hSSTR2, and done so in a manner that the chimeric hSSTR2 was unchanged in function.

This is the first to utilize the HA-tagged human somatostatin receptor subtype 2 in an Ad5 vector. Inclusion of the HA-tag allows the human somatostatin receptor subtype 2 protein product to be identified in cells by flow cytometry, or by immunohistochemistry.

EXAMPLE 2

Animal Models

Athymic nude mice were utilized for the animal model. Human ovarian cancer cells (SKOV3.ip1) were implanted either subcutaneously or intraperitoneally. At defined times after implantation, the Ad5 vector targeting the ovarian tumor cells was administered. This was accomplished by either direct injection or via intraperitoneal injection.

Human non-small cell lung cancer cells were implanted subcutaneously. At defined times after implantation, the Ad5 vector encoding the somatostatin receptor subtype 2 gene (AdhSSTR2) was administered by direct injection.

EXAMPLE 3

Specificity of *in vivo* Binding and Histology Analysis

Control experiments to verify specificity include dilution of specific activity of the radiolabeled peptide in order to saturate the human somatostatin receptor subtype 2 receptors at the tumor site. Additional controls were used. One was an irrelevant peptide without affinity for the receptor under study, while another was a control adenovirus encoding the thyrotropin

releasing hormone receptor which does not bind somatostatin analogues. Histology analysis of the tumors was conducted. These studies determine the level and uniformity of the reporter gene expression in the tumors.

EXAMPLE 4

Recombinant Adenovirus Vector Expressing HSV-TK and hSSTR2

Herpes simplex virus thymidine kinase (HSV-TK) gene was employed as a therapeutic agent. Adenovirus vectors were derived encoding the tumor cell targeting motifs within the HI loop, as well as isogenic controls. These vectors were then used in treatment regimens. Analysis of treated groups included reduction of tumor mass within the peritoneum, as well as survival.

A double expression cassette, which replaces an E1 region of the viral genome, contains herpes simplex virus-thymidine kinase and human somatostatin receptor subtype 2 genes each driven by an immediate-early cytomegalovirus promoter (CMV_{PR}) and followed by a polyadenylation signal (pA) (Figure 1). Expression of herpes simplex virus-thymidine kinase allows for therapeutic application of the vector in combination with ganciclovir, whereas expression of the human somatostatin receptor subtype 2 gene provides an opportunity for the vector biodistribution studies via gamma camera imaging. An RGD motif incorporated into the HI loop of the adeonvirus fiber protein results in expanded tropism of the vector by allowing the virus to utilize cellular integrins as primary receptors for virus attachment.

EXAMPLE 5

Expression of hSSTr2 and CD Genes in Ovarian Cancer Cells

An adenoviral vector which contains the SSTr2 gene and another therapeutic gene, such as cytosine deaminase (CD) gene, could be used to non-invasively determine the level of *in vivo* expression of the therapeutic gene indirectly by imaging the SSTr2 expression. The CD enzyme converts non-toxic 5-fluorocytosine (5-FC) into the toxic 5-fluorouracil (5-FU). An initial step towards validating this system is to ensure that both SSTr2 and CD are expressed simultaneously. An experiment was conducted with SK-OV-3.ip1 cells that were infected with an adenovirus encoding the bacterial gene for CD (AdCMVCD) and with AdCMVSSTr2 at 10, 100, or 300 moi of each adenovirus. Twenty-four hr later the cells were split into two flasks and grown for an additional 24 hr after which one flask was harvested for a tritiated 5-FC to 5-FU conversion assay and the other flask used in a ^{125}I-Tyr^{1}-somatostatin binding assay as described above.

The results of the tritiated 5-FC conversion assay are shown in Figure 2A. The percentage of tritiated 5-FU produced from tritiated 5-FC was 9%, 45%, and 78% when the cells were infected at 10, 100, and 300 moi, respectively. Cells infected with a control adenovirus demonstrated only 3% conversion. Figure 2B shows the specific binding of ^{125}I-Tyr^{1}-somatostatin to 50 µg of membrane preparation was 0.4%, 2%, and 5% of the total radioactivity added when the cells were infected at 10, 100, and 300 moi. Uninfected SK-OV-3.ip1 membrane preparations demonstrated < 0.2% binding of ^{125}I-Tyr^{1}-somatostatin. Thus,

both SSTr2 and CD can be expressed in cells after adenoviral co-infection suggesting that a two-gene vector encoding for SSTr2 and CD would yield similar results. Similarly, A-427 cells co-infected with an adenovirus encoding the gene for TK (AdCMVTK) and AdCMVSSTr2 expressed both gene products 48 hr after infection.

EXAMPLE 6

Expression of hSSTR2 in Lung Cancer Cells

The adenovirus vector containing the human somatostatin receptor subtype 2 gene was used to infect human lung cancer A427 cells. A cell membrane preparation was prepared from these infected cells and 50 _g was incubated with ^{111}In-labeled octreotide. There was 80% binding of the ^{111}In-labeled octreotide to the cell membrane preparation, which was specifically blocked by excess unlabeled octreotide.

EXAMPLE 7

Imaging Gene Transfer to A427 Cancer Cells in Culture

Gamma camera imaging and gamma counting of internalized [^{111}In]-DTPA-D-Phe^1-octreotide in A-427 cells infected with 10 pfu per cell of AdSSTr2 is shown in Figures 3A-3C. The image immediately after addition of [^{111}In]-DTPA-D-Phe^1-octreotide is shown in Figure 3A and the amount of internalized radioactivity after a 1 h incubation and wash is shown in Figure 3B. The internalized radioactivity could be visualized when the percentage of infected cells in the mixture of uninfected and infected A-427 cells was >25%. Gamma counting results of the

internalized radioactivity for 100%, 75%, 50%, 25%, 10%, 5%, 1% and 0% infected A-427 cells were (mean ± SD) 2.13 ± 0.15, 1.39 ± 0.19, 0.92 ± 0.07, 0.51 ± 0.03, 0.22 ± 0.02, 0.11 ± 0.01, 0.04 ± 0.003, and 0.03 ± 0.003 % dose/mg total protein, respectively (Figure 3C). Internalization was inhibited to <0.02 % dose/mg total protein by addition of excess unlabeled octreotide which demonstrates the specificity of [^{111}In]-DTPA-D-Phe^1-octreotide binding and internalization. These studies demonstrated the expression and internalization of SSTr2 on A-427 cells following AdSSTr2 infection and binding of radiolabeled peptide. The internalization of SSTr2 is important for the intracellular accumulation and retention of radiolabeled octreotide analogues.

EXAMPLE 8

Imaging Gene Transfer to A427 Tumors in Nude Mice

Induction of SSTr2 expression in A-427 tumors *in vivo* was evaluated by imaging tumor accumulation of [^{111}In]-DTPA-D-Phe^1-octreotide. These studies utilized ^{111}In-DTPA-D-Phe^1-octreotide to non-invasively image SSTr2 expression since [^{90}Y] is a pure beta-emitter and [^{90}Y]-SMT 487 would not be suitable for this purpose. Gamma camera images of a representative mouse from the first group at 5.5 h after *i.v.* injection of [^{111}In]-DTPA-D-Phe^1-octreotide at 48 h and 96 h after a single intratumoral AdSSTr2 (right side) or AdTRHr (left side) injection are shown in Figures 4A and 4B, while images of a mouse from the second group 48 h and 96 h after a second intratumoral injection of AdSSTr2 or AdTRHr are shown in Figures 4C and 4D. These results show that imaging could detect accumulation of [^{111}In]-

DTPA-D-Phe^1-octreotide in tumors injected with AdSSTr2 compared to much lower levels in tumors injected with AdTRHr. The retention of radioactivity in the kidneys and excretion through the bladder is observed. The localization of [^{111}In]-DTPA-D-Phe^1-octreotide in AdSSTr2-infected tumors was similar 48 and 96 h after one or two AdSSTr2 injections. This tumor uptake was important to validate the dosing regimen that was used in the therapy studies.

The ROI analysis and tissue counts after the second imaging session for each group of animals are shown in Figures 5A and 5B. The ROI analysis in Figure 5A shows tumor uptake of [^{111}In]-DTPA-D-Phe^1-octreotide of ~2.8% ID/g 48 and 96 h after a single intratumoral AdSSTr2 injection compared to ~1.5% ID/g 48 and 96 h after a second intratumoral AdSSTr2 injection. Uptake of [^{111}In]-DTPA-D-Phe^1-octreotide in AdTRHr-injected tumors was <0.3% ID/g at both time points. Figure 5B shows the biodistribution of [^{111}In]-DTPA-D-Phe^1-octreotide. The uptake in tumors after a single or double injection of AdSSTr2 (~1.5% ID/g) was greater than in normal tissues (<0.5% ID/g except kidney) and the AdTRHr-injected tumors (0.08% ID/g) for both groups of animals. This uptake of [^{111}In]-DTPA-D-Phe^1-octreotide in AdSSTr2-injected tumors was similar to that previously reported in rats bearing pancreatic tumors that natively express SSTr2. The kidneys had ~18% ID/g in both groups of animals, which agrees with the results of other studies (44). The uptake in AdSSTr2-injected tumors by tissue counting was similar to the ROI analysis for two injections of AdSSTr2, but not a single injection of AdSSTr2. This is likely due to an overestimate of the ROI after a

single AdSSTr2 injection. Since the tumors were smaller for the single injection of AdSSTr2, it is hypothesized that some normal tissue surrounding the tumor was induced to express SSTr2 and included in the tumor ROI analysis. Thus, this could account for the discrepancy between the ROI analysis and the tissue counting. These studies showed a high level of SSTr2 expression in tumors up to 4 days following one or two direct intratumoral AdSSTr2 injections.

Therapy experiments were conducted using [^{90}Y]-SMT 487 based on the high level of SSTr2 tumor expression as determined by [^{111}In]-DTPA-D-Phe^{1}-octreotide imaging. Previous studies have shown favorable biodistribution of [^{90}Y]-SMT 487 in rats bearing pancreatic tumors that natively express SSTr2 (47) and relatively low radiation dose estimates to normal organs in humans by measuring the kinetics of [^{86}Y]-SMT 487 in baboons using positron-emission tomography (48). No significant animal weight loss was observed throughout the experiment. The change in median A-427 tumor size relative to the size on the day of the first AdSSTr injection is shown in Figure 6A. Mice that received 2 intratumoral injections of AdSSTr2 and 4 doses of 400 μCi or 500 μCi [^{90}Y]-SMT 487 had median tumor quadrupling times of 40 and 44 days, respectively (Figure 6B). The log-rank test revealed a statistically significant difference in time to tumor quadrupling between the AdSSTr2 + [^{90}Y]-SMT 487 treatment groups and the control groups ($p < 0.02$). The median tumor quadrupling times of the no treatment group and the no virus + 4 doses of 500 μCi [^{90}Y]-SMT 487 group were 16 and 25 days, respectively. The difference in time to tumor quadrupling between the untreated

and no virus + [^{90}Y]-SMT 487 control groups was significant ($p = 0.0008$) which is likely due to nonspecific irradiation of the tumor since the A-427 tumors are negative for SSTr2.

The median tumor areas at the time of treatment were 47-68 mm^2 and the tumor doubling times (7-9 days) were not significantly different among groups. The differences in median tumor area between groups began to appear at the beginning of the second week of treatment. A second experiment showed differences in the median time to tumor doubling when the initial median tumor areas of the groups were 58-132 mm^2 (data not shown). Possible reasons for the differences between these experiments could be that a smaller fraction of the radiation dose was deposited in the smaller tumors due to the long path length of [^{90}Y] emissions or that the smaller tumors were still in an exponential phase of growth that was not inhibited by the first week of treatment. Anderson *et al.* showed therapeutic efficacy with a [^{64}Cu]-labeled octreotide derivative in rats bearing *s.c.* pancreatic tumors that natively express SSTr2 (49). This study suggested that [^{64}Cu] may be more appropriate for therapy of smaller tumors than [^{90}Y] due to the differences in the path length of their particulate emissions (49).

Figures 7A and 7B show the imaging of the expression of two genes (SSTr2 and TK) following Ad transfer to A427 tumors. 5 x 10^8 pfu AdSSTr2 (left tumor) or AdTKSSTr2 (right tumor) (Figure 7A) or 5 x 10^8 pfu AdTK (left tumor) or 5 x 10^8 pfu AdTKSSTr2 (right tumor) (Figure 7B) were injected into *s.c.* A427 tumor xenografts and animals imaged 2 days later at 5 h after *i.v.* injection of ^{99m}Tc-P2049 and ^{131}I-FIAU.

EXAMPLE 9

Immunohistochemistry

After imaging, the tumors were removed and analyzed by immunohistochemistry. Ad5-CMVTRHr-injected tumors showed minimal background staining, primarily in scattered macrophages. Ad5-CMVhSSTr2-injected tumors showed cells expressing somatostatin receptors in 3 of the 4 tumors that were examined. Of interest, the negative tumors had low uptake of the radiolabeled peptide (data not shown). The location of the positive areas appeared to be along the Ad5 needle tract and at the termination of the probable injection site. In addition, areas of necrosis were noted frequently at the terminations of the probable injection tracts for the Ad5-CMVhSSTr2-injected tumors. Figure 8A shows cells expressing somatostatin receptor along an apparent injection tract. Figure 8B shows no staining in a similarly stained frozen section from the matching control tumor from the same mouse.

EXAMPLE 10

Imaging Gastrin Releasing Peptide Receptor (GRPr) Expression

A technique was developed to image gastrin releasing peptide receptor (GRPr) expression using a ^{99m}Tc-labeled bombesin (BBN) analogue. The BBN analogue (QWAVGHLM, SEQ ID No. 6) with an Aoc linker was HYNIC-modified, purified by reverse phase HPLC, and analyzed by mass spectrometry. The HYNIC-peptide was radiolabeled with ^{99m}Tc using tricine as the transchelator and purified again by HPLC. Binding specificity and

affinity of the ^{99m}Tc-labeled BBN analogue for GRPr were verified by Scatchard analysis using BNR-11 cells (3T3 cells stably expressing GRPr). GRPr expression was induced in the footpad of mice after local injection of a recombinant GRPr-expressing adenoviral vector (Figure 9A). In two experiments male CD1 mice (n=8/experiment) were injected in the left rear footpad (10^9 infectious particles) with either an adenoviral vector encoding GRPr (Ad-CMVGRPr) or a negative control adenoviral vector encoding β-galactosidase (AdLacZ). Mice were injected IV 48 hours later with ^{99m}Tc-BBN analogue (0.5 μg, 1.5 MBq), imaged with a gamma camera using a pinhole collimator, and terminated. The HYNIC-modified BBN analogue, confirmed by mass spectroscopic analysis, was radiolabeled with ^{99m}Tc (6 MBq/μg). Scatchard analysis demonstrated specific, high affinity binding to GRPr-expressing cells (Kd=2-5 nM). Following IV administration, the ^{99m}Tc-BBN analogue cleared from the circulation by 2 h, with 50% of the dose excreted. Imaging and tissue biodistribution demonstrated significant ($p<0.05$), specific retention of the ^{99m}Tc-BBN analogue in the footpad of mice injected with AdGRPr (Experiment 1: 1.3 ± 0.2% dose/g; Experiment 2: 0.9 ± 0.1% dose/g) compared to mice injected with AdLacZ (Experiment 1: 0.5 ± 0.1% dose/g, Experiment 2: 0.5 ± 0.1% dose/g) (Figure 9B). These results demonstrate that *in vivo* imaging with a ^{99m}Tc-BBN analogue measured local induction of receptor resulting from injection of Ad-CMVGRPr.

EXAMPLE 11

Radiolabeling of TETA-Octreotide with ^{64}Cu

TETA (Aldrich Chemical Co., Milwaukee, WI) was conjugated to octreotide as described elsewhere (43). $^{64}CuCl_2$ (initial specific activity = ~ 5,000 Ci/mmol) was produced and purified at the University of Missouri-Columbia Research Reactor and used to label TETA-octreotide as previously described (43). Briefly, the TETA-octreotide was mixed with ^{64}Cu-acetate in 0.1 M ammonium acetate buffer, pH 5.5 and incubated at room temperature for 1 hour. Gentisic acid (1 mg/ml) was added to the mixture to reduce the effects of radiolysis. Reactions products were purified using a C-18 SepPak. The mixture was added to the SepPak, rinsed with 5 ml of 0.1 M ammonium acetate, pH 5.5 to remove uncomplexed ^{64}Cu, and rinsed with ethanol to elute the ^{64}Cu-TETA-octreotide product. Purity was confirmed by reverse phase HPLC and thin layer chromatography.

EXAMPLE 12

Competitive Binding Assay

A427 and SKOV3.ip1 cells were maintained in Dulbecco's Modified Eagles Medium containing 10% fetal bovine serum and cultured at 37°C in a humidified atmosphere with 5% CO_2 and seeded so that they were ~80% confluent at the time they were infected. The A427 cells were infected at 0 and 10 pfu/cell with AdhSSTR2, while the SKOV3.ip1 cells were infected with 0 and 100 pfu/cell of AdhSSTR2 because they are less easily transduced (44). The cells were grown for 48 hours and then harvested to form membrane preparations as previously

described (44). The membrane preparations were then diluted with buffer (10 mM HEPES, 5 mM $MgCl_2$, 1 mM EDTA, 0.1% BSA, 10 μg/ml leupeptin, 10 μg/ml pepstatin, 0.5 μg/ml aprotinin, and 200 μg/ml bacitracin, pH 7.4) to 0.5 mg/ml. One-hundred microliters (50 μg) of membrane preparation were added to Multiscreen Durapore filtration plates (type FB, 1.0 μm borosilicate glass fiber over 1.2 μm Durapore membrane; Millipore, Bedford, MA) in triplicate and washed with buffer (10 mM HEPES, 5 mM $MgCl_2$, 1 mM EDTA and 0.1% BSA, pH 7.4). One-hundred microliters of ^{64}Cu-TETA-octreotide (0.05 nM) were added to each well and incubated for 90 min at room temperature. The samples were then washed twice with ice cold buffer, the filters allowed to dry, and the individual wells punched out and counted in a gamma counter. Non-specific binding was assessed using a 1000-fold molar excess of octreotide to inhibit binding of ^{64}Cu-TETA-octreotide.

The result shows that membrane preparations from A427 cells infected with 10 pfu/cell of AdhSSTR2 or SKOV3.ip1 cells infected with 100 pfu/cell of AdhSSTR2 demonstrated 37% and 20% binding of ^{64}Cu-TETA-octreotide, respectively compared to < 1.0% binding with uninfected cells or infected cells blocked with an excess of unlabeled octreotide (Figure 10).

EXAMPLE 13

^{64}Cu-TETA-Octreotide Biodistribution Studies

Tumor localization and pharmacokinetics of ^{64}Cu-TETA-octreotide was investigated in mice bearing *i.p.* SKOV3.ip1 human ovarian tumors induced to express hSSTR2 with

AdhSSTR2. Mice bearing *i.p.* SKOV3.ip1 tumors infected with 1 x 10^9 pfu AdhSSTR2 or AdLacZ 5 days after tumor cell inoculation followed by *i.p.* injection of ^{64}Cu-TETA-octreotide 2 days later had median (25th-75th percentile range) tumor uptakes of 11.4 (7.6-17.0) %ID/g and 1.6 (1.6-1.8) %ID/g (p=0.002) at 4 h after ^{64}Cu-TETA-octreotide administration respectively (Figure 11). A larger uptake of ^{64}Cu-TETA-octreotide was also observed in the liver, small intestine, spleen, peritoneal lining, uterus, and pancreas of mice administered AdhSSTR2 compared to mice given AdLacZ. This may be due to AdhSSTR2 infection of these organs. Mice given AdhSSTR2 had tumor-to-blood, kidney, and liver ratios of 27.3, 2.7, and 2.2 at 4 h after ^{64}Cu-TETA-octreotide administration respectively. Mice administered ^{64}Cu-TETA-octreotide 2 or 4 days after *i.p.* injection of AdhSSTR2 had similar median tumor uptake of 11.2 (10.6-12.9) %ID/g and 16.4 (12.7-27.4) %ID/g (p=0.076) 4 hours later (Figure 12). Other normal tissues also demonstrated similar uptake except for the liver, which had significantly greater uptake 4 days after AdhSSTR2 administration than 2 days after administration (p=0.009). In a separate experiment, mice killed 4 or 18 hours after injection of ^{64}Cu-TETA-octreotide showed a median tumor uptake of 24.3 (17.0-31.1) %ID/g at 4 hours which declined to 4.9 (2.9-8.0) %ID/g at 18 hours (Figure 13). Pharmacokinetic analysis demonstrated that clearance of ^{64}Cu-TETA-octreotide from the tumor, blood, liver, and kidney was best fit using a two compartment model. The radioactivity cleared from tumor with an α half-life of 1.2 hours and a β half-life of 27.1 hours. In contrast, blood demonstrated an initial clearance half-life of 0.3 hours followed by accumulation of radioactivity

with a doubling time of 46.2 hours. These studies demonstrate that ^{64}Cu-TETA-octreotide localized in human ovarian tumors induced to express hSSTR2 with AdhSSTR2 *in vivo*. In addition, ^{64}Cu-TETA-octreotide has been demonstrated to be useful in therapy studies, indicating it should have therapeutic efficacy in this human ovarian cancer model induced to express hSSTR2 due to its high uptake in tumor and its comparable biological half-life in tumor (27.1 hours) with the physical half-life of ^{64}Cu (12.8 hours).

Figure 14 shows surviving proportion of athymic nude mice that were injected *i.p.* with 3 x 10^7 SKOV3.ip1 cells. One group of 5 animals received 1 x 10^9 pfu AdSSTr2 intratumorally on Day 5 followed by 1.4 mCi ^{64}Cu-TETA-octreotide *i.p.* on Day 7. Another group of 5 animals received 1 x 10^9 pfu AdSSTr2 on Days 5 and 19, and received 1.4 and 0.7 mCi ^{64}Cu-TETA-octreotide *i.p.* on Days 7 and 21, respectively. Another group of 5 animals received 1 x 10^9 pfu AdSSTr2 on Day 5 and 2.0 mCi ^{64}Cu-TETA-octreotide on Day 7. An unrelated group of 5 animals served as a control.

EXAMPLE 14

Construction and Confirmation of Recombinant Adenoviral Vectors

Recombinant adenoviral vectors encoding the GRPr gene under the control of the DF3 (AdDF3GRPr) or erbB-2 (AderbGRPr) promoters were constructed. The schema used to generate the recombinant adenoviral vectors AdDF3GRPr is shown in Figure 15. AderbGRPr was generated using standard methods.

The methodology for recombinant adenovirus construction is based upon *in vivo* homologous recombination between the recombinant adenoviral shuttle vector and the adenoviral packaging plasmid pJM17. The adenoviral shuttle vector containing the GRPr gene with the DF3 promoter element, pACDF3GRPrpLpARS(+), was constructed and used to derive the corresponding adenoviral vector. The resulting adenoviral vector, AdDF3GRPr, would be predicted to contain the GRPr expression cassette inserted in place of deleted adenoviral E1 sequences (Figure 16A). A similar result would be expected for AderbGRPr generated from pACerbGRPrpLpARS(+) (map not shown).

Cotransfection of the adenoviral shuttle vector pACDF3GRPrpLpARS(+) or pACerbGRPrpLpARS(+) and the packaging plasmid pJM17 in the E1A transcomplementing cell line 293 resulted in multiple areas of cytopathic effect consistent with adenoviral replication. Analysis of the viral DNA by PCR demonstrated the presence of recombinant adenoviruses possessing characteristics consistent with the GRPr expressing vectors predicted in Figure 15. Amplification of AdDF3GRPr or AderbGRPr genomic DNA containing the GRPr gene with GRPr-specific primers yielded the expected PCR fragment of 974 bp in both vectors (Figure 13B). Analysis of AdDF3GRPr and AderbGRPr genomic DNA yielded the predicted bands for the DF3 and erbB-2-specific primers, respectively (lanes 2 and 6, Figure 16B). Analysis for E1A sequences using adenovirus E1A-specific primers indicated the predicted PCR product of 1070 bp from genomic DNA of the Ad2 adenovirus. In contrast, this fragment was absent

in amplification of AdDF3GRPr and AderbGRPr DNA, confirming the absence of E1A sequences in these recombinant adenoviruses. The PCR analysis is consistent with the derivation of E1A(-), GRPr encoding recombinant adenoviruses under the control of either the DF3 or erbB-2 promoter elements and also indicated that no wild-type virus had been rescued by propagation.

To verify the overall integrity of the adenoviral vectors, restriction analysis of genomic DNA of AdDF3GRPr and AderbGRPr was performed (Figure 16C). Analysis with a series of restriction endonuclease confirmed that the overall configuration of the recombinant genomes corresponded to the predicted structure. These results demonstrate the production of replication defective adenoviral vectors that encode the GRPr gene under control of the DF3 and erbB-2 promoter elements.

EXAMPLE 15

Tumor Cell Specific Expression Employing the erbB-2 Promoter Element

The ability of the AderbGRPr vector to direct specific gene expression was tested in three human breast cancer cell lines, SK-BR-3, ZR-75-1 erbB-2 positive and MDA-MB-231 erbB-2 negative (45,46). Specific binding of ^{125}I-BBN to the induced GRPr receptor served as the assay to assess gene expression. The amount of binding was quantified as the percent radioactivity bound compared to total radioactivity added. The AdCMVGRPr virus showed high levels of GRPr gene expression that increased with increasing MOI at 50, 200 and 500 (Figure 17) in the three breast cancer cell lines tested. The percent ^{125}I-BBN binding for

AdCMVGRPr at MOI 50, 200, and 500 were 46%, 54% and 66% for MDA-MB-231, 54%, 73% and 77% for ZR-75-1 and 68%, 72% and 74% for SK-BR-3, respectively. The BNR-11 cells served as a positive control and demonstrated 58% ^{125}I-BBN binding. However, only the two erbB-2 positive cell lines showed high level BBN binding following infection with AderbGRPr (Figure 17) that also increased as the MOI was increased. The percent ^{125}I-BBN binding for AderbGRPr at MOI 50, 200, and 500 were 8%, 7% and 12% for MDA-MD-231, 29%, 38% and 56% for ZR-75-1 and 15%, 28% and 50% for SK-BR-3, respectively. The level of GRPr gene expression was not as great for the erbB-2 promoter as it was for the CMV promoter. At an MOI of 500 the percent binding of AderbGRPr versus AdCMVGRPr was 18%, 73% and 68% for MDA-MB-231, ZR-75-1 and SK-BR-3, respectively. Therefore, specific gene expression employing the erbB-2 promoter was achieved in an adenoviral vector at high levels relative to the CMV promoter.

EXAMPLE 16

Tumor Cell Specific Expression Employing the DF3 Promoter Element

The same breast cancer cell lines were tested with the AdDF3GRPr vector employing the same binding assay. Specific GRPr gene expression was observed employing the AdDF3GRPr vector (Figure 18). Increased gene expression was observed with increasing MOI (50, 200 and 500) with the AdDF3GRPr vector in the ZR-75-1 and SK-BR-3 cell lines. The percent ^{125}I-BBN binding for AdDF3GRPr at MOI 50, 200, and 500 were 10%, 11% and 10% for MDA-MB-231, 25%, 51% and 62% for ZR-75-1 and 18%, 41%

and 65% for SK-BR-3 cells, respectively. At an MOI of 500 the percent binding of AdDF3GRPr versus AdCMVGRPr was 16%, 102% and 88% for MDA-MB-231, ZR-75-1 and SK-BR-3 cells, respectively. The results successfully demonstrate specific and high level gene expression employing the DF3 promoter element in breast cancer cell lines.

A Genetic Radio-Isotope Targeting Strategy (GRITS) was used in pancreatic and cholangiocarcinoma tumor models, and the DF3 promoter was tested in two human pancreatic cell lines, BXPC-3 and ASPC-1, and two human cholangiocarcinoma cell lines, SK-ChA-1 and Oz. Figure 19 shows specific GRPr gene expression in one pancreatic, ASPC-1, and one cholangiocarcinoma, SK-ChA-1, cell line. The percent ^{125}I-BBN binding for AdCMVGRPr at MOI 50, 200, and 500 were 21%, 31% and 48% for BXPC-3; 36%, 63% and 64% for ASPC-1; 21%, 39% and 70% for SK-ChA-1 and 45%, 58% and 70% for Oz cells, respectively. The percent ^{125}I-BBN binding for AdDF3GRPr at MOI 50, 200, and 500 were 2%, 4%, and 3% for BXPC-3 and 14%, 20% and 18 % for ASPC-1 cells, respectively. However, the DF3 mediated GRPr expression in ASPC-1 was not as great as the other DF3 positive cell lines and did not increase with increasing MOI. The SK-ChA-1 cell line gave results similar to the breast cancer cell lines with 17%, 33% and 51% compared to 5%, 5% and 10% for Oz cells at MOIs of 50, 200 and 500 respectively with AdDF3GRPr. Therefore, the DF3 promoter can be used to achieve tumor-specific gene expression in breast, pancreatic and cholangiocarcinoma cells expressing DF3. Weak tumor-specific gene expression was observed in one pancreatic cell line.

EXAMPLE 17

Immunohistochemical Analysis of MUC1 (DF3) Expression and Correlation with ^{125}I-BBN Binding to AdDF3GRPr Infected Cells

MUC1 and cytokeratin expression was analyzed in the panel of human breast, pancreatic, and cholangiocarcinoma cell lines by immunohistochemistry. The two breast cancer cell lines with the highest level of MUC1 expression, ZR-75-1 and SK-BR-3 had the highest GRPr expression following infection with AdDF3GRPr detected by ^{125}I-BBN binding (Table 1, Figures 20 and 21). MDA-MB-231 had low MUC1 expression and low GRPr expression following infection with AdDF3GRPr (Table 1, Figure 20). A similar result was observed for the cholangiocarcinoma cell lines. SKChA-1 cells had a higher level of MUC1 expression compared to Oz cells which corresponded to a higher level of ^{125}I-BBN binding to AdDF3GRPr infected cells (Table 1 and Figure 20). The pancreatic cell lines showed a different relationship. While BXPC-3 cells had an intermediate level of MUC1 expression, GRPr expression after infection with AdDF3GRPr was very low (Table 1 and Figure 21). However, GRPr expression after infection with AdCMVGRPr was lower in BXPC-3 cells than for the other cell lines. ASPC-1 cells had low level MUC1 expression but a higher level of GRPr expression following AdDF3GRPr infection than BXPC-3 cells. GRPr expression was higher in AdCMVGRPr infefcted ASPC-1 cells than BXPC-3 cells. All cell lines were positive for control cytokeratin staining. Therefore, the expression of MUC1 correlated well with GRPr expression using AdDF3GRPr in breast

and cholangiocarcinoma cell lines, but not with the pancreatic cell lines.

TABLE 1

Immunostaining Scores: MUC1/Cytokeratin and Percentage of ^{125}I-BBN Binding to AdDF3GRPr or AdCMVGRPr Infected Cells at 500 MOI

Cell line	Score		% Binding	
	MUC1	Cytokeratin	AdDF3GRPr	AdCMVGRPr
ZR-75-1	2.8	2.6	61.7	61.1
SK-ChA-1	2.1	2.3	51.4	69.9
SK-BR-3	1.3	2.0	65.3	74.3
BXPC-3	1.3	1.8	3.2	48.1
Oz	1.1	2.2	10.1	70.2
ASPC-1	0.7	2.3	17.6	64.4
MDA-MB-231	0.4	1.2	10.3	62.8

EXAMPLE 18

Replicative Adenovirus

Most of the current adenoviral vectors used for gene therapy have the E1 and E3 regions of the adenoviral genome deleted. The E1 region is essential for viral replication, while the E3 region is not required for viral growth and its removal allows

for larger cDNA inserts. Adenoviral vectors with an E1 deletion are replication-deficient and thus are capable of infecting a cell only once. Therefore, the cell does not die as a result of infection. The desired cDNA is usually cloned into a shuttle (expression) plasmid that contains a portion of the E1 region of the viral genome. The large size of the adenoviral genome prevents the use of a single plasmid system. Thus, a system called homologous recombination is used whereby the cDNA recombinant shuttle plasmid and a rescue plasmid containing the rest of the adenoviral genome are co-transfected into a packaging cell line (Figure 22). The 293 human transformed primary embryonal kidney cell is the standard packaging cell line that has been stably transfected with the E1 region of the adenoviral genome (50). This allows the E1-deleted vector to be made at high titer and remain replication-deficient. Another method of adenoviral generation allows for recombination in bacteria. This method, described by He *et al.*, permits broad screening of recombinants before introduction into 293 cells (51). The main advantage of using adenoviral vectors is their high *in vivo* transduction efficiency. Another advantage is their ability to infect non-dividing as well as dividing cells. The capability to produce adenoviral vectors at high titers is also important. Disadvantages of using adenoviral vectors include host immune response against the vector preventing re-administration, transient expression because it is non-integrating, and lack of cell-specific infection resulting in gene delivery to normal cells.

Another replication-competent vector that has been constructed and is being evaluated is an adenovirus encoding

SSTr2 that contains a 24 base pair deletion (Δ24) in the E1A region (AdΔ24SSTr2). The Δ24 should allow the adenovirus to replicate only in cancers that have disruption of the Rb protein. AdΔ24SSTr2 was used to infect A-427 cells at 1 and 10 moi. Forty-eight hr after infection, the cells were harvested for a membrane preparation and a binding assay was conducted with ^{125}I-Tyr^{1}-somatostatin. The membrane preparations infected at 1 and 10 moi showed 18% and 16% binding, respectively, which was inhibited to < 8% with an excess of unlabeled somatostatin. The ability of AdΔ24SSTr2 to replicate was confirmed by seeding uninfected A-427 cells into the original flask of A-427 cells that were harvested for the membrane preparation. The hypothesis is that AdΔ24SSTr2 left in the flask could infect the newly seeded A-427 cells. This was confirmed by performing a binding assay on these cells 48 hr after seeding which resulted in 18% binding from both the original 1 and 10 moi flasks. Three subsequent passages in this manner resulted in 15-17% binding.

Figure 23 shows partial E1-defective adenovirus strategy for increasing the expression of hSSTr2 throughout the tumor volume.

EXAMPLE 19

Plate Imaging of Multiple Vectors

Four different vectors (Ad-TK, Ad-TK-hSSTr2, Ad-TK-hSSTr2 (RGD) and Ad-hSSTr2) were used to infect SKOV3.ip cells, and the internalization imaging of the vectors were evaluated. Figures 24-28 show the time course imaging study (initial, 20 minutes, 60 minutes, 90 minutes and 120 minutes, respectively).

After imaging, the cells were harvested, counted in a gamma counter and the percentages of internally bound radioactivity were standardized for the total amount of protein. Figure 29 shows the comparison of percentage dose internally bound per µg protein (^{99m}Tc-P2045/µg protein) between the cells infected with Ad-TK-SSTr2 (A) and with Ad-TK-SSTr2-RGD (B).

Plates were imaged using 2 different gamma energy windows on a Technicare 420/550 mobile gamma camera using a high resolution parallel hole collimator. Region of interest analyses were confirmed by gamma counter analysis on the removed cells. Only cells infected with an Ad virus encoding hSSTr2 showed internal binding of ^{99m}Tc-P2045, while only cells infected with an Ad virus encoding TK showed internal binding of ^{125}I-FIAU.

EXAMPLE 20

In Vivo Imaging

Human lung cancer cells (A427) were injected *s.c.* in the right and left flanks of 8 nude mice (2 groups of 4/group) (see Figure 30 for the schema of a reporter system to image gene transfer). After 14 days all right tumors were directly injected with Ad-TK-hSSTr2 (5 x 10^8 plaque forming units). The left tumors were injected with the same dose of Ad encoding TK alone (Ad-TK, Group A) or Ad encoding hSSTr2 alone (Ad-hSSTr2, Group B). The expression of hSSTr2 following gene transfer was monitored using a new ^{99m}Tc-labeled somatostatin-analogue, P2045 (Diatide, Inc.), while TK enzymatic activity was monitored with ^{13}I-2'-deoxy-2'-fluro-_-D-arabinofuranosyl-5-iodouracil

(FIAU). ^{99m}Tc-P2045 (54 MBq/nmol, 22 MBq) and ^{131}I-FIAU (23 MBq/nmol, 5.6 MBq) were injected *i.v.* 48 h later. Mice were imaged using a gamma camera (2 windows) equipped with a pinhole collimator at 3 min, 5 h, and 26 h after injection of the radiotracers, and then terminated. Radiotracers in tumors and other tissues were determined by region of interest (ROI) and gamma counter analyses.

The results showed that at 5 h, ~85% of both radiotracers were eliminated in the urine. At 5 h, ROI analyses showed the Ad-TK-hSSTr2 injected right tumors (n = 8) accumulated 2.0 ± 0.3% and 0.5 ± 0.1% injected dose (ID) for ^{99m}Tc-P2045 and ^{131}I-FIAU, respectively (Figure 31). At 26 h, ROI analyses showed the same tumors decreased to 1.5 ± 0.2% and 0.2 ± 0.03% ID for ^{99m}Tc-P2045 and ^{131}I-FIAU, respectively. At 26 h, the Ad-TK-hSSTr2 injected tumors (n = 8, mean weight = 0.08g) accumulated 11.1 ± 2.9% ID/g for ^{99m}Tc-P2045 and 1.6 ± 0.4% ID/g for ^{131}I-FIAU, by gamma counter analyses. Left Group A tumors accumulated 3.7 ± 1.3% ID/g for ^{131}I-FIAU, while left Group B tumors accumulated 9.0 ± 2.5% ID/g for ^{99m}Tc-P2045. At that time, the left Group A and B tumors (negative controls, n = 4/group) averaged 0.3 ± 0.1% ID/g for both ^{99m}Tc-P2045 and ^{131}I-FIAU. Gamma counter and ROI analyses were in agreement for the levels of tumor uptake for the radiotracers. The tumor uptake values for the two radiotracers were positively correlated (r^2 = 0.80).

In conclusion, the ^{99m}Tc-P2045 showed 7-fold greater accumulation in Ad-TK-hSSTr2 injected tumors as compared with ^{131}I-FIAU at 26 h. The rapid blood clearance and high retention of

^{99m}Tc -P2045 in Ad-TK-hSSTr2-injected tumors offers great potential for this agent to image expression of the hSSTr2 reporter gene. Since ^{99m}Tc-P2045 was linearly correlated with ^{131}I-FIAU uptake, the ^{99m}Tc-P2045 imaging provides a convenient assessment of TK gene transfer. Imaging hSSTr2 expression with ^{99m}Tc-P2045 is thus a highly sensitive procedure for detecting Ad-mediated gene transfer of both the reporter and therapeutic genes.

In vivo imaging was also done on intraperitoneal ovarian tumors. Three mice having SKOV3.ip1 tumors were utilized. One group was injected with Ad-hSSTr2 vector 48 hours before the injection of a radiotracer, and the other received no Ad vector. Both groups were imaged 5 h after injection of the radiotracer, (*e.g.* ^{99m}Tc-P2045). Figure 32A shows the imaging obtained on the non-Ad group, while Figure 32B shows the Ad-treated group. Images of mice bearing SKOV3.ip1 tumors (injected previously *i.p.* with Ad-hSSTr2) showed uptake of ^{99m}Tc-P2045 at locations of the tumors.

EXAMPLE 21

Plate Imaging of ^{125}I-FIAU Internal Binding Using TK Gene Driven by Cox-2 Promoter

Ad-Cox2L-TK vector was used in this study. MKN-28 cell line (permissive for Cox-2 expression) and KATO-3 cell line (negative for Cox-2 expression) were used for the plate imaging. Uninfected cells (no Ad) were controls. Internal binding of ^{125}I-FIAU was imaged according to the method described above. Figure 33A shows the initial images of ^{125}I-FIAU in both MKN-28

and KATO-3 cells, while Figure 33B shows the final images of ^{125}I-FIAU, which was taken after 1 hr incubation.

MKN-28 cells infected 48 h earlier with Ad-Cox-2-TK showed increased specific internal binding of ^{125}I-FIAU relative to uninfected cells. Such binding was specific since it was inhibited with excess unlabeled FIAU.

EXAMPLE 22

Imaging hSSTr2 Reporter Gene Transfer Using the HSV

Herpes virus encoding hSSTr2 was used to infect A427 cells. ^{99m}Tc-P2045 was used to monitor the expression of hSSTr2 following gene transfer. 48 hours later, the internalization of ^{99m}Tc-P2045 was imaged. Excess P2045 was used to show the specificity. Two sets of triplicates were tested in a 12-well plate. The initial and final images are shown in Figures 34A and 34B.

A427 cells infected with the Herpes virus encoding hSSTr2 showed increased specific internal binding of ^{99m}Tc-P2045, relative to no internal binding with uninfected cells. Such binding was specific since it was inhibited with excess unlabeled P2045.

EXAMPLE 23

Imaging hSSTr2 Reporter Gene Transfer Using Ad-hSSTr2 and ^{188}Re-P2045

Ad-hSSTr2 vector was used to infect A427 cells. The infected cells were undergone 100, 75, 50 and 25% positive cell dilution. ^{188}Re-P2045 was used to monitor the expression of hSSTr2 following gene transfer (_-shield was required on collimator). 48 hours later, the internalization of ^{188}Re-P2045 was

imaged. Excess P2045 was used to show the specificity. The initial and final images are shown in Figures 35A and 35B.

It shows that internal binding of Re-188 can be imaged in spite of a low abundant gamma-ray emission and _-emission. A427 cells infected with the Ad virus encoding hSSTr2 showed increased specific internal binding of ^{188}Re-P2045, relative to no internal binding with uninfected cells. Such binding was specific since it was inhibited with excess unlabeled P2045.

Discussion

^{64}Cu is a positron emitter which can be detected by positron emission tomography (PET). Such detection is very sensitive with high resolution. A mouse is imaged with a subcutaneous SKOV3.ip1 ovarian tumor or A427 lung tumor following intratumoral injection of AdCMVhSSTR2 and intravenous injection of ^{64}Cu-TETA-octreotide. Other possible radioisotopes used for imaging are ^{99m}Tc, ^{111}In, ^{124}I, ^{18}F, ^{123}I, ^{11}C, ^{131}I, ^{67}Cu, ^{211}At, ^{177}Lu, ^{186}Re, ^{212}Bi, ^{47}Sc, ^{105}Rh, ^{109}Pd, ^{153}Sm, ^{188}Re, ^{198}Au, ^{199}Au, ^{75}Br, ^{76}Br, ^{77}Br, ^{13}N, ^{34m}Cl, ^{38}Cl, ^{52m}Mn, ^{55}Co, ^{62}Cu, ^{68}Ga, ^{72}As, ^{76}As, ^{72}Se, ^{73}Se, ^{75}Se and ^{94m}Tc. Besides ^{64}Cu, radioisotopes ^{32}P, ^{90}Y, ^{125}I, ^{212}Pb, ^{213}Bi, ^{111}In, ^{123}I, ^{131}I, ^{67}Cu, ^{211}At, ^{177}Lu, ^{186}Re, ^{175}Yb, ^{212}Bi, ^{47}Sc, ^{105}Rh, ^{109}Pd, ^{153}Sm, ^{188}Re, ^{198}Au, ^{199}Au and ^{77}Br may also be used for therapy. Some of the radioisotopes can be detected by PET or single photon emission computed tomography (SPECT). Others can be detected by planar imaging.

The demonstration of enhanced binding/gene transfer to ovarian and lung cancer cells *in vitro* would warrant their evaluation in stringent models relevant to human diseases. In this

regard, a number of adenoviral-vector based strategies for carcinoma of the ovary were developed and an orthotopic human/murine xenograft model for the analysis of the therapeutic efficacy of these approaches was employed (41-42). The present invention provides the herpes simplex virus thymidine kinase (HSV-TK) gene and cytosine deaminase (CD) gene as examples of the therapeutic agents. Adenovirus vectors were derived encoding the tumor cell targeting motifs within the HI loop, as well as isogenic controls.

As adenoviral vectors were developed to target ovarian cancer and lung cancer specifically, they were utilized for the experiments to develop and validate the technology for *in vivo* gene transfer imaging. These measures would provide a bridge to the phase I clinical testing of this gene transfer system in humans.

Advances in clinical oncology have been made utilizing clinical trial methodology to incorporate novel therapeutics into clinical practice. The majority of clinical protocols have investigated various traditional cancer therapies (surgery, pharmacologic agents, and radiation). The presently disclosed gene transfer imaging system will be investigated in phase I/II trial in the context of human ovarian cancer.

The following references were cited herein:

1. Kaminski, M.S., *et al.*, *N. Engl. J. Med.*, 329:459-465, 1993.
2. Press, O.W., *et al.*, *N. Engl. J. Med.*, 329:1219-1224, 1993.
3. Goldenberg, D., *et al.*, *Semin. Cancer Biol.*, 1:217-225, 1990.
4. Blumenthal, R.D., *et al.*, *Int. J. Cancer*, 52:1-7, 1992.
5. Buchsbaum, D.J., *et al.*, *Med. Phys.*, 20:551-567, 1993.

6. Buchsbaum, D., *In:* D. Goldenberg (ed.), Cancer Therapy with Radiolabeled Antibodies, 115-140, Boca Raton: CRC Press, 1995.

7. Wahl, R.L., *Cancer*, 73:989-992, 1994.

8. Buchsbaum, D., *Antibody, Immunoconj. Radiopharm.*, 4:693-701,1991.

9. Scheinberg, *et al., Cancer Res.* (Suppl) 50:962s-963s, 1990.

10. Meredith, R.F., *et al., J. Nucl. Med.*, 35:1017-1022, 1994.

11. Welt, S., *et al., J. Clin. Oncol.*, 12:1561-1571, 1994.

12. Goldenberg, D.M., *Am. J. Med.*, 94:297-312, 1993.

13. Meredith, R.F., *et al., J. Nucl. Med.* 35:1017, 1994.

14. Divgi, C., *et al., J. Nucl. Med.* 36:586, 1995.

15. Kvols, L.K., *et al., N. Engl. J. Med.*, 315:663, 1986.

16. Fischman, A.J., *et al., J. Nucl. Med.*, 34:2253-2263, 1993.

17. Buchegger, F., *et al., J. Nucl. Med.*, 31, 1035, 1990.

18. Sharkey, R.M., *et al., J. Natl. Cancer Inst.*, 83, 627, 1991.

19. Yokota, T., *et al., Cancer Res.*, 52, 3402, 1992.

20. Bender, H., *et al., Cancer Res.*, 52, 121, 1992.

21. Colapinto, E.V., *et al., Cancer Res.*, 50, 1822, 1990.

22. Milenic, D.E., *et al., Cancer Res.*, 51, 6363, 1991.

23. Rowlinson, G., *et al., Cancer Res.*, 47, 6528, 1987.

24. Stewart, J., *et al., Int. J. Radiat. Oncol. Biol.*, 16, 405, 1989.

25. Zalutsky, M.R., *et al., Cancer Res.*, 50, 4105, 1990.

26. Kozak, R.W., *et al., Cancer Res.*, 49, 2639, 1989.

27. Quadri, S.M., *et al., J. Nucl. Med.*, 34:938-945, 1993.

28. Greiner, J.W., *et al., Cancer Res.*, 53, 600, 1993.

29. Kuhn, J.A., *et al., Cancer Res.*, 51, 2335, 1991.

30. Shrivastav *et al., Int. J. Radiat. Oncol. Biol.*, 16, 721, 1989.

31. Msirikale, *et al., Int. J. Radiat. Oncol. Biol..,* 13, 1839, 1987.

32. Kalofonos, H., *et al., Cancer Res.,* 50, 159, 1990.

33. Blumenthal, R.D., *et al., Cancer Res.,* 48, 5403, 1988.

34. Blumenthal, R.D., *et al., J. Natl. Cancer Inst.,* 84, 399, 1992.

35. Morton, B.A., *et al., Cancer Res.* (Suppl.), 50, 1008s, 1990.

36. Invitrogen Corp., Carlsbad, CA.

37. Becker, T.C., *et al., Methods. Cell. Biol.,* 43:161, 1994.

38. Alemany, R., *et al., J. Virol. Methods,* 68: 147, 1997,

39. Koller, K.J., *et al., Anal. Biochem.,* 250:51, 1997.

40. He, T-C. *et al., Proc. Natl. Acad. Sci. USA* 95, 2509-2514, 1998.

41. Deshane, J., *et al., Gynecol. Oncol,* 64:378, 1997.

42. Rosenfeld, M.E., *et al., J. Mol. Med.,* 74: 455, 1996.

43. Anderson, C. J., *et al., J. Nucl. Med., 36:* 2315-2325, 1995.

44. Rogers, *Clin. Cancer Res., 3:* 383-393, 1999.

45. Kury FD, *et al.,Oncogene,* 5:1403-1408, 1990.

46. Ring CJA, *et al., Gene Ther,* 3:1094-1103, 1996.

47. Stolz B, *et al., Eur J Nucl Med 25:* 668-674, 1998.

48. Rosch F, *et al., Eur J Nucl Med 26:* 358-366, 1999.

49. Anderson CJ, *et al., J Nucl Med 39:* 1944-1951, 1998.

50. Graham FL, *et al., J Gen Virol* 1977;36:59-74.

51. He T, *et al., Proc Natl Acad Sci USA* 1998;95:2509-14.

Any patents or publications mentioned in this specification are indicative of the levels of those skilled in the art to which the invention pertains. These patents and publications are herein incorporated by reference to the same extent as if each individual publication was specifically and individually indicated to be incorporated by reference.

One skilled in the art will readily appreciate that the present invention is well adapted to carry out the objects and obtain the ends and advantages mentioned, as well as those inherent therein. The present examples along with the methods, procedures, treatments, molecules, and specific compounds described herein are presently representative of preferred embodiments, are exemplary, and are not intended as limitations on the scope of the invention. Changes therein and other uses will occur to those skilled in the art which are encompassed within the spirit of the invention as defined by the scope of the claims.

WHAT IS CLAIMED IS:

1. A method for monitoring therapeutic gene transfer and expression into a subject, comprising the steps of:

administering to said subject a vector encoding at least one therapeutic gene and a gene for a membrane expressed targeting molecule, wherein both said genes are capable of being expressed in said subject;

administering a radiolabeled ligand to said subject, wherein said ligand has a high affinity for said membrane expressed targeting molecule; and

imaging said subject by detecting the binding of said radiolabeled ligand with said membrane expressed targeting molecule, wherein said binding is directly proportional to the transfer and expression of said therapeutic gene into said subject.

2. The method of claim 1, wherein said membrane expressed targeting molecule is an antigen, a receptor or modification thereof.

3. The method of claim 2, wherein said receptor is selected from the group consisting of human somatostatin subtype 2 receptor, gastrin releasing peptide receptor, vasoactive intestinal peptide receptor and dopamine receptor.

4. The method of claim 1, wherein said ligand is an antibody, a peptide, a drug, a growth factor, a hormone, a vitamin, or a protein.

5. The method of claim 1, wherein said therapeutic gene is selected from the group consisting of herpes simplex virus thymidine kinase, cytosine deaminase, p53, p16, bax, tumor antigens, antiangiogenesis molecules, pro-angiogenesis molecules, pro-apoptosis molecules, anti-apoptosis molecules, platelet factor-4, soluble Flt-1, angiopoietin-2, thrombospondin-1, angiostatin, endostatin, Fas, FasLigand, cytokines, GM-CSF, IL-2, IL-4, IL-6, IL-7, IL-12, TNF-α and interferon.

6. The method of claim 1, wherein said vector is selected from the group consisting of an adenoviral vector, a retroviral vector, an adeno-associated viral vector, herpes simplex viral vector, vaccinia virus vector, a liposome, plasmid DNA and a synthetic vector.

7. The method of claim 1, wherein said ligand is labeled by radioisotopes selected from the group consisting of ^{99m}Tc, ^{111}In, ^{124}I, ^{18}F, ^{64}Cu, ^{123}I, ^{11}C, ^{131}I, ^{67}Cu, ^{211}At, ^{177}Lu, ^{186}Re, ^{212}Bi, ^{47}Sc, ^{105}Rh, ^{109}Pd, ^{153}Sm, ^{188}Re, ^{198}Au, ^{199}Au, ^{75}Br, ^{76}Br, ^{77}Br, ^{13}N, ^{34m}Cl, ^{38}Cl, ^{52m}Mn, ^{55}Co, ^{62}Cu, ^{68}Ga, ^{72}As, ^{76}As, ^{72}Se, ^{73}Se, ^{75}Se and ^{94m}Tc.

8. A recombinant adenoviral vector encoding at least one therapeutic gene and a gene for a membrane expressed targeting molecule.

9. The recombinant adenoviral vector of claim 8, wherein said membrane expressed targeting molecule is human somatostatin subtype 2 receptor or a modification thereof.

10. The recombinant adenoviral vector of claim 9, wherein the gene for said human somatostatin subtype 2 receptor is tagged with the HA sequence at the N-terminus.

11. The recombinant adenoviral vector of claim 8, wherein said adenoviral vector is further tropism-modified by incorporating the tumor cell targeting motifs in the HI loop of adenovirus fiber protein.

12. The recombinant adenoviral vector of claim 8, wherein said therapeutic gene is selected from the group consisting of herpes simplex virus thymidine kinase, cytosine deaminase, p53, p16, bax, tumor antigens, antiangiogenesis molecules, pro-angiogenesis molecules, pro-apoptosis molecules, anti-apoptosis molecules, platelet factor-4, soluble Flt-1, angiopoietin-2, thrombospondin-1, angiostatin, endostatin, Fas, FasLigand, cytokines, GM-CSF, IL-2, IL-4, IL-6, IL-7, IL-12, TNF-α and interferon.

13. A method of treating an individual having a tumor, comprising the step of:

administering to said individual the recombinant adenoviral vector of claim 8.

14. The method of claim 13, wherein said tumor is selected from the group consisting of ovarian tumor, colon tumor, lung tumor, pancreatic tumor, prostate tumor, breast tumor, head and neck tumor, and glioma tumor.

15. The method of claim 13, wherein said vector is administered systemically or locally.

16. The method of claim 13, wherein said vector is administered by direct injection or via intraperitoneal injection.

17. The method of claim 13, further comprising the step of: administering to said individual with 5-fluorocytosine.

18. The method of claim 13, further comprising the step of: administering to said individual with ganciclovir.

19. The method of claim 13, further comprising the step of: administering to said individual with a radiolabeled peptide, wherein said peptide has a high affinity for a membrane expressed targeting molecule.

20. The method of claim 19, wherein said peptide is labeled by radioisotopes selected from the group consisting of ^{32}P, ^{90}Y, ^{125}I, ^{212}Pb, ^{213}Bi, ^{111}In, ^{64}Cu, ^{123}I, ^{131}I, ^{67}Cu, ^{211}At, ^{177}Lu, ^{186}Re, ^{212}Bi, ^{47}Sc, ^{105}Rh, ^{109}Pd, ^{153}Sm, ^{188}Re, ^{175}Yb, ^{198}Au, ^{199}Au and ^{77}Br.

21. A method for controlling expression of a reporter gene and/or a therapeutic gene transferred to a target cell, comprising the steps of:

placing said reporter gene and/or therapeutic gene under control of a tissue-specific promoter and/or an inducible promoter or fragments thereof; and

expressing said reporter gene and/or therapeutic gene in said target cell, wherein the expression of said reporter gene and/or therapeutic gene is controlled by said promoter(s) or fragments.

22. The method of claim 21, wherein said tissue-specific promoter is selected from the group consisting of a prostate specific antigen promoter, a carcinoembryonic antigen promoter, erbB-2 promoter, MUC1 promoter, insulin promoter, alpha fetoprotein promoter, E2F promoter, myosin light chain 2 promoter, Cox-2 promoter, oligodendrocyte-specific and myelin basic protein promoter.

23. The method of claim 21, wherein said inducible promoter is selected from the group consisting of tetracycline-inducible promoter and multidrug resistance gene promoter.

24. The method of claim 21, wherein said fragments are cis-acting control sequences.

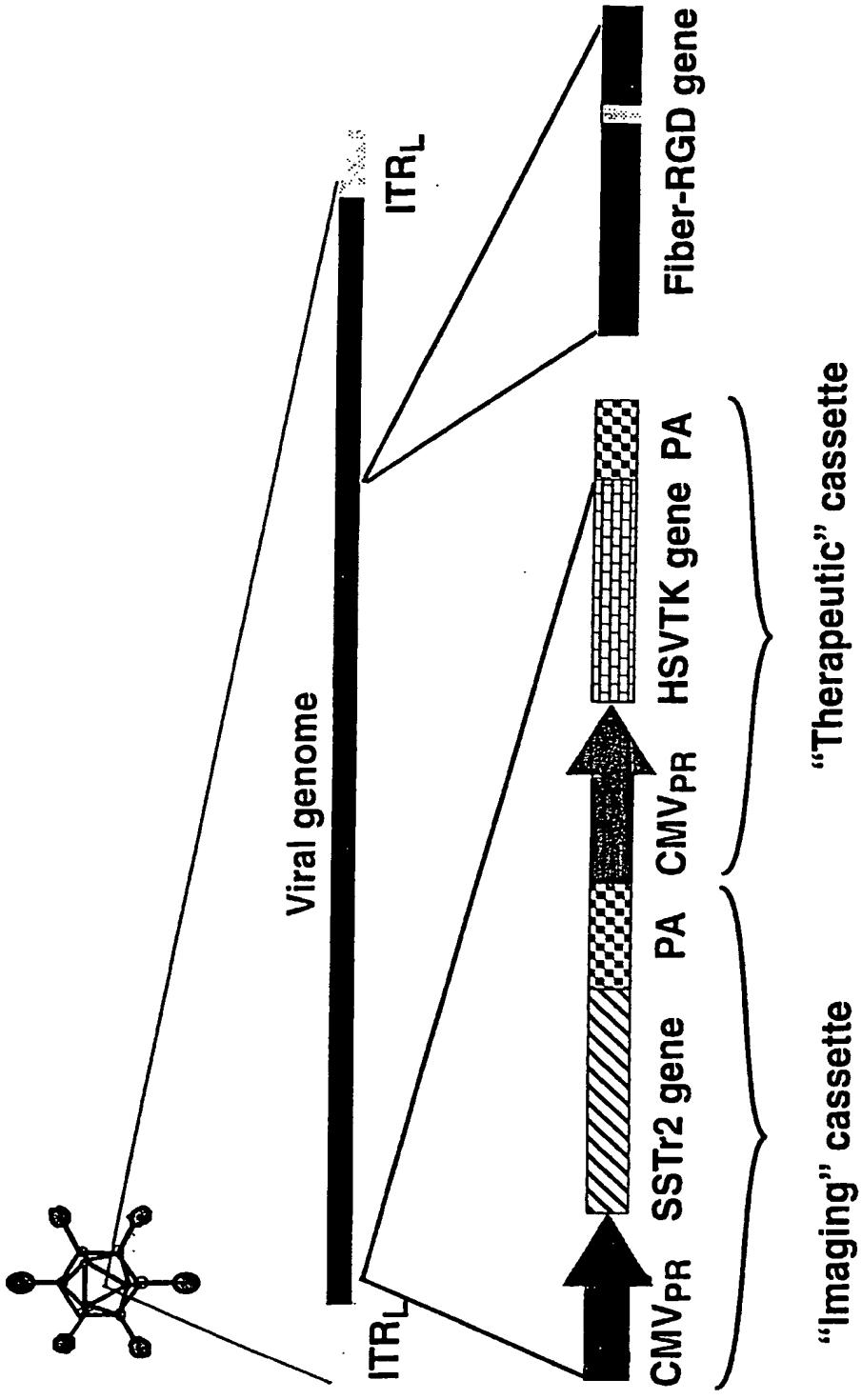
Fiber-RGD gene
ITR$_L$
Viral genome
HSVTK gene PA
CMV$_{PR}$
"Therapeutic" cassette
SSTr2 gene PA
CMV$_{PR}$
"Imaging" cassette
ITR$_L$

Fig. 1

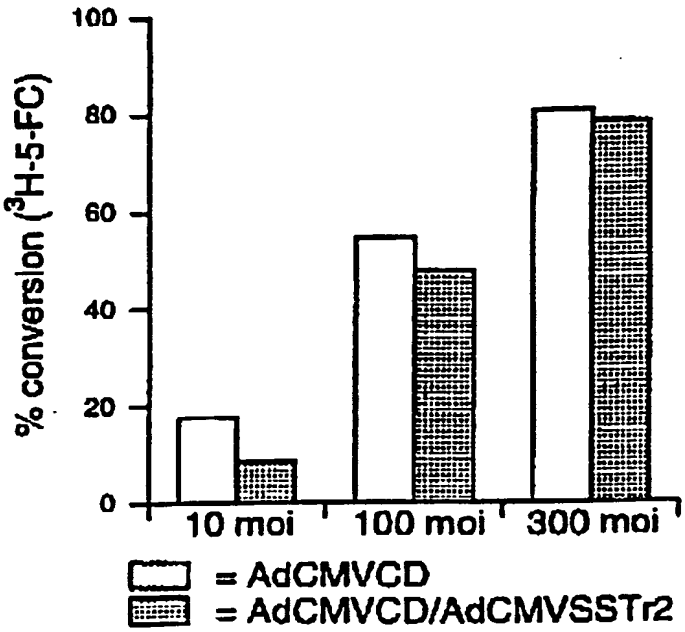
100
80
60
40
20
0
% conversion (^{3}H-5-FC)
10 moi
100 moi
300 moi
= AdCMVCD
= AdCMVCD/AdCMVSSTr2

Fig. 2A

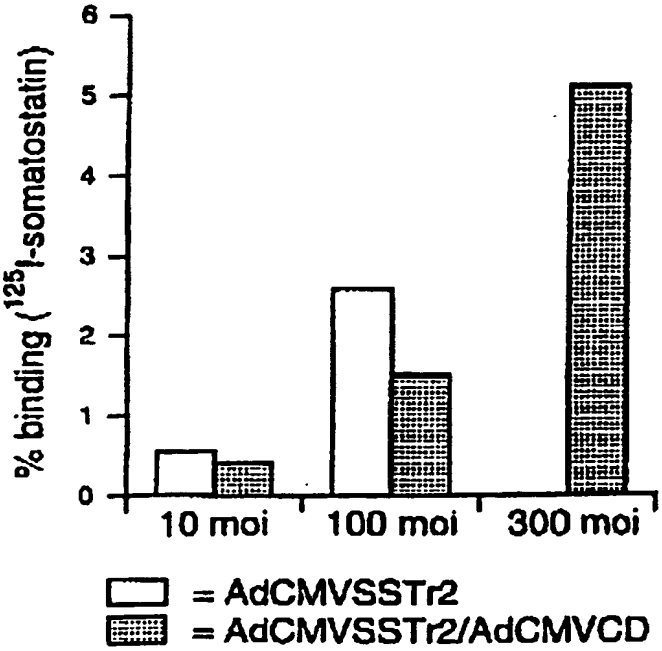
6
5
4
3
2
1
0
% binding (^{125}I-somatostatin)
10 moi
100 moi
300 moi
= AdCMVSSTr2
= AdCMVSSTr2/AdCMVCD

Fig. 2B

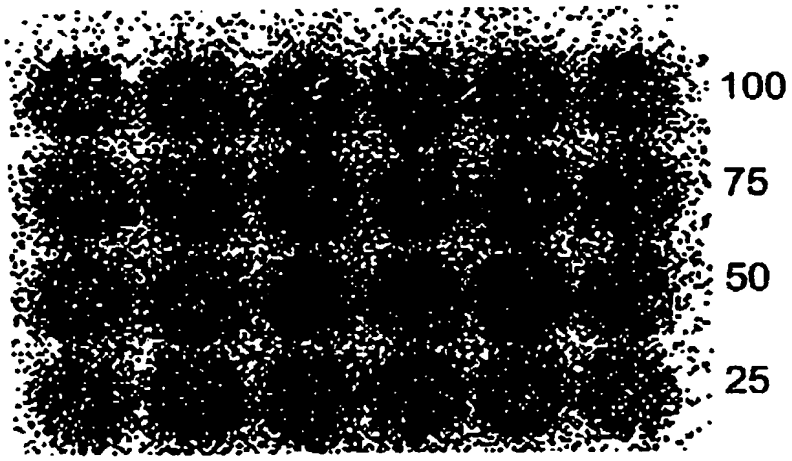

Fig. 3A

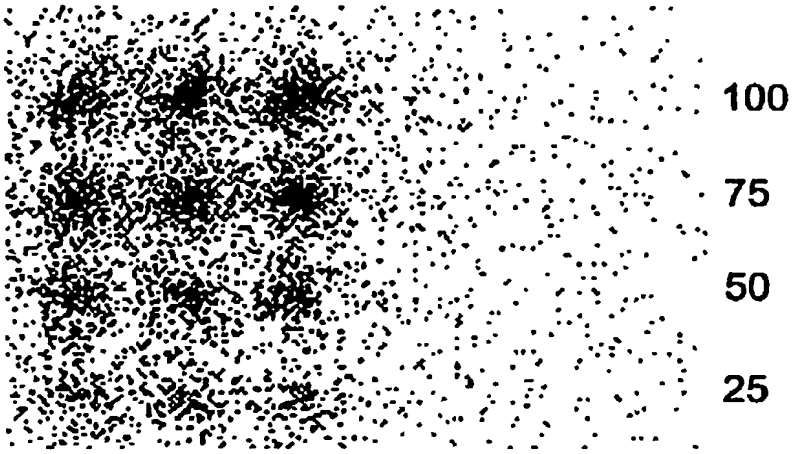

Fig. 3B

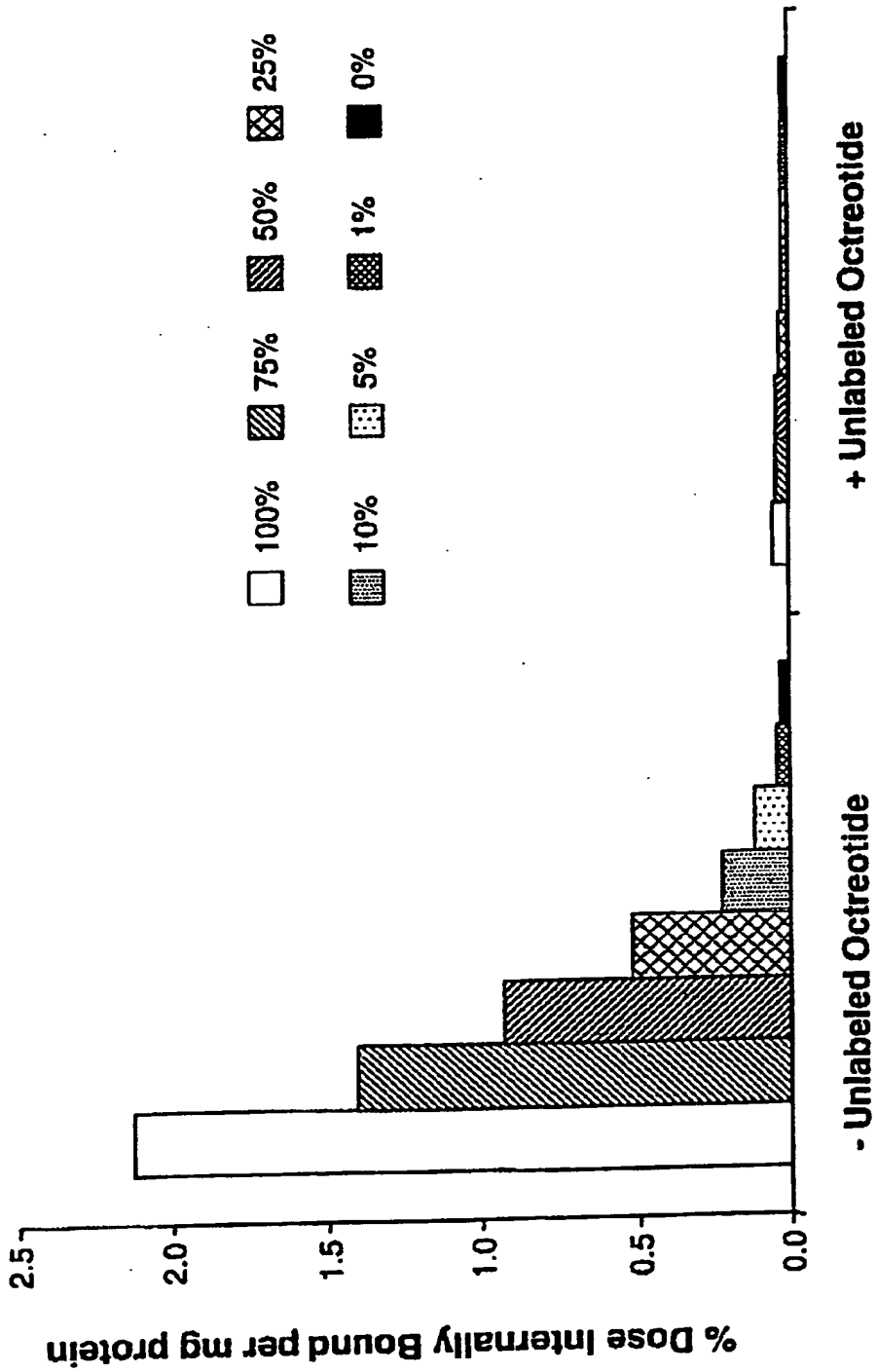
% Dose Internally Bound per mg protein
2.5
2.0
1.5
1.0
0.5
0.0
100%
75%
50%
25%
10%
5%
1%
0%
- Unlabeled Octreotide
+ Unlabeled Octreotide

Fig. 3C

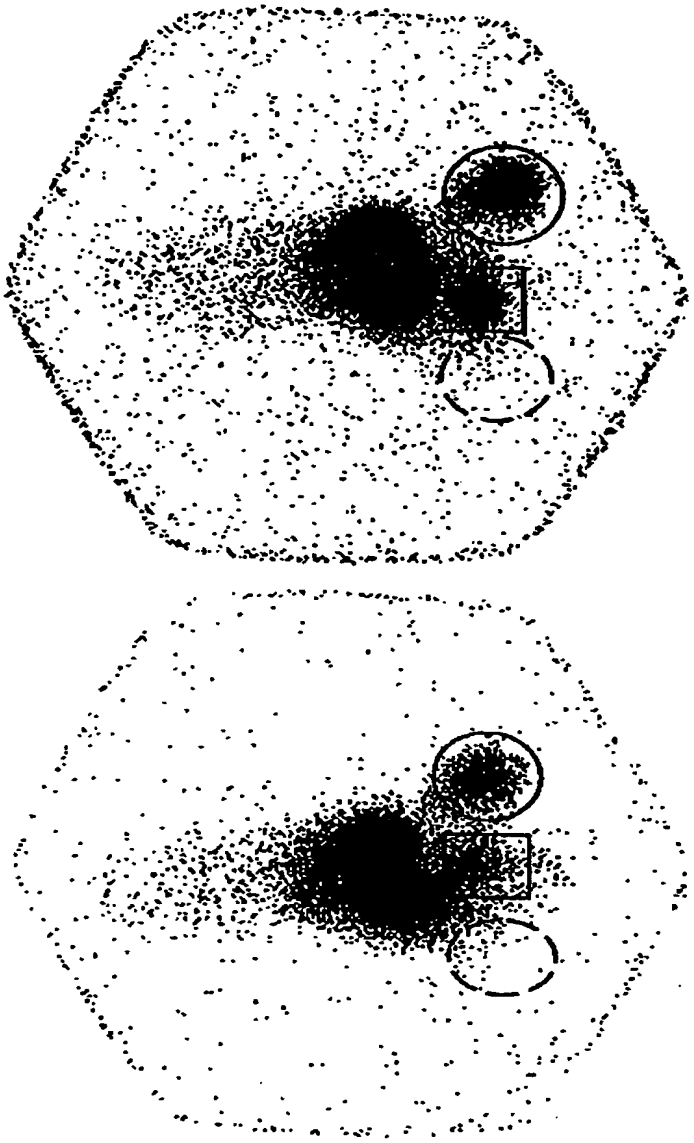

Fig. 4B

Fig. 4A

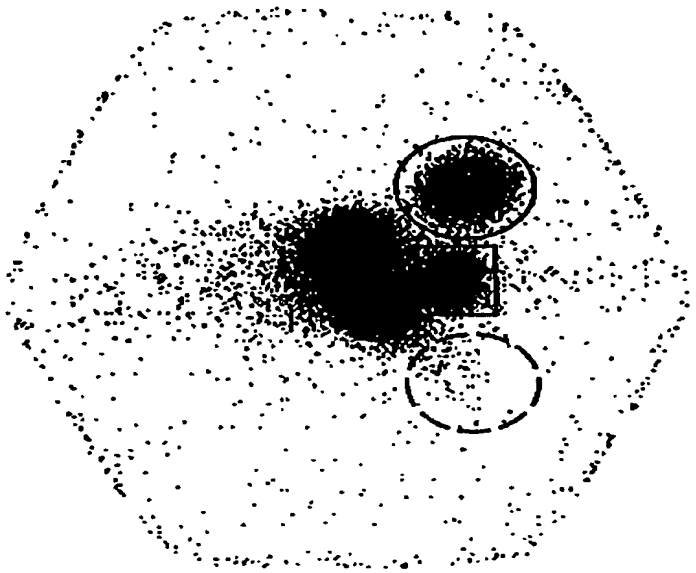

Fig. 4D

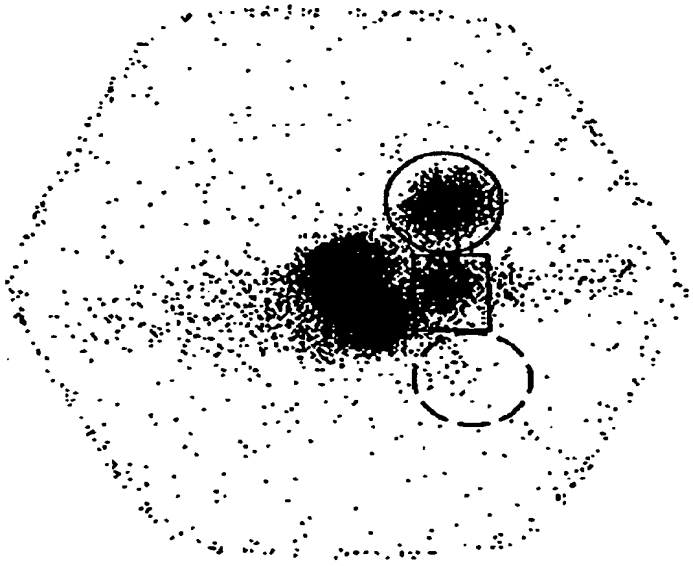

Fig. 4C

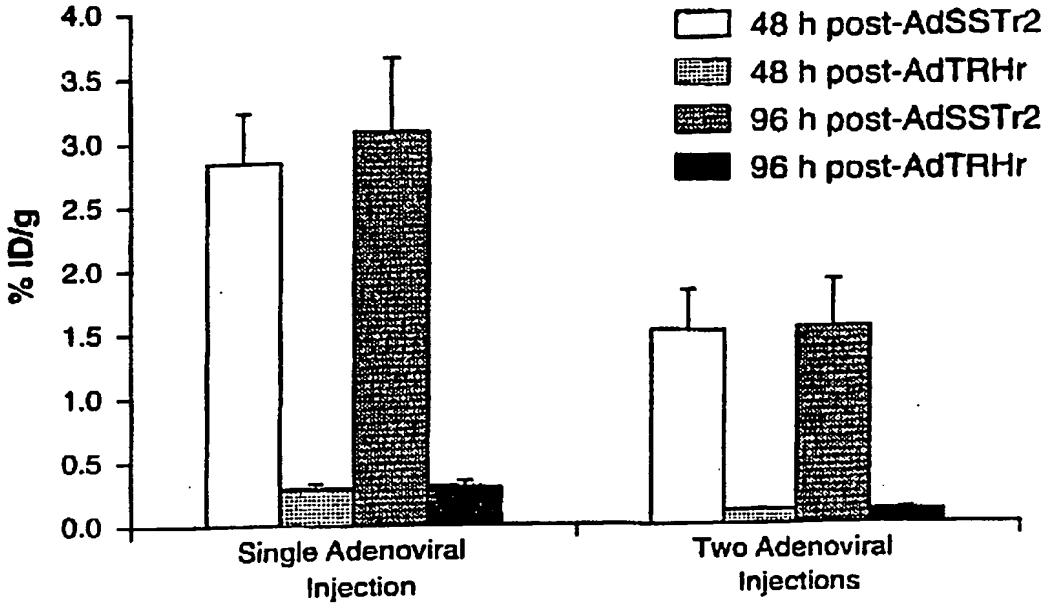
4.0
3.5
3.0
2.5
2.0
1.5
1.0
0.5
0.0
% ID/g
48 h post-AdSSTr2
48 h post-AdTRHr
96 h post-AdSSTr2
96 h post-AdTRHr
Single Adenoviral Injection
Two Adenoviral Injections

Fig. 5A

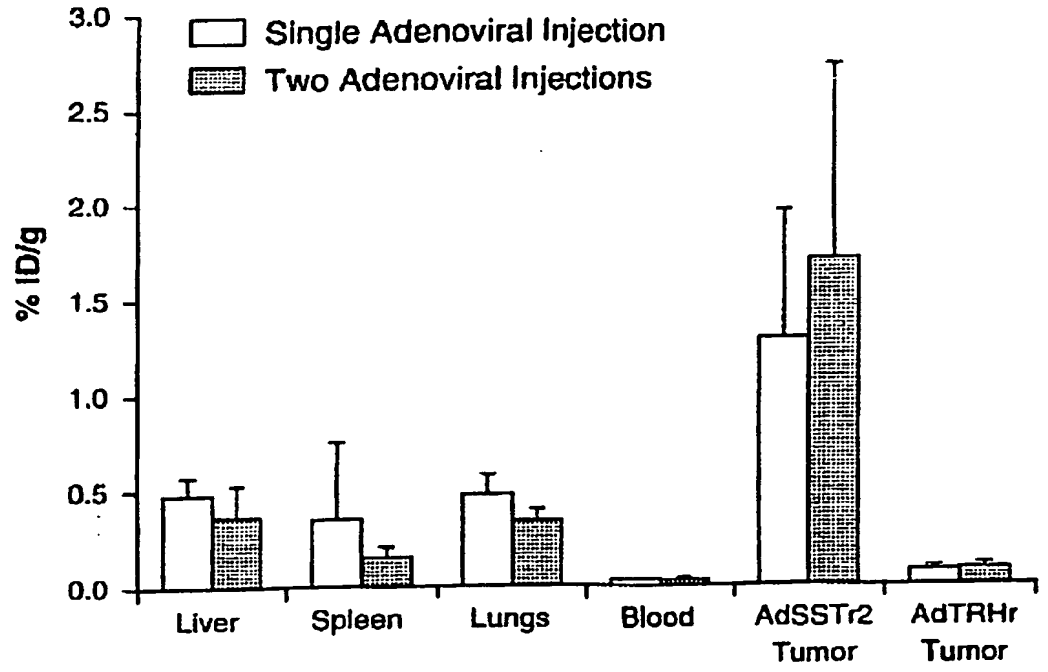
3.0
2.5
2.0
1.5
1.0
0.5
0.0
% ID/g
Single Adenoviral Injection
Two Adenoviral Injections
Liver
Spleen
Lungs
Blood
AdSSTr2 Tumor
AdTRHr Tumor
Tissue

Fig. 5B

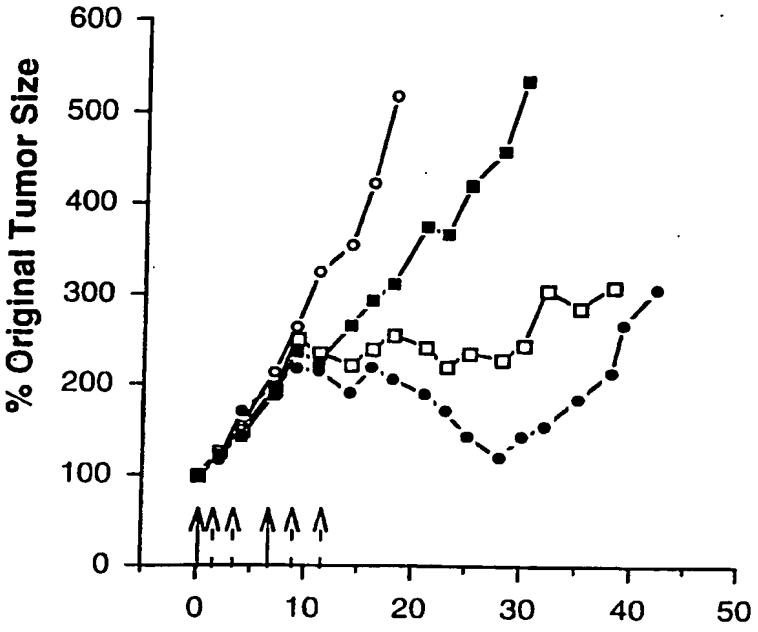
% Original Tumor Size
600
500
400
300
200
100
0
0
10
20
30
40
50

Fig. 6A

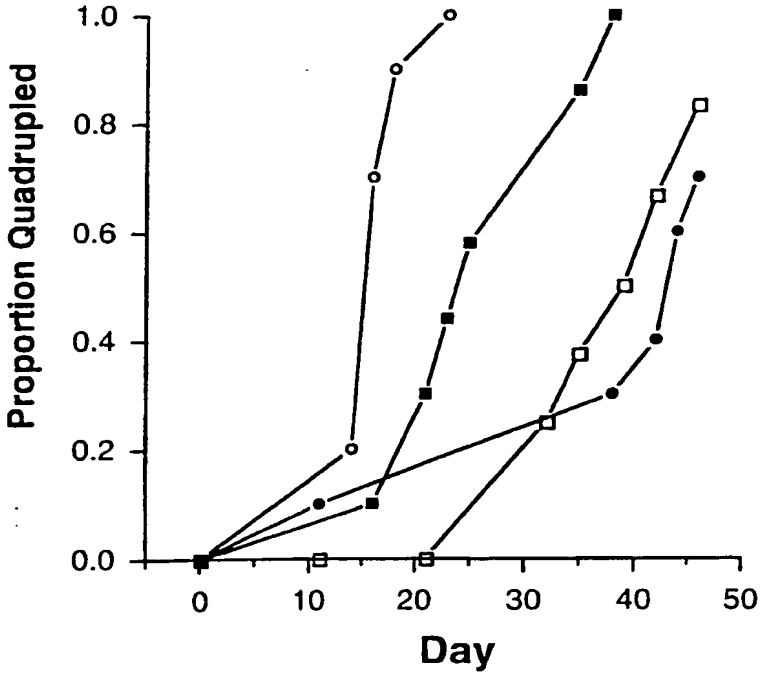
Proportion Quadrupled
1.0
0.8
0.6
0.4
0.2
0.0
0
10
20
30
40
50
Day

Fig. 6B

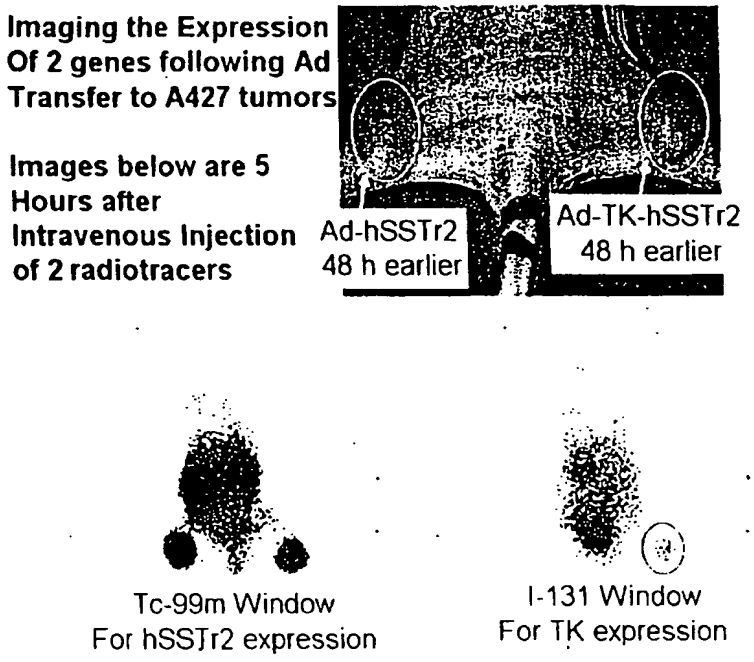
Imaging the Expression
Of 2 genes following Ad
Transfer to A427 tumors
Images below are 5
Hours after
Intravenous Injection
of 2 radiotracers
Ad-hSSTr2
48 h earlier
Ad-TK-hSSTr2
48 h earlier
Tc-99m Window
For hSSTr2 expression
I-131 Window
For TK expression

Fig. 7A

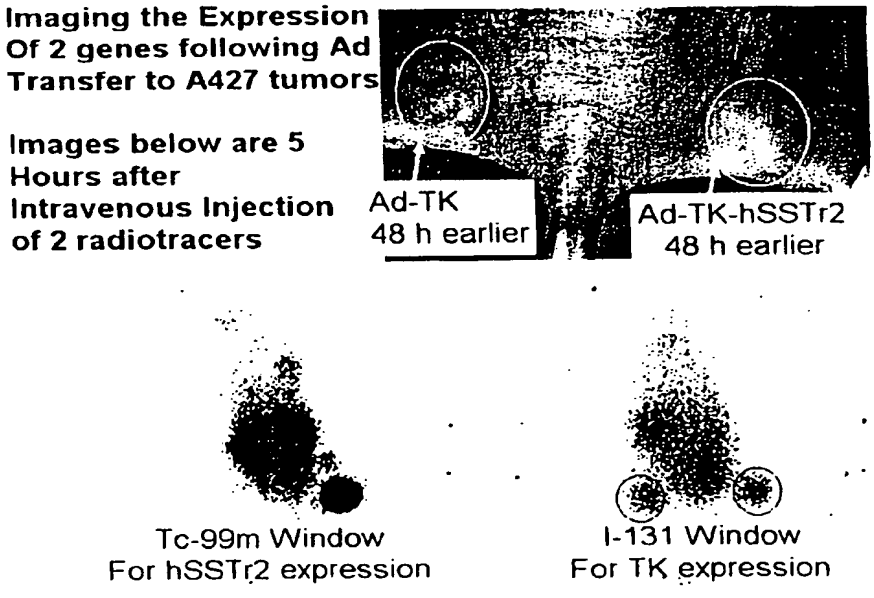
Imaging the Expression
Of 2 genes following Ad
Transfer to A427 tumors
Images below are 5
Hours after
Intravenous Injection
of 2 radiotracers
Ad-TK
48 h earlier
Ad-TK-hSSTr2
48 h earlier
Tc-99m Window
For hSSTr2 expression
I-131 Window
For TK expression

Fig. 7B

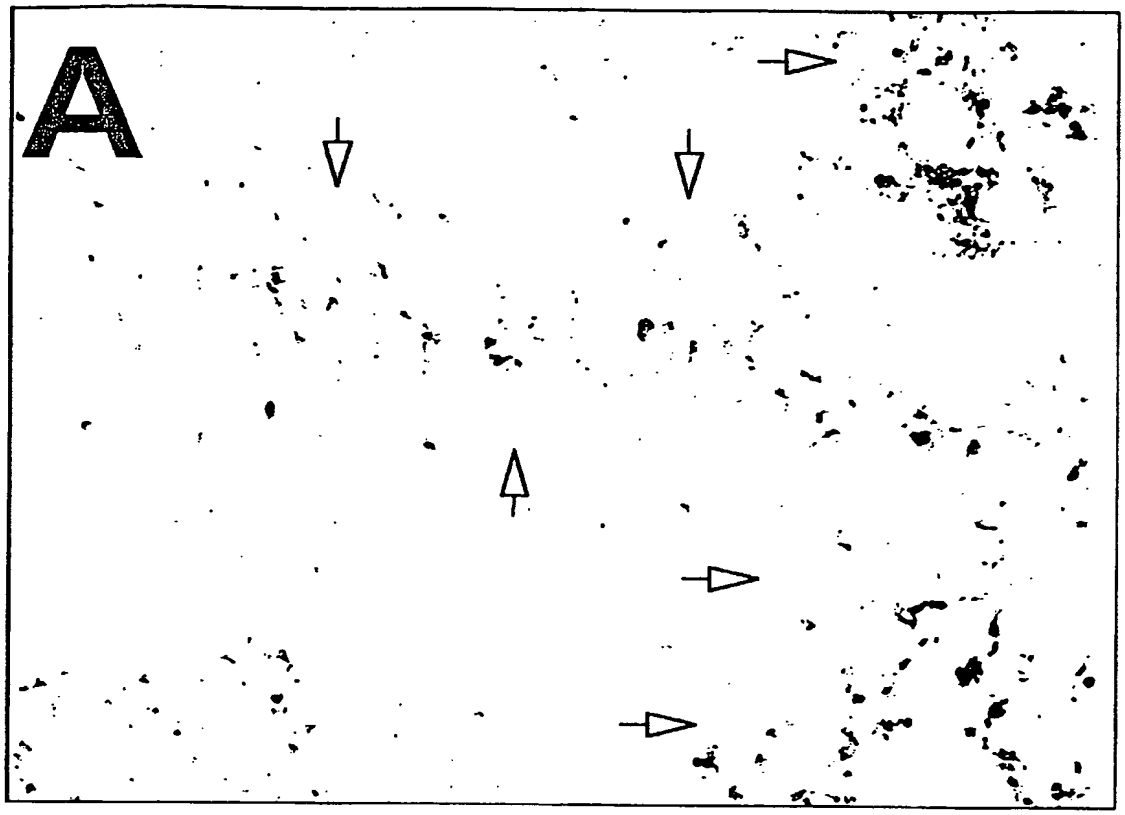

Fig. 8A

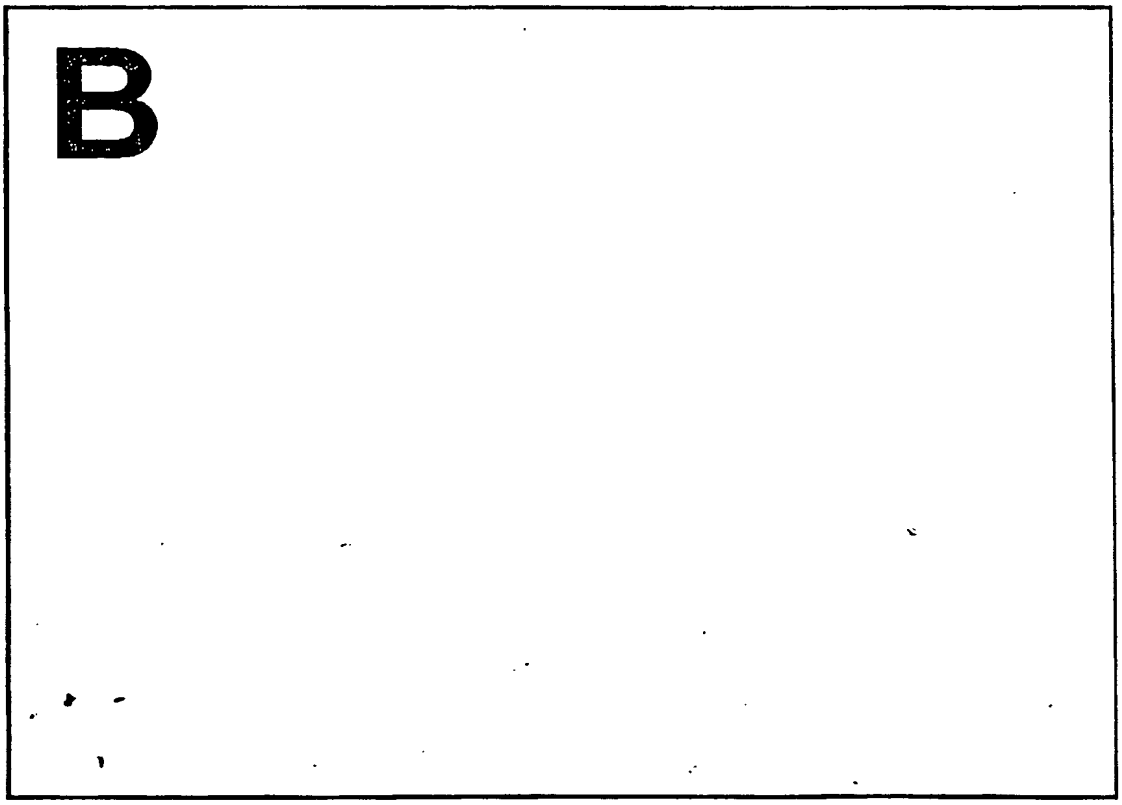

Fig. 8B

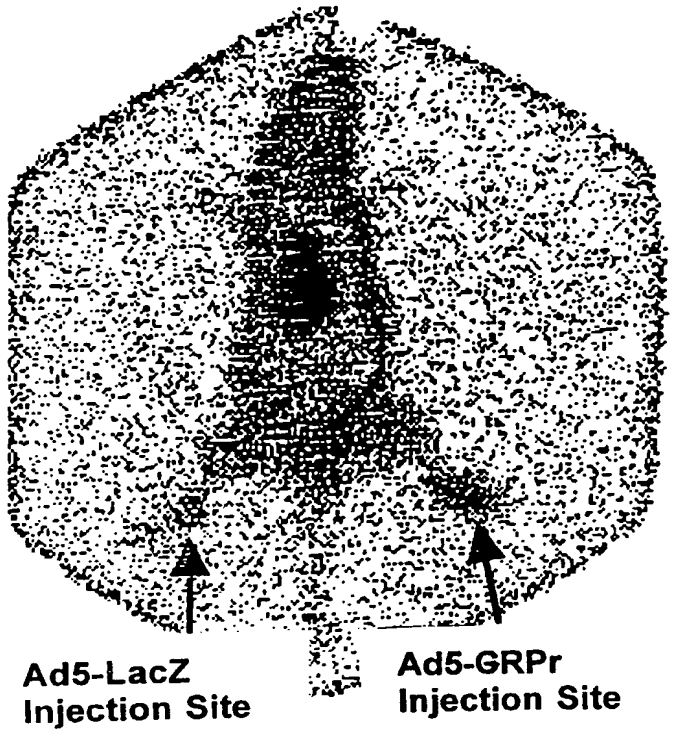
Ad5-LacZ
Injection Site
Ad5-GRPr
Injection Site

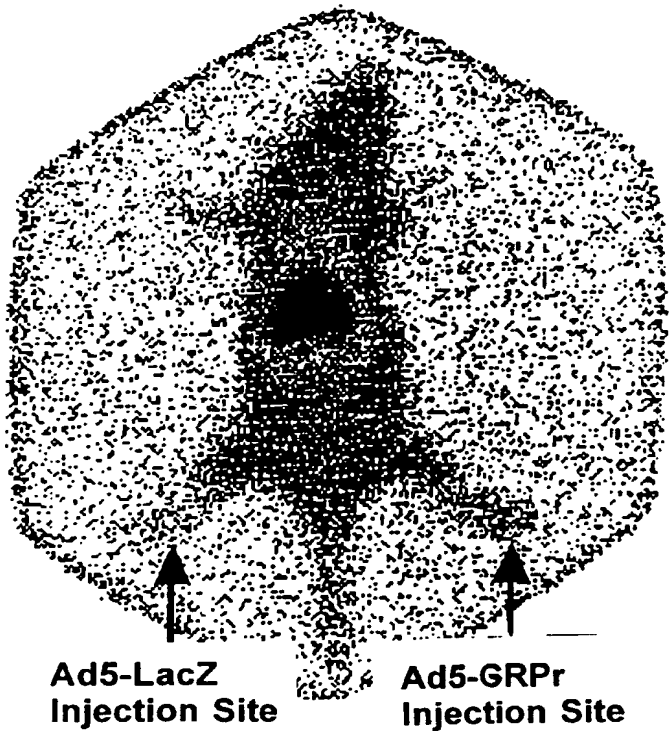
Ad5-LacZ
Injection Site
Ad5-GRPr
Injection Site

Fig. 9A

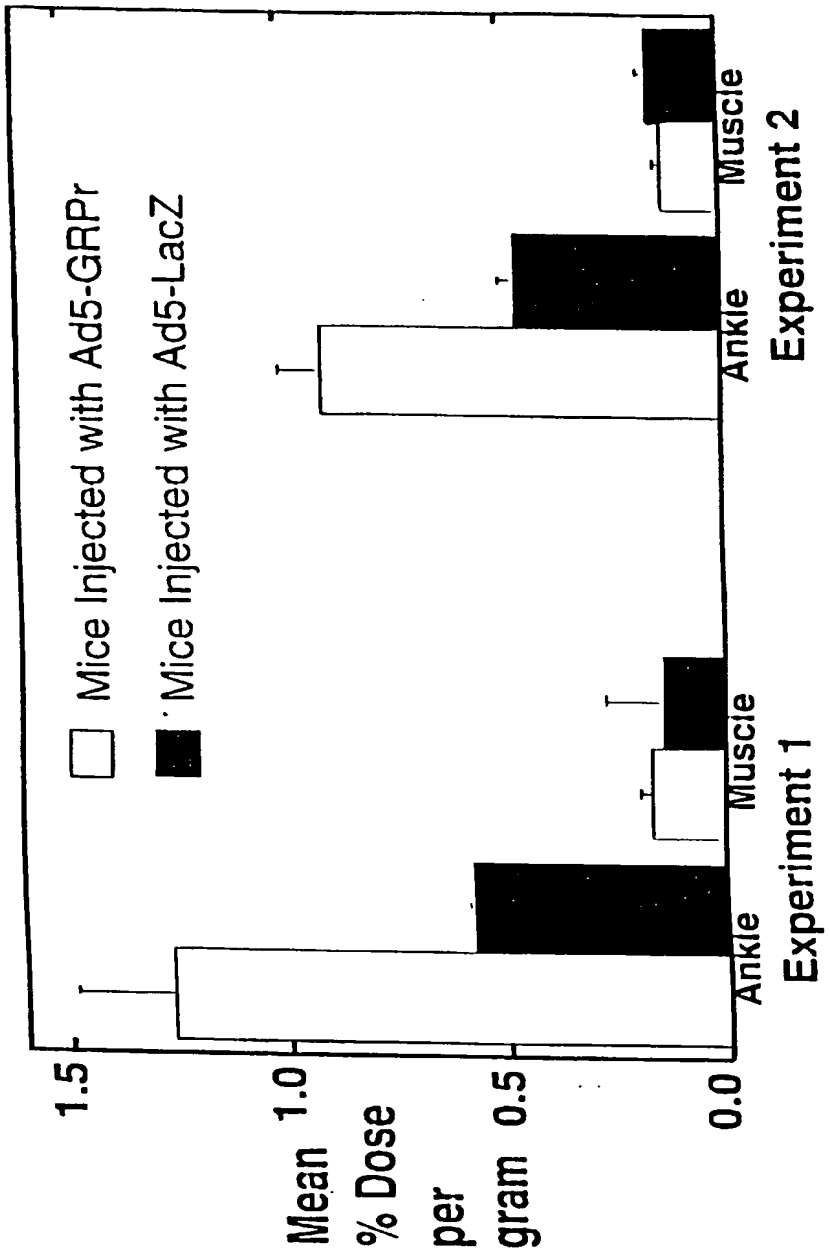
Mice Injected with Ad5-GRPr
Mice Injected with Ad5-LacZ
Mean % Dose per gram
1.5
1.0
0.5
0.0
Ankle
Muscle
Experiment 1
Ankle
Muscle
Experiment 2

Fig. 9B

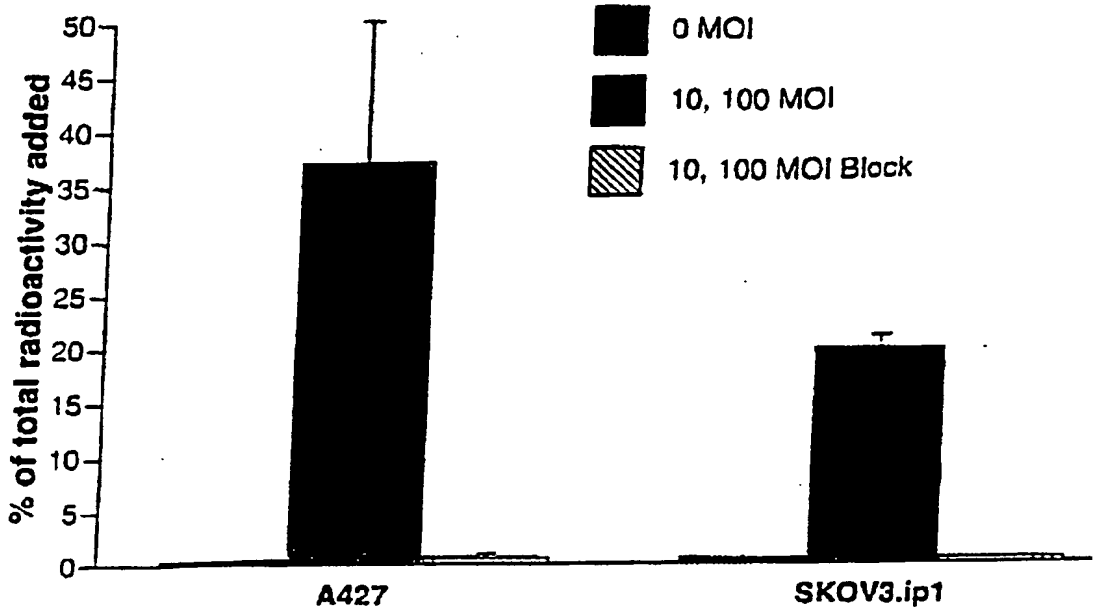
% of total radioactivity added
50
45
40
35
30
25
20
15
10
5
0
0 MOI
10, 100 MOI
10, 100 MOI Block
A427
SKOV3.ip1

Fig. 10

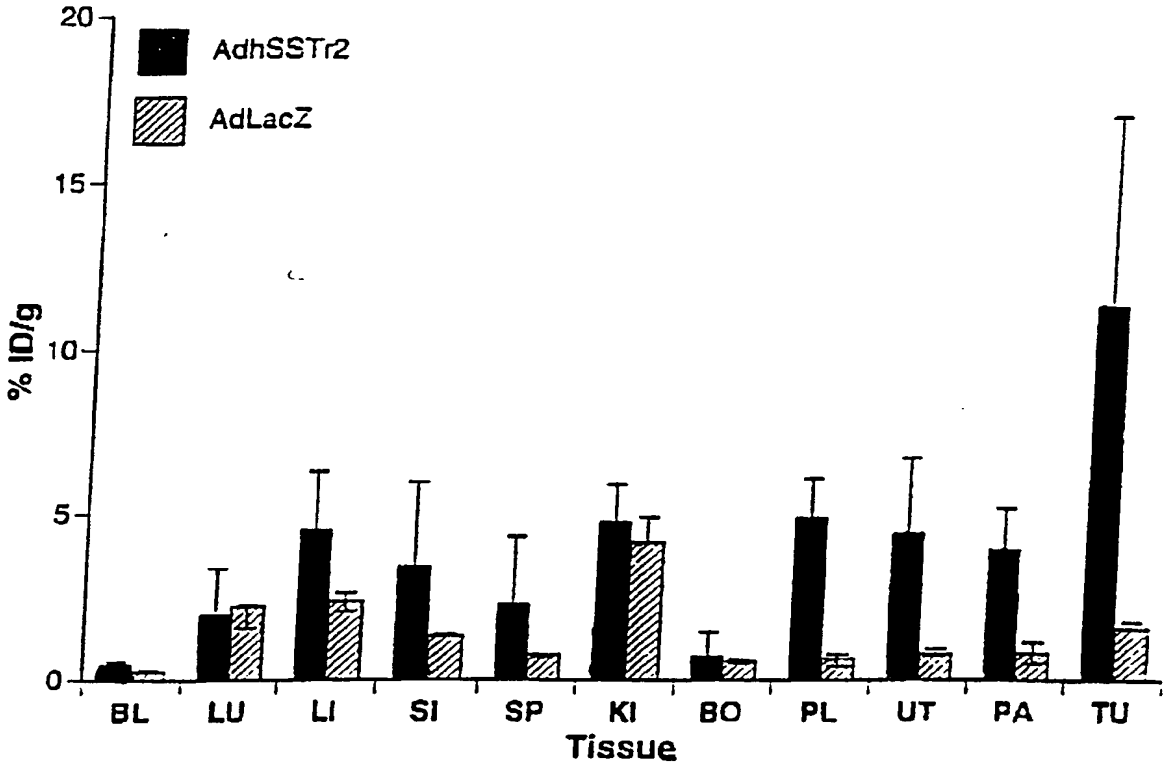
% ID/g
20
15
10
5
0
AdhSSTr2
AdLacZ
BL
LU
LI
SI
SP
KI
BO
PL
UT
PA
TU
Tissue

Fig. 11

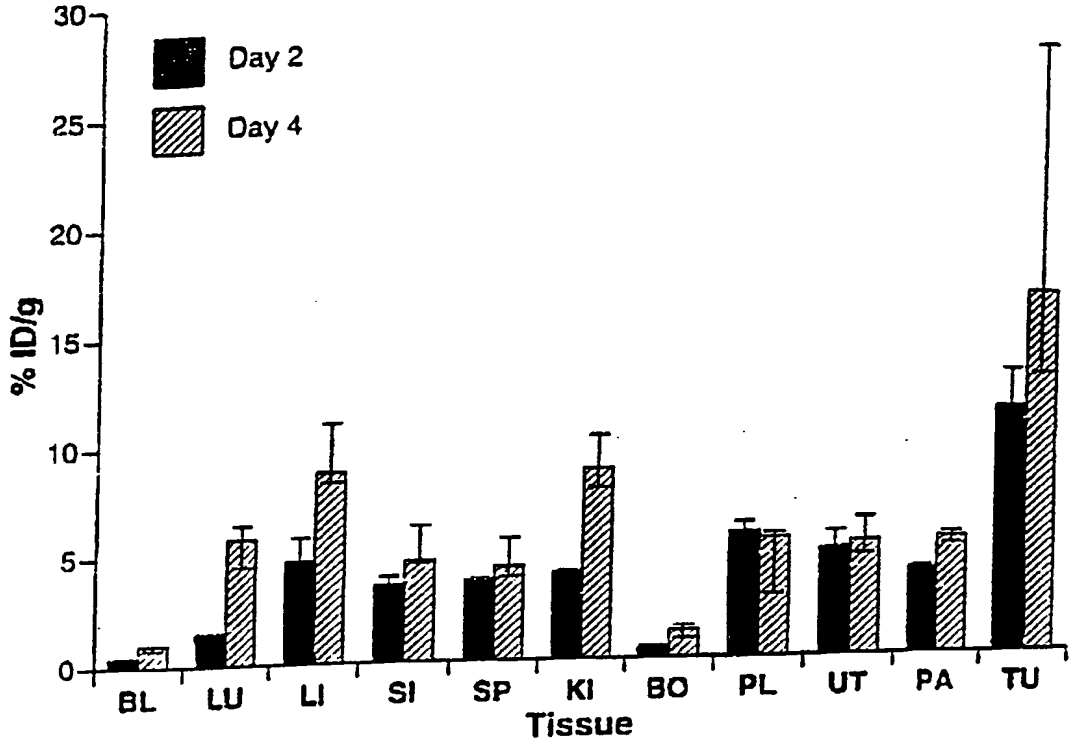
30
25
20
15
10
5
0
% ID/g
Day 2
Day 4
BL
LU
LI
SI
SP
KI
BO
PL
UT
PA
TU
Tissue

Fig. 12

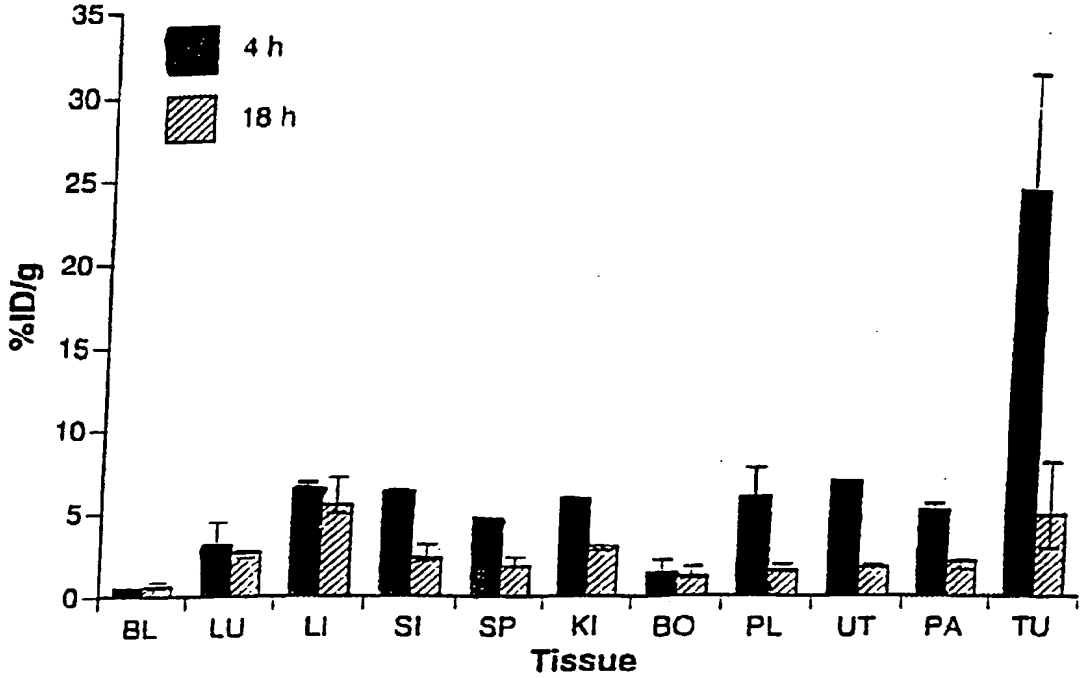
35
30
25
20
15
10
5
0
%ID/g
4 h
18 h
BL
LU
LI
SI
SP
KI
BO
PL
UT
PA
TU
Tissue

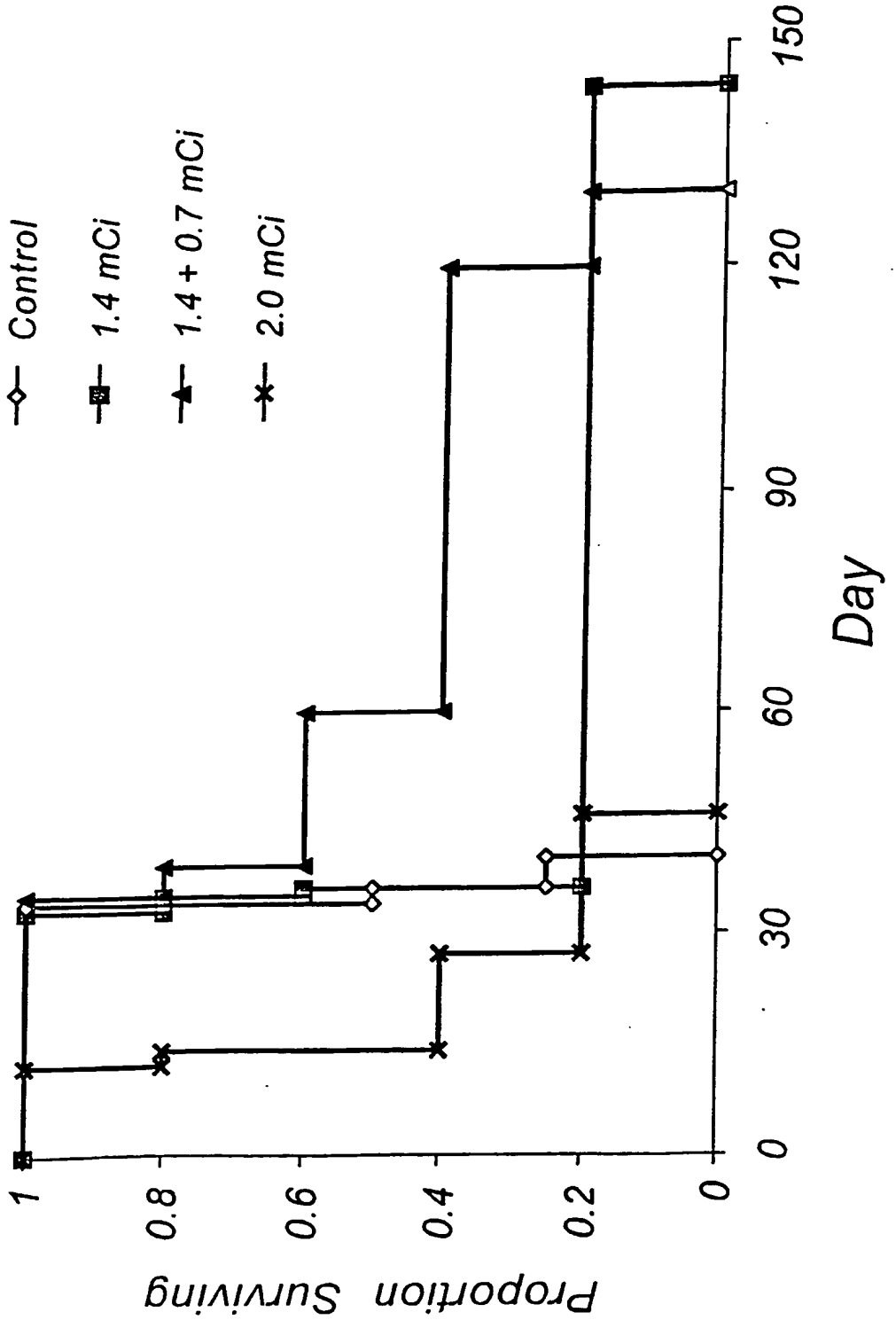
Control
1.4 mCi
1.4 + 0.7 mCi
2.0 mCi
Proportion Surviving
1
0.8
0.6
0.4
0.2
0
0
30
60
90
120
150
Day

Fig. 14

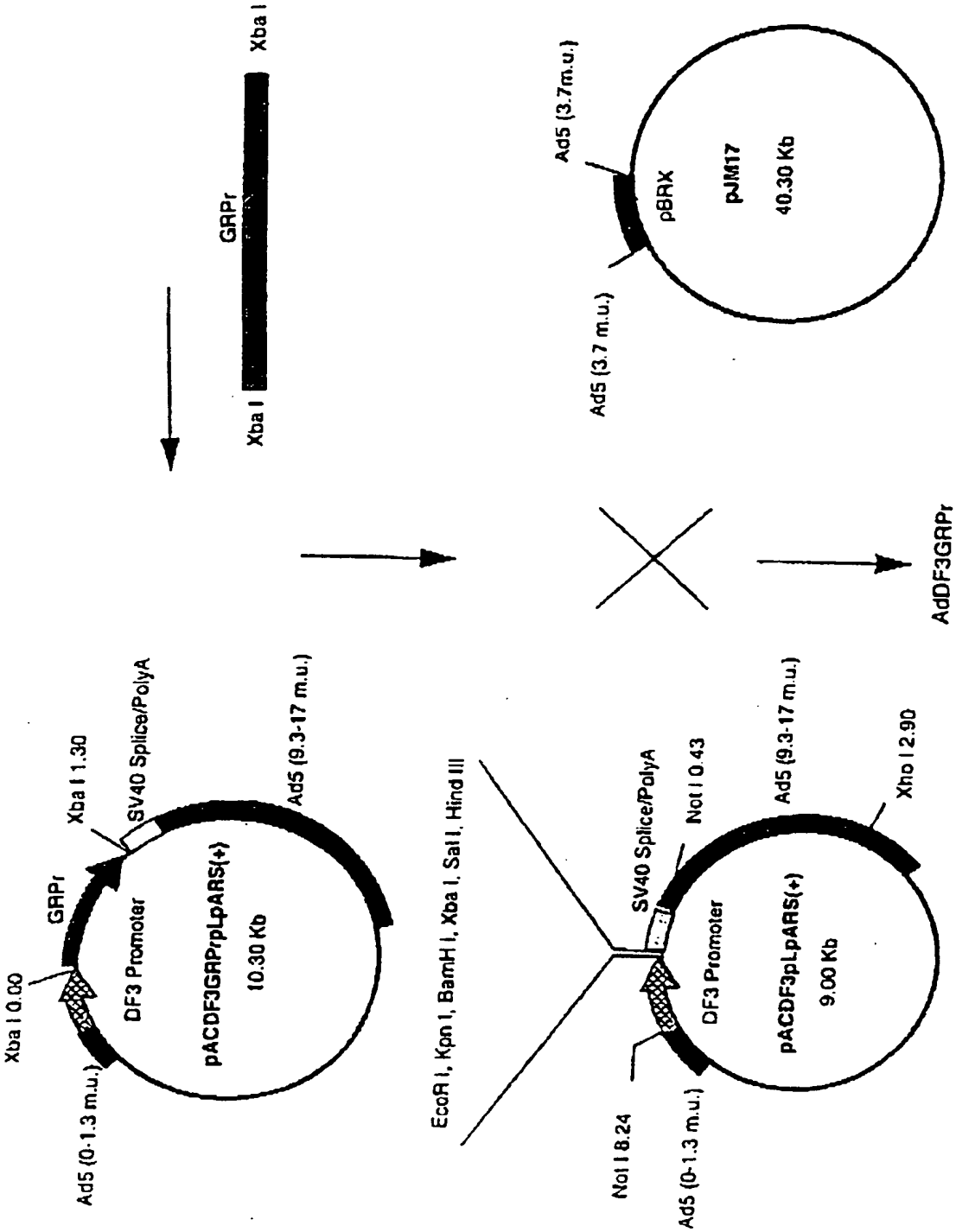
Xba I
GRPr
Xba I
Ad5 (3.7m.u.)
pBRX
pJM17
40.30 Kb
Ad5 (3.7 m.u.)
Xba I 0.00
GRPr
Xba I 1.30
SV40 Splice/PolyA
Ad5 (9.3-17 m.u.)
DF3 Promoter
pACDF3GRPrpLpARS(+)
10.30 Kb
Ad5 (0-1.3 m.u.)
EcoR I, Kpn I, BamH I, Xba I, Sal I, Hind III
SV40 Splice/PolyA
Not I 0.43
Ad5 (9.3-17 m.u.)
Xho I 2.90
DF3 Promoter
pACDF3pLpARS(+)
9.00 Kb
Not I 8.24
Ad5 (0-1.3 m.u.)
AdDF3GRPr

Fig. 15

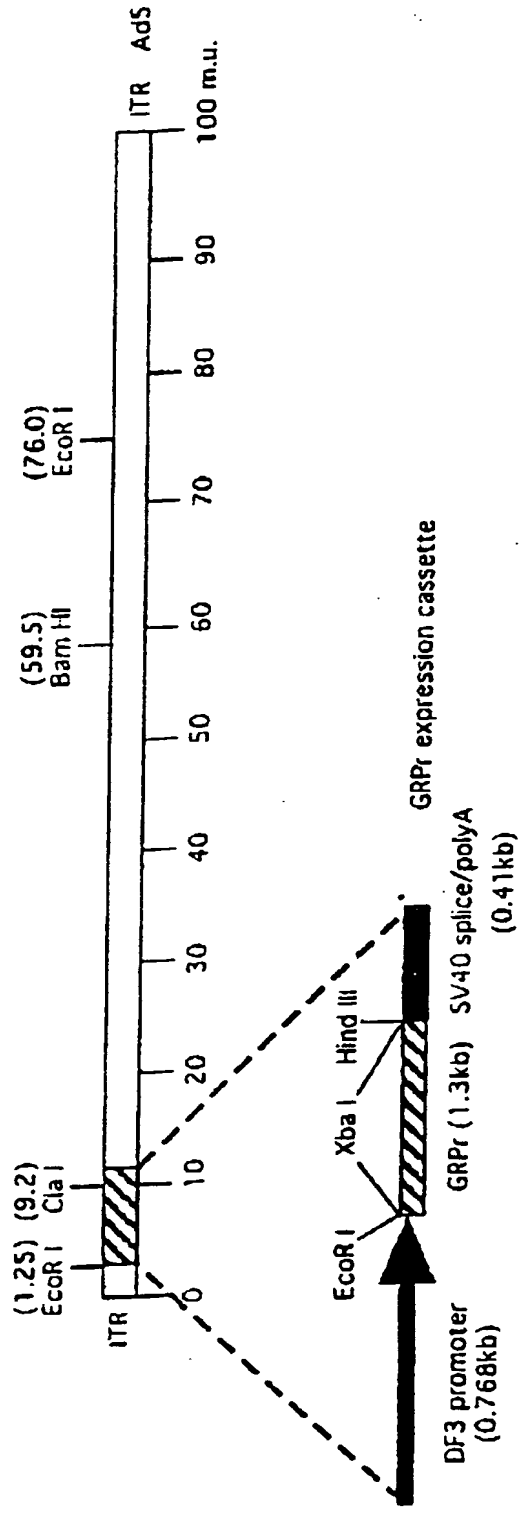
ITR
Ad5
100 m.u.
90
80
70
60
50
40
30
20
10
0
(76.0)
EcoR I
(59.5)
Bam HI
(9.2)
Cla I
(1.25)
EcoR I
ITR
GRPr expression cassette
SV40 splice/polyA
(0.41kb)
GRPr (1.3kb)
Hind III
Xba I
EcoR I
DF3 promoter
(0.768kb)

Fig. 16A

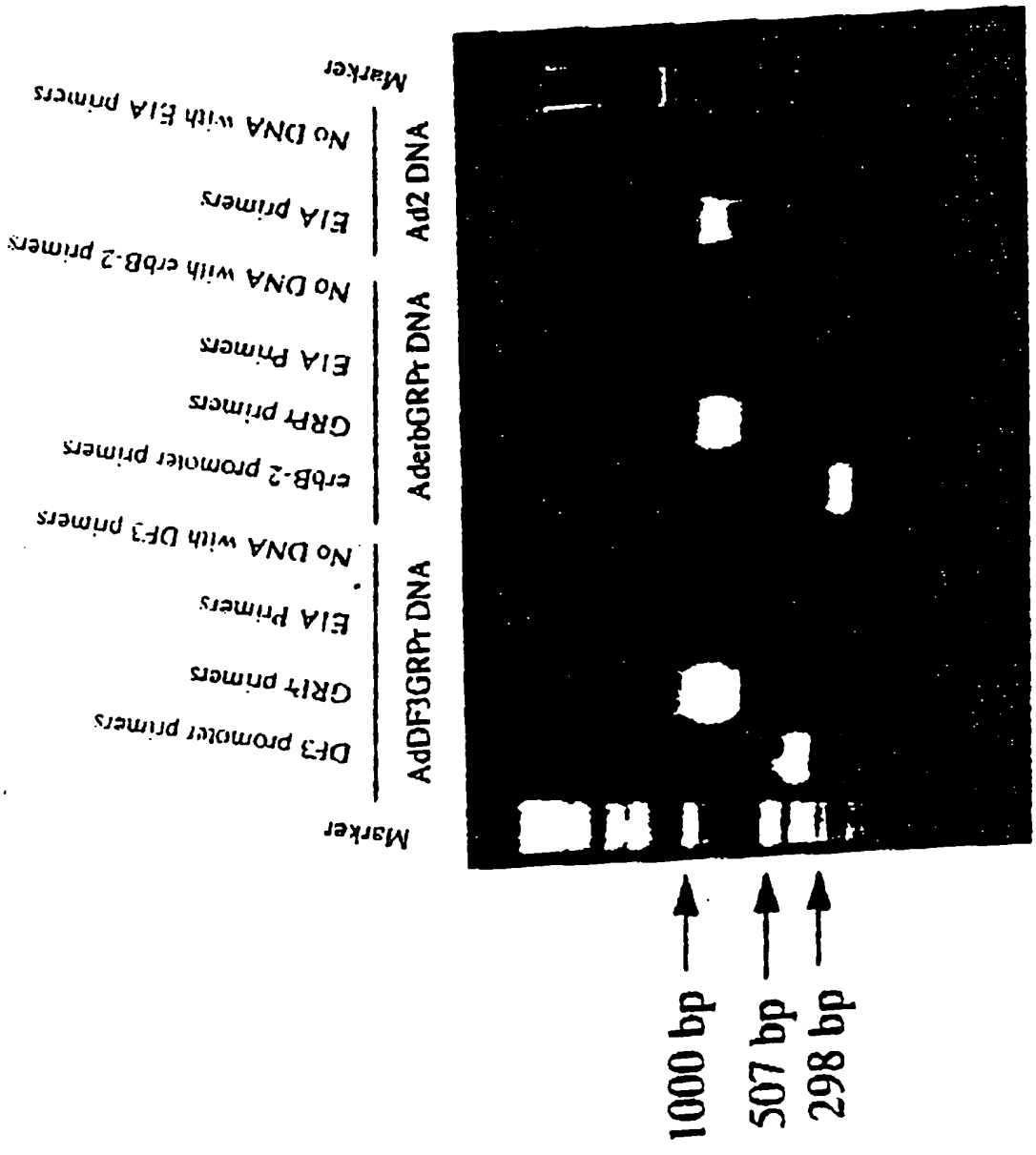
Marker
AdDF3GRPr DNA
DF3 promoter primers
GRPr primers
EIA Primers
No DNA with DF3 primers
AdeibGRPr DNA
erbB-2 promoter primers
GRPr primers
EIA Primers
No DNA with erbB-2 primers
Ad2 DNA
EIA primers
No DNA with EIA primers
Marker
1000 bp
507 bp
298 bp

Fig. 16B

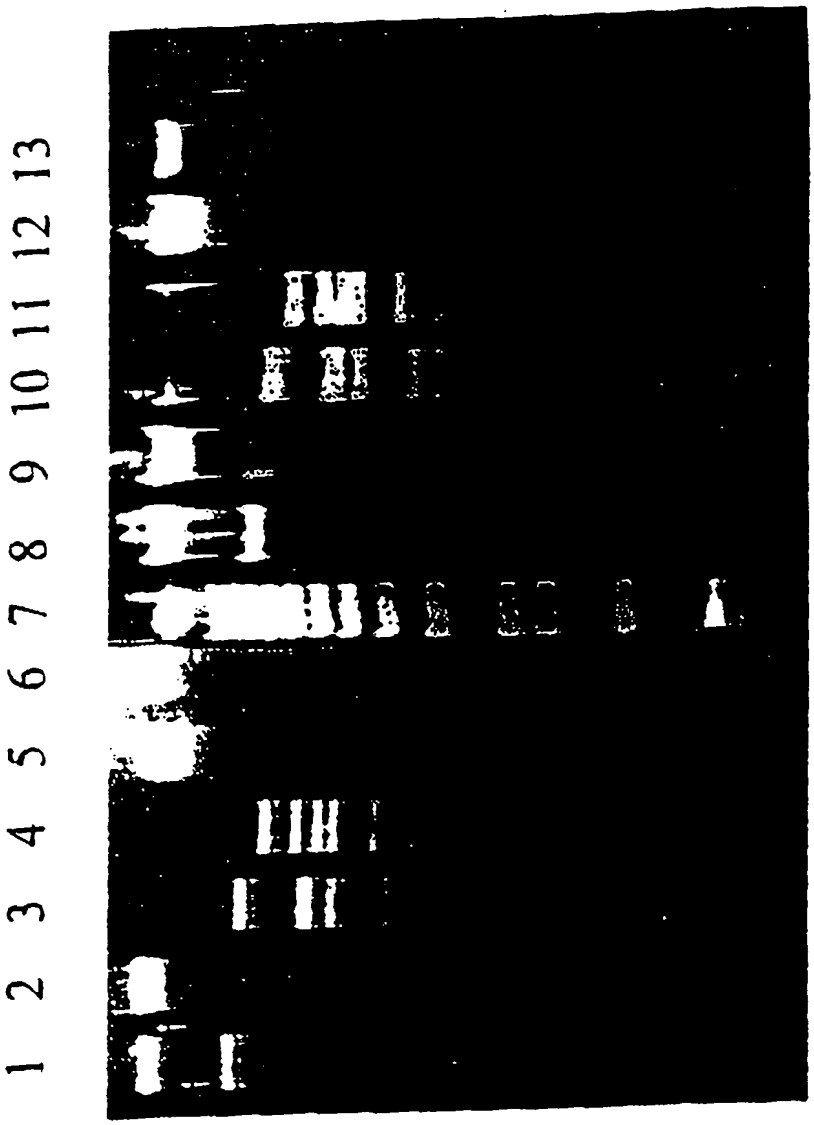

Fig. 16C

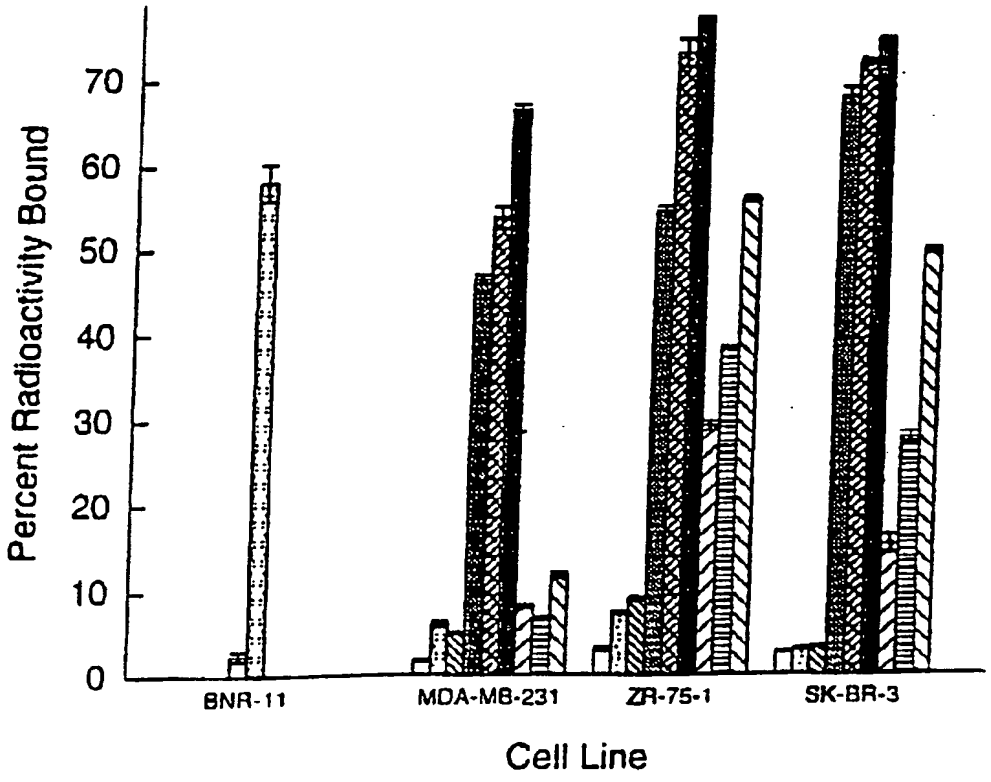
Percent Radioactivity Bound
70
60
50
40
30
20
10
0
BNR-11
MDA-MB-231
ZR-75-1
SK-BR-3
Cell Line

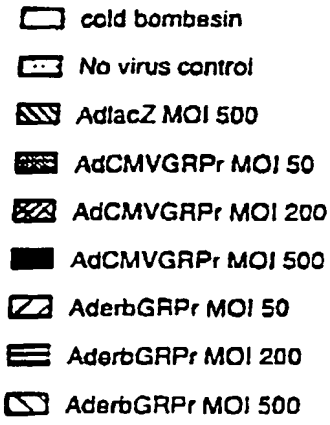
cold bombesin
No virus control
AdlacZ MOI 500
AdCMVGRPr MOI 50
AdCMVGRPr MOI 200
AdCMVGRPr MOI 500
AderbGRPr MOI 50
AderbGRPr MOI 200
AderbGRPr MOI 500

Fig. 17

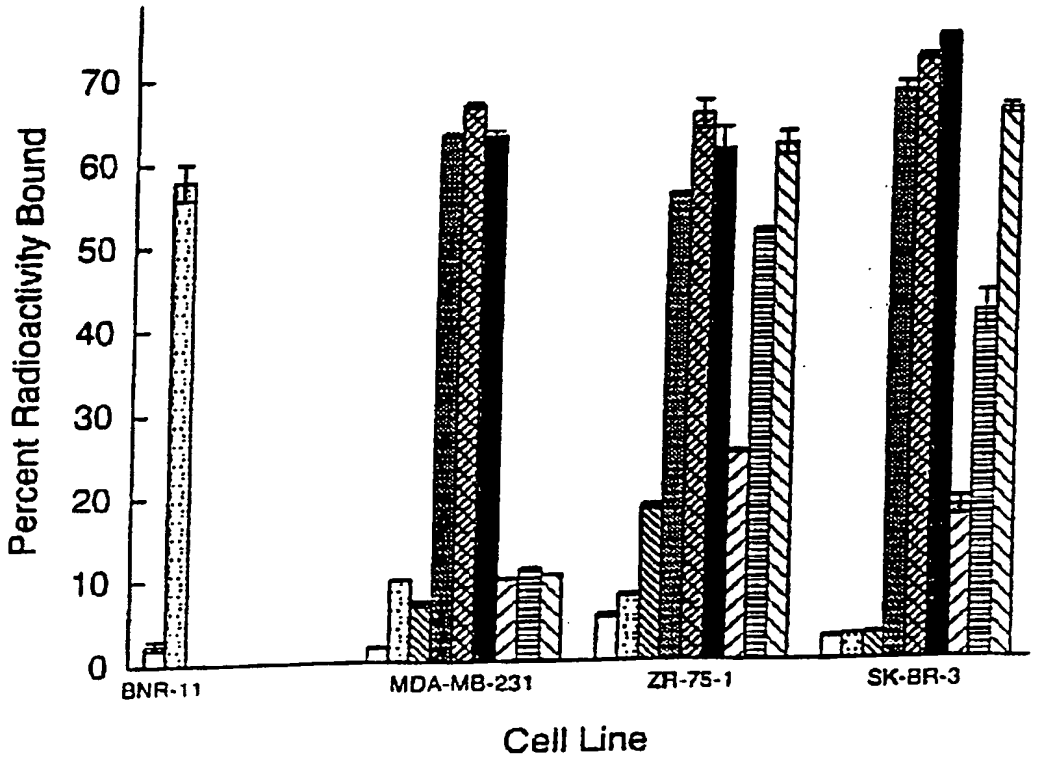
Percent Radioactivity Bound
0
10
20
30
40
50
60
70
BNR-11
MDA-MB-231
ZR-75-1
SK-BR-3
Cell Line
cold bombesin
No virus control
AdlacZ MOI 500
AdCMVGRPr MOI 50
AdCMVGRPr MOI 200
AdCMVGRPr MOI 500
AderbGRPr MOI 50
AderbGRPr MOI 200
AderbGRPr MOI 500

Fig. 18

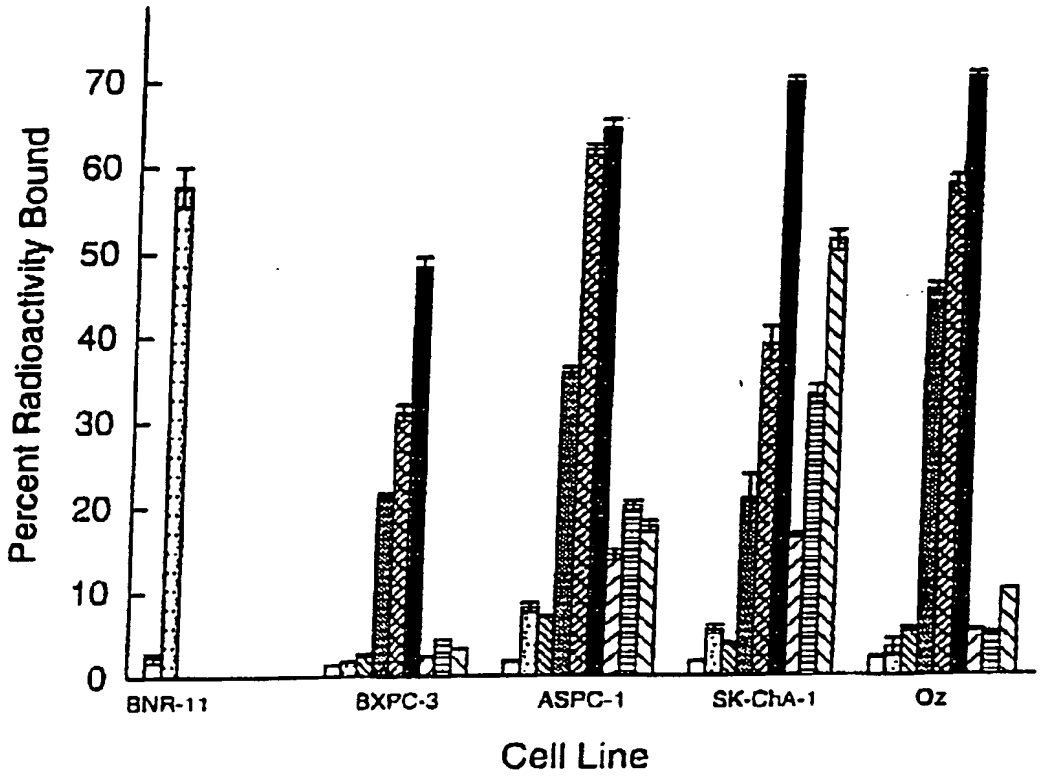
Percent Radioactivity Bound
70
60
50
40
30
20
10
0
BNR-11
BXPC-3
ASPC-1
SK-ChA-1
Oz
Cell Line
cold bombesin
No virus control
AdlacZ MOI 500
AdCMVGRPr MOI 50
AdCMVGRPr MOI 200
AdCMVGRPr MOI 500
AderbGRPr MOI 50
AderbGRPr MOI 200
AderbGRPr MOI 500

Fig. 19

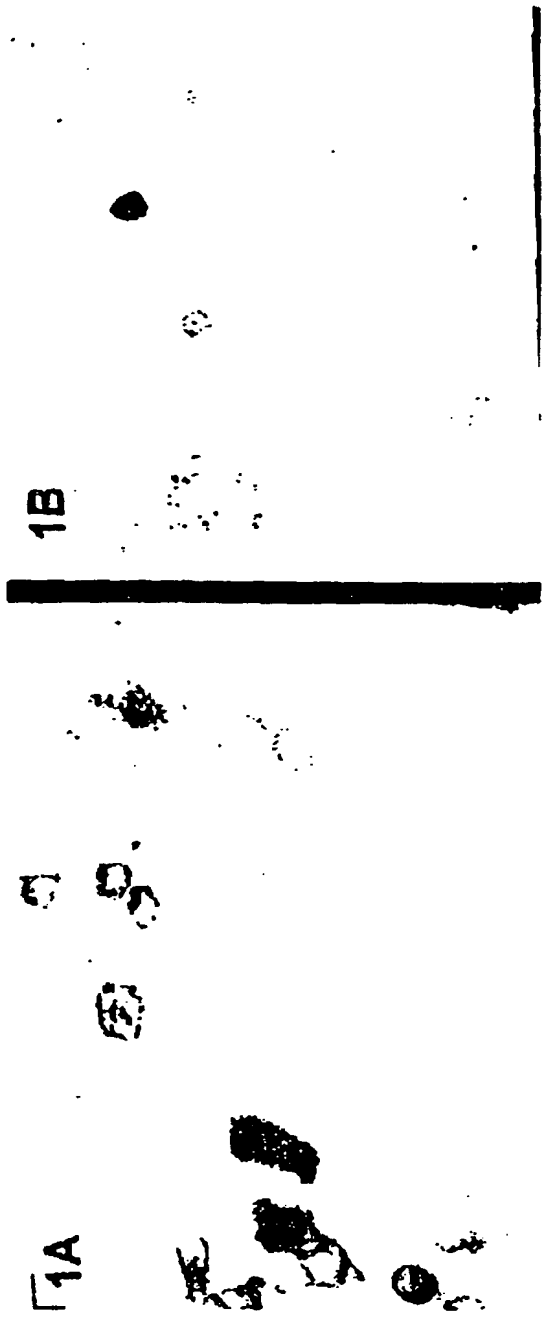

Fig. 20A

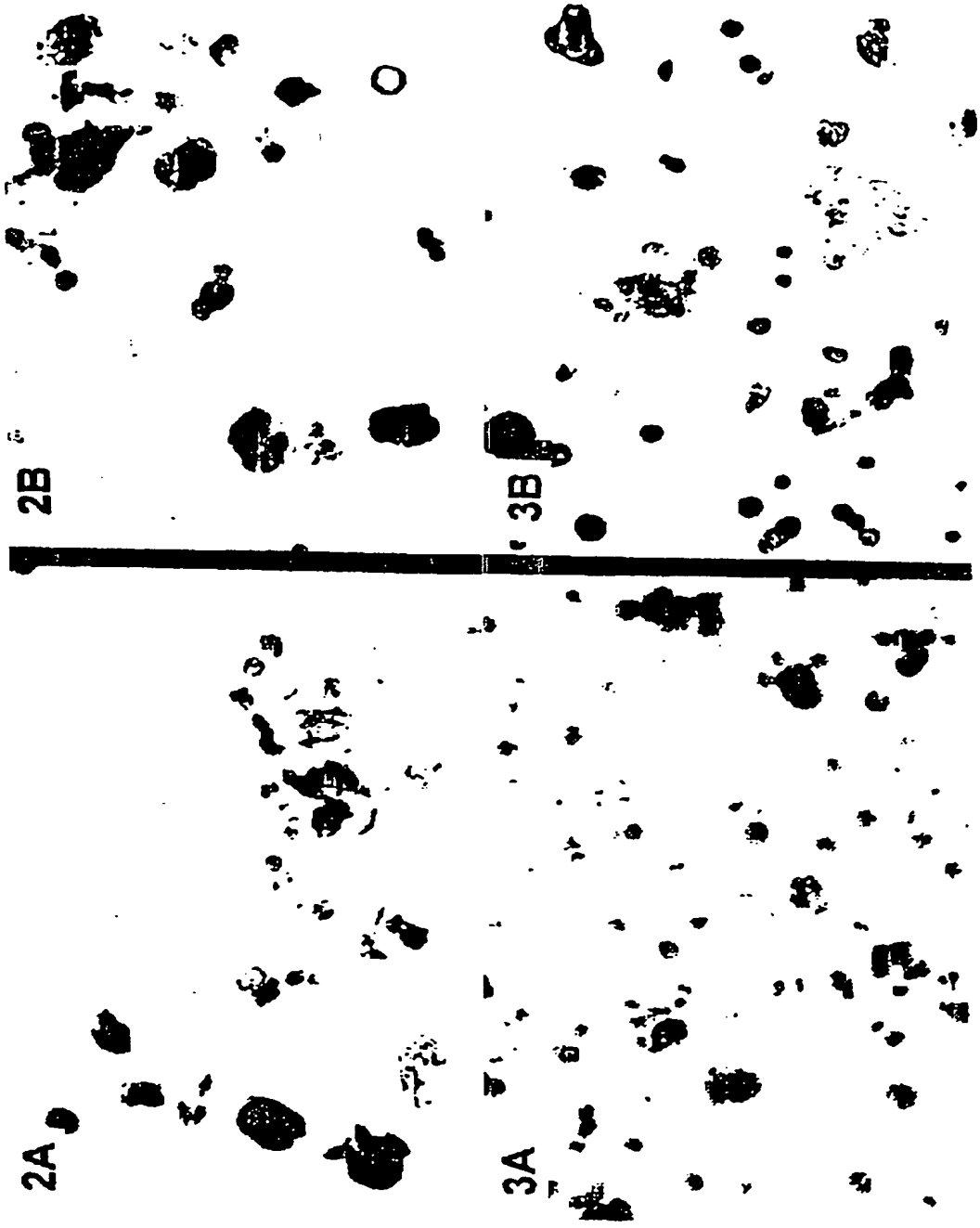

Fig. 20B

Fig. 21A

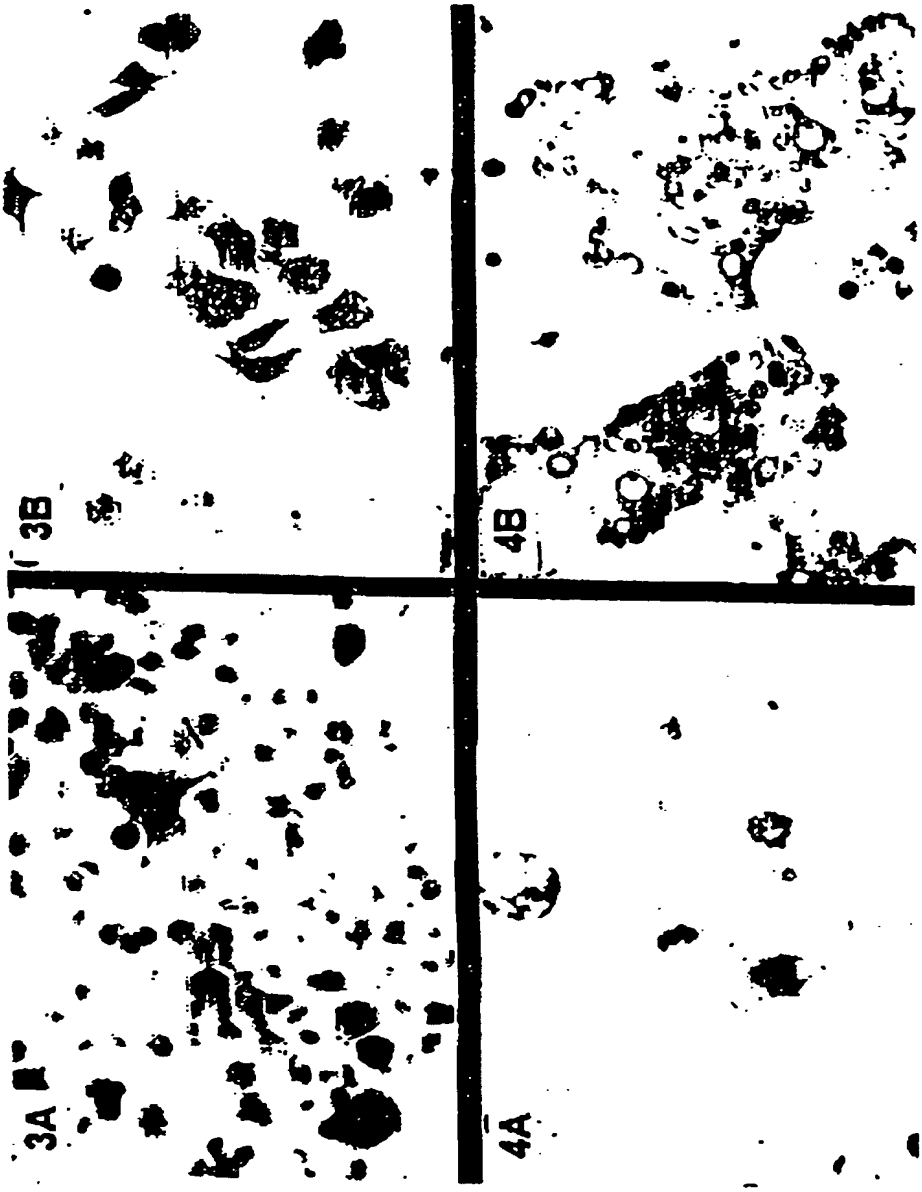

Fig. 21B

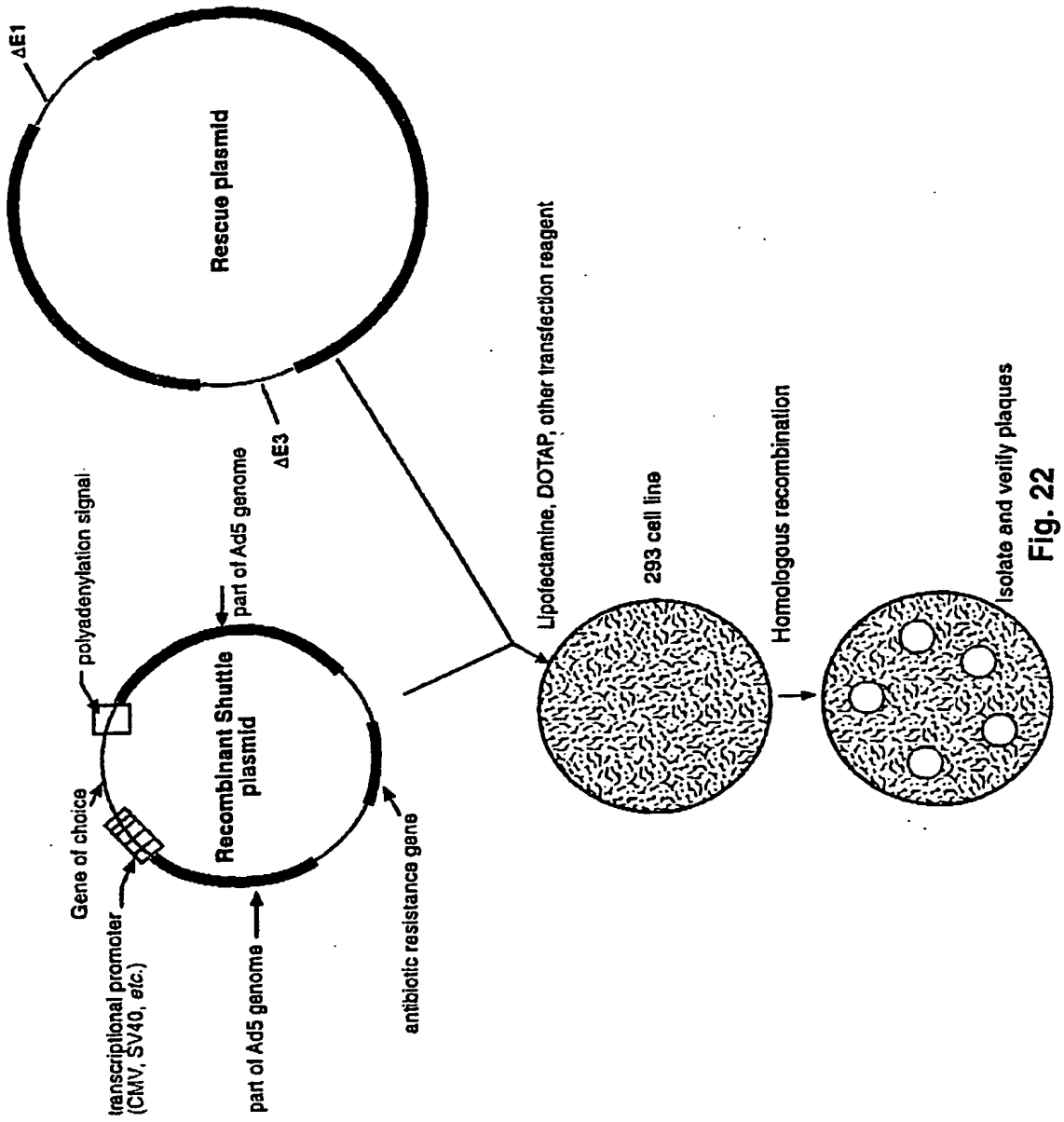
ΔE1
Rescue plasmid
ΔE3
part of Ad5 genome
polyadenylation signal
Recombinant Shuttle plasmid
Gene of choice
transcriptional promoter (CMV, SV40, etc.)
part of Ad5 genome
antibiotic resistance gene
Lipofectamine, DOTAP, other transfection reagent
293 cell line
Homologous recombination
Isolate and verify plaques

Fig. 22

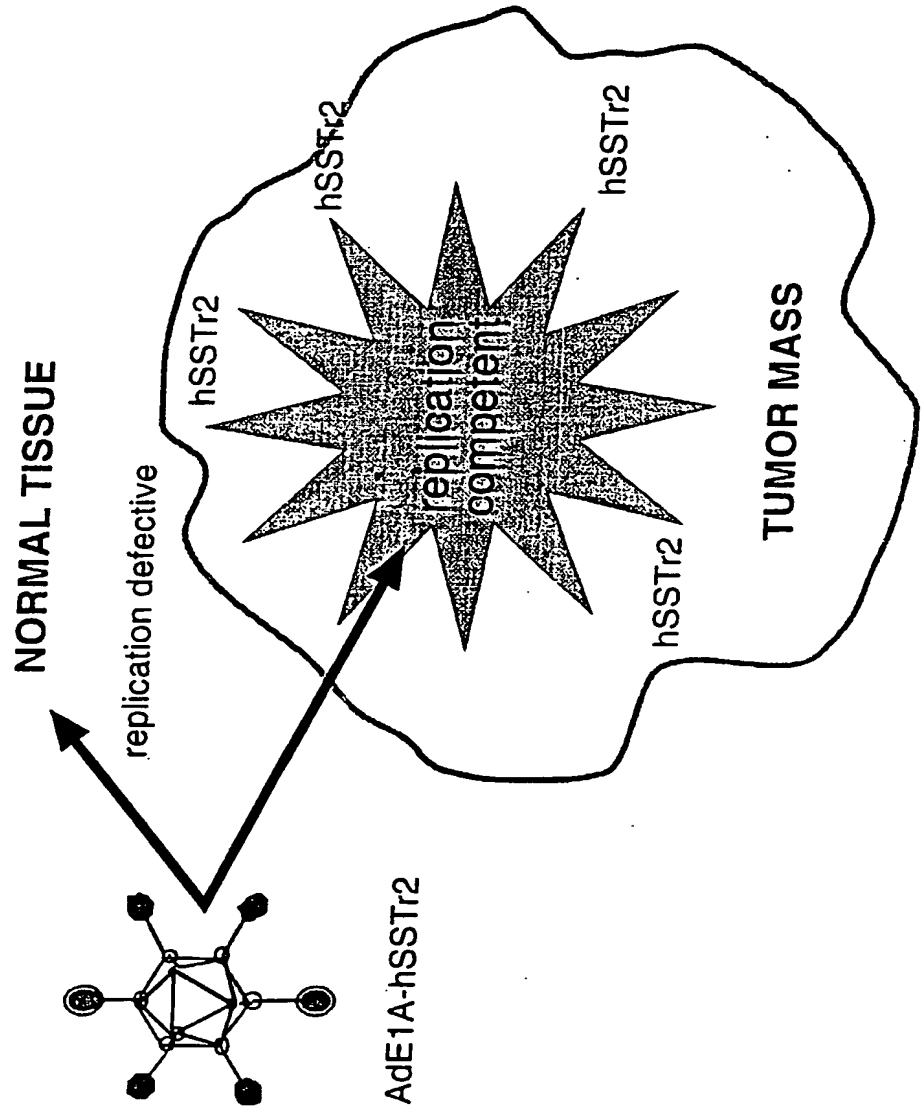
NORMAL TISSUE
replication defective
AdE1A-hSSTr2
hSSTr2
hSSTr2
hSSTr2
hSSTr2
replication competent
TUMOR MASS

Fig. 23

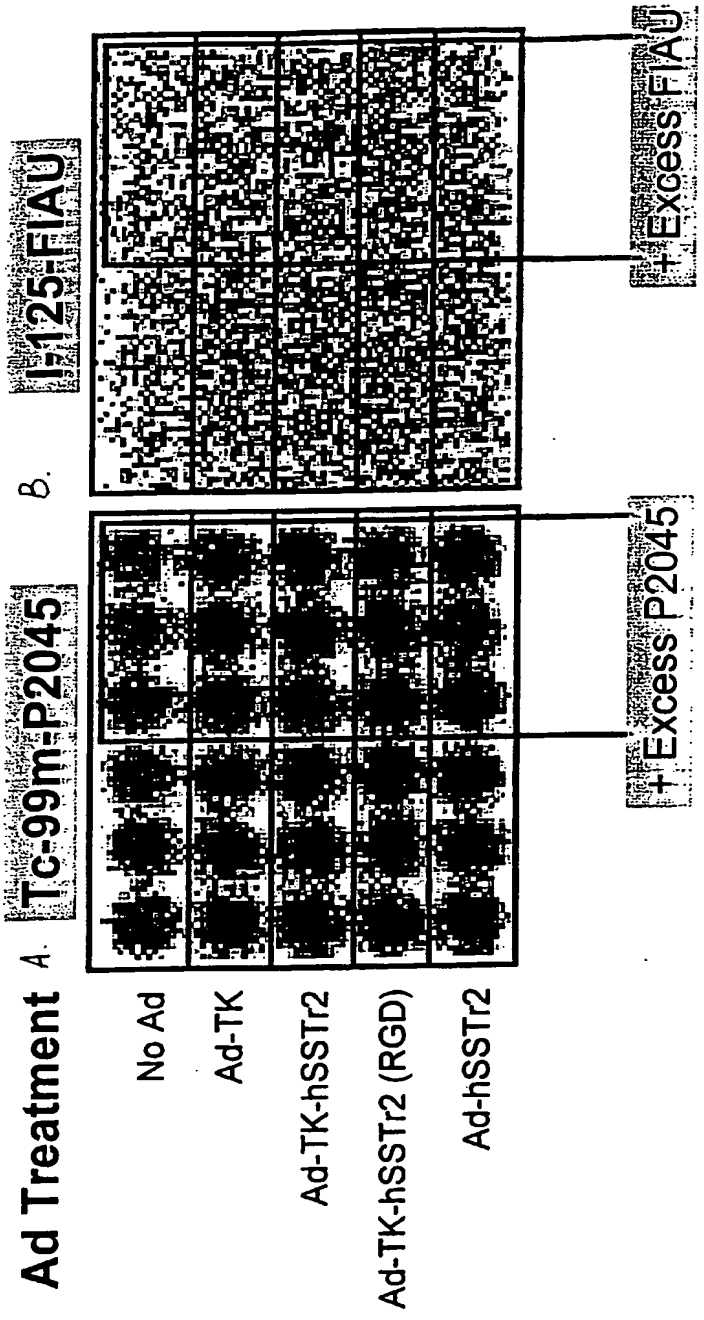

Fig. 24A

Fig. 24B

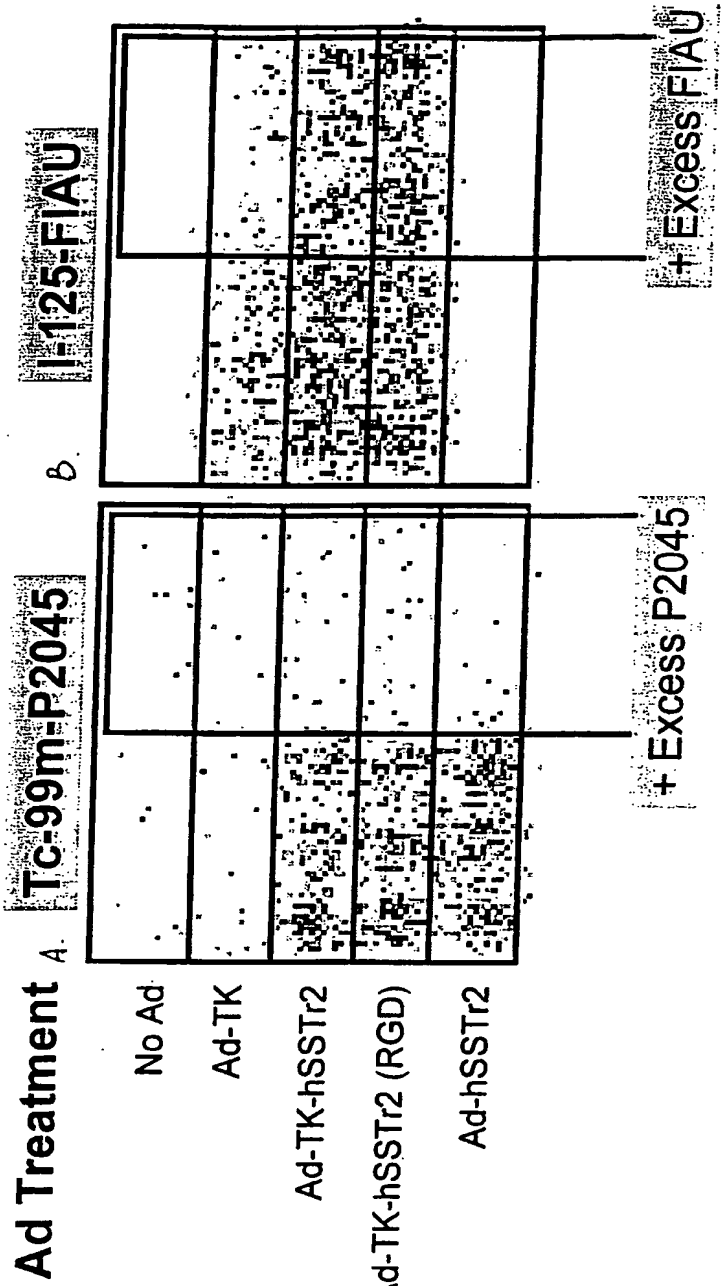

Fig. 25A

Fig. 25B

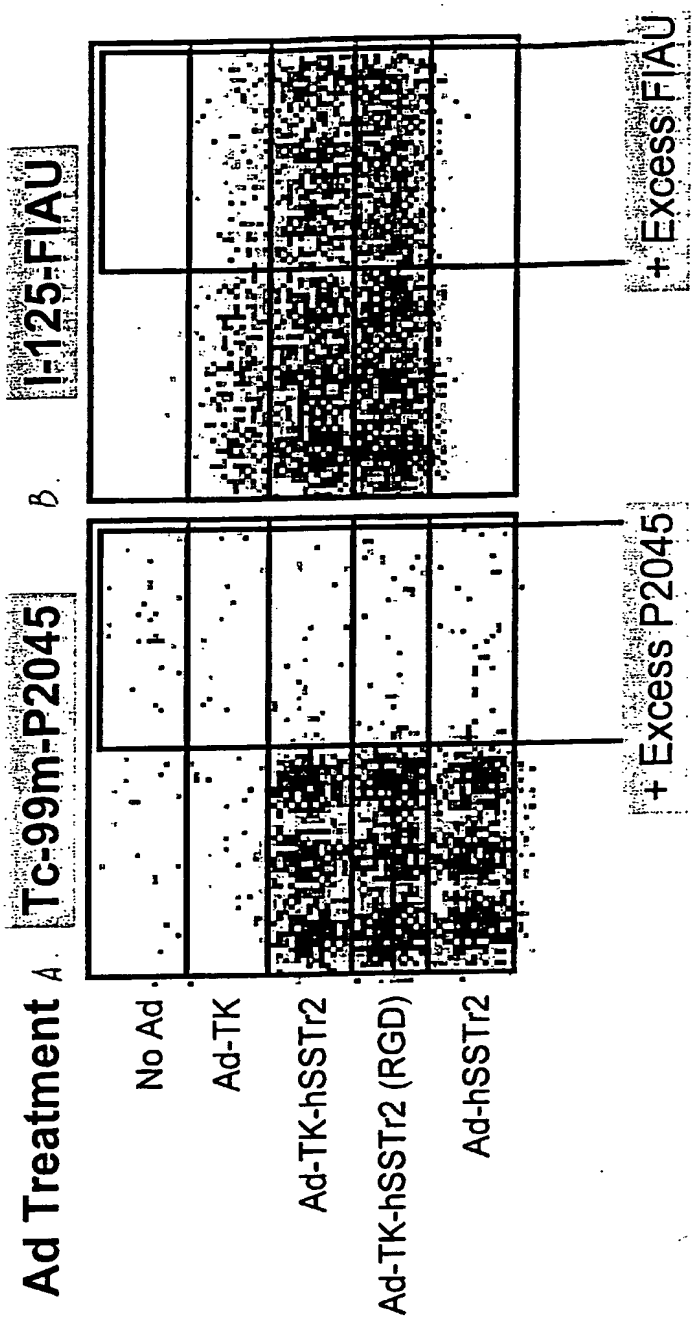

Fig. 26A

Fig. 26B

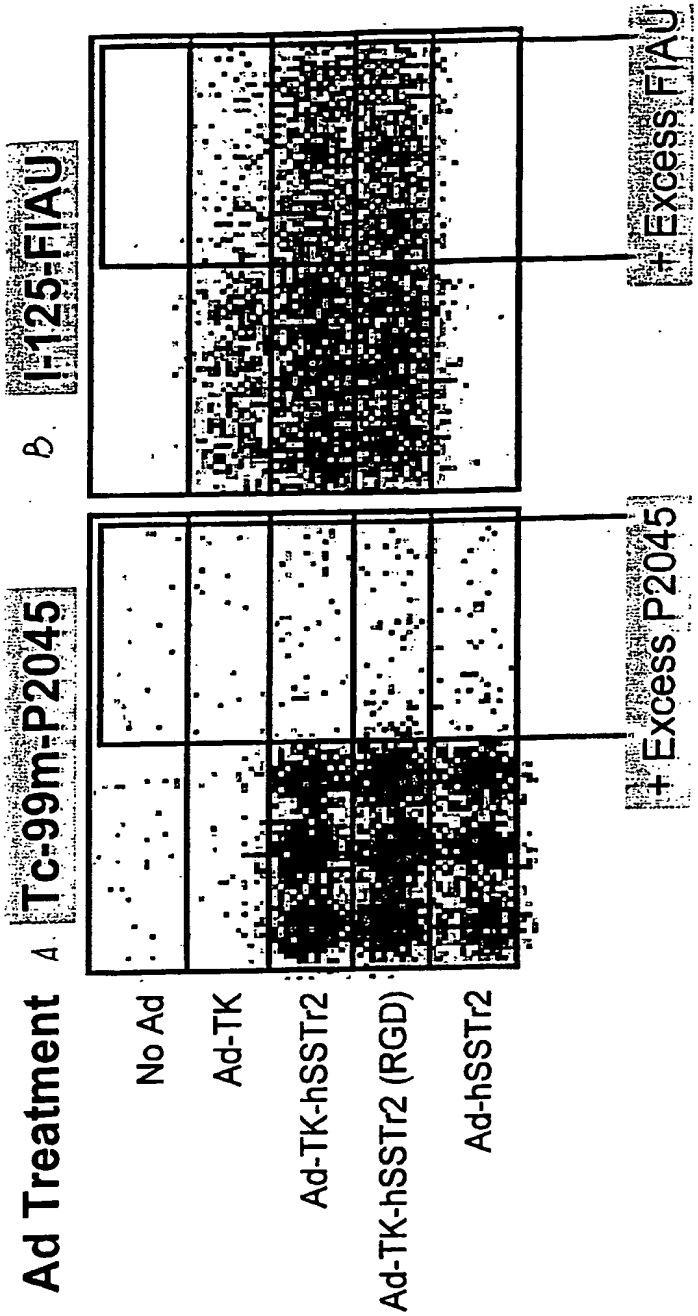

Fig. 27A

Fig. 27B

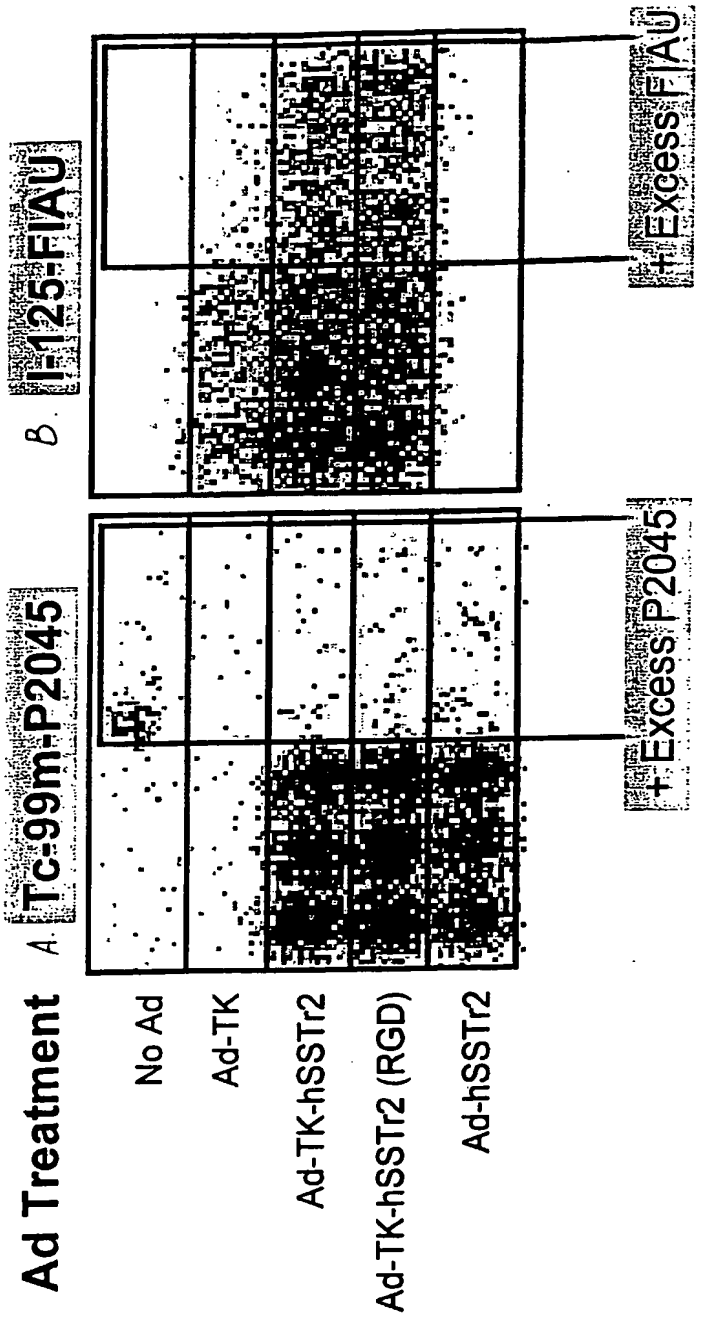

Fig. 28A

Fig. 28B

Fig. 29A

"Non-RGD"

Ad-TK-hSSTr2

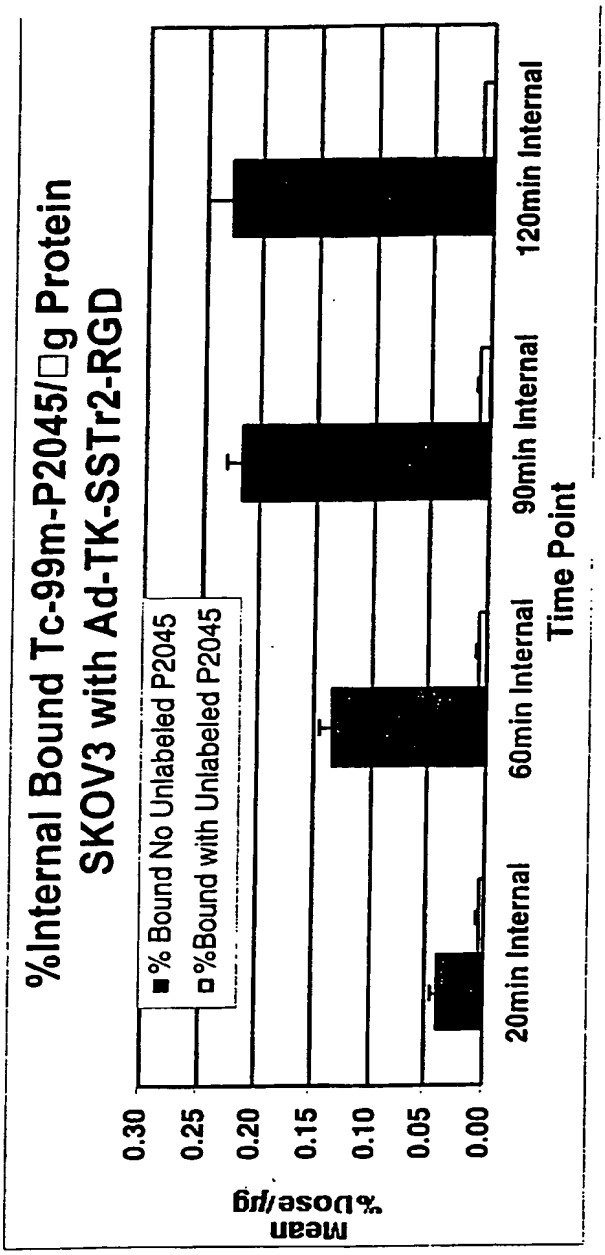

Ad-TK-hSSTr2

"RGD"

Fig. 29B

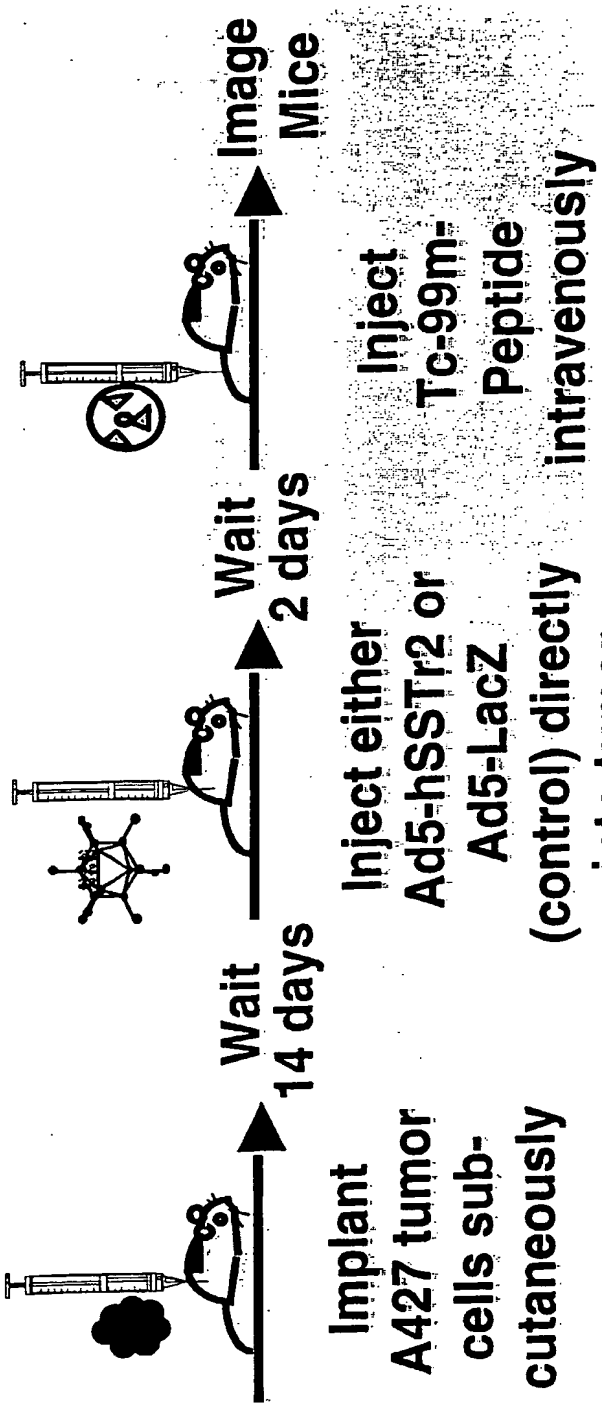
Implant A427 tumor cells sub-cutaneously
Wait 14 days
Inject either Ad5-hSSTr2 or Ad5-LacZ (control) directly into tumor
Wait 2 days
Inject Tc-99m-Peptide intravenously
Image Mice

Fig. 30

Imaging Gene Transfer to subcutaneous A-427 Tumors

Images at 5 hr after i.v. injection

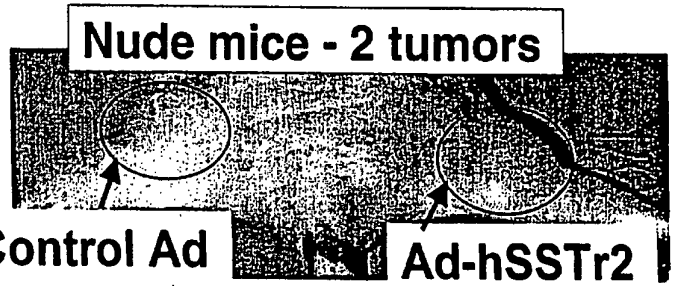

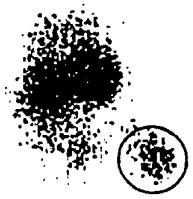

In-111-
Octreotide

Tc-99m-
P829

Tc-99m-
P2045

Fig. 31

Imaging Gene Transfer to IP Ovarian tumors

3 mice with IP SKOV3.ip1 tumors - No Ad injection
-Imaged 5 h after Tc-99m-peptide

Fig. 32A

3 mice with IP SKOV3.ip1 tumors - Ad-hSSTr2 IP 48 h earlier
- Imaged 5 h after Tc-99m-P2045

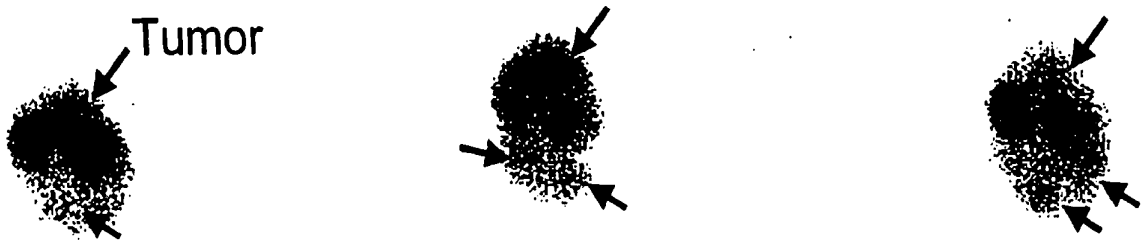

Fig. 32B

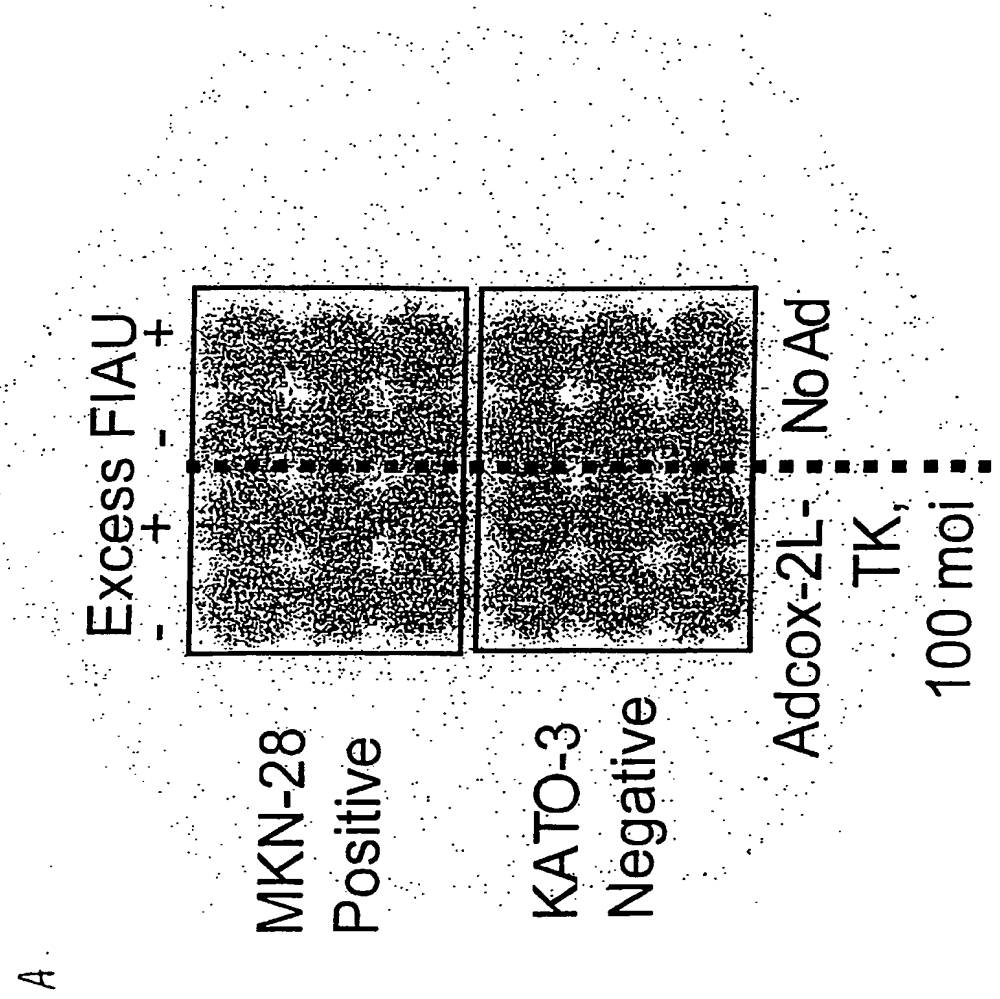
A
MKN-28
Positive
KATO-3
Negative
Excess FIAU
+
-
+
-
Adcox-2L-
TK,
100 moi
No Ad

Fig. 33A

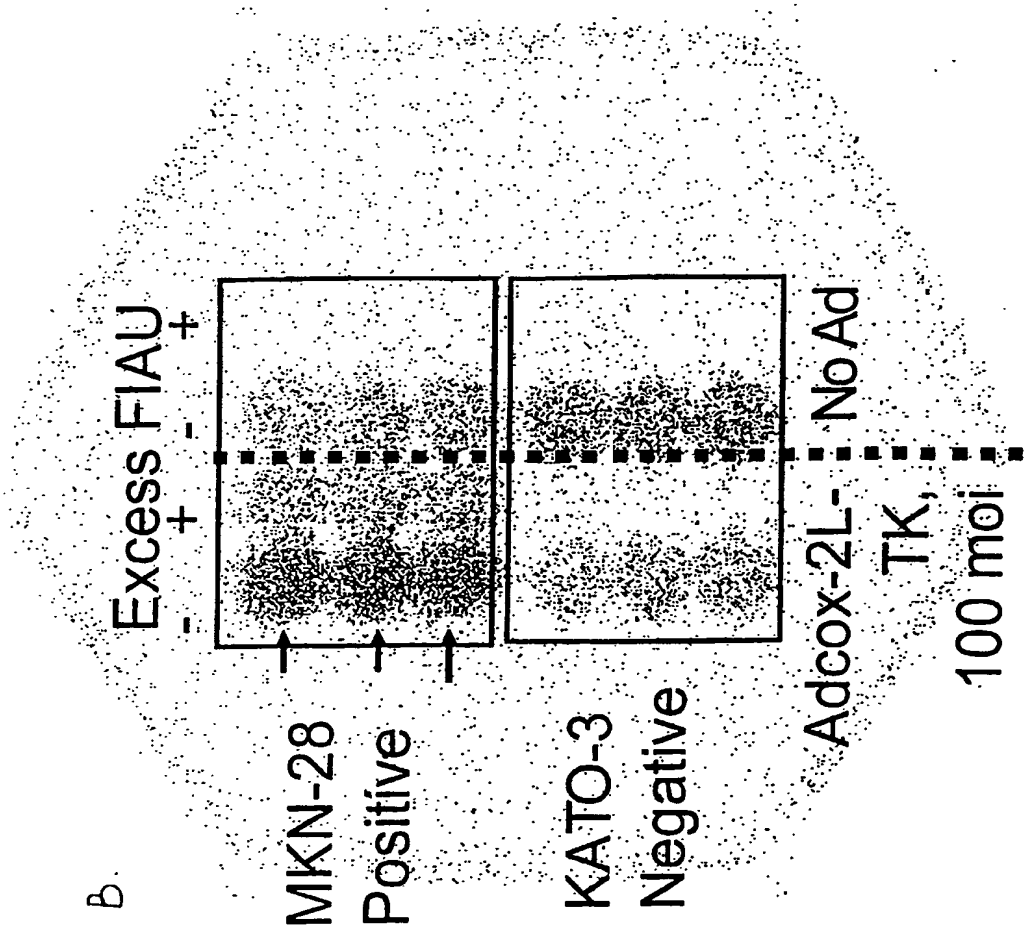
B.
MKN-28
Positive
KATO-3
Negative
Adcox-2L- TK, 100 moi
No Ad
Excess FIAU
+
-
+
-

Fig. 33B

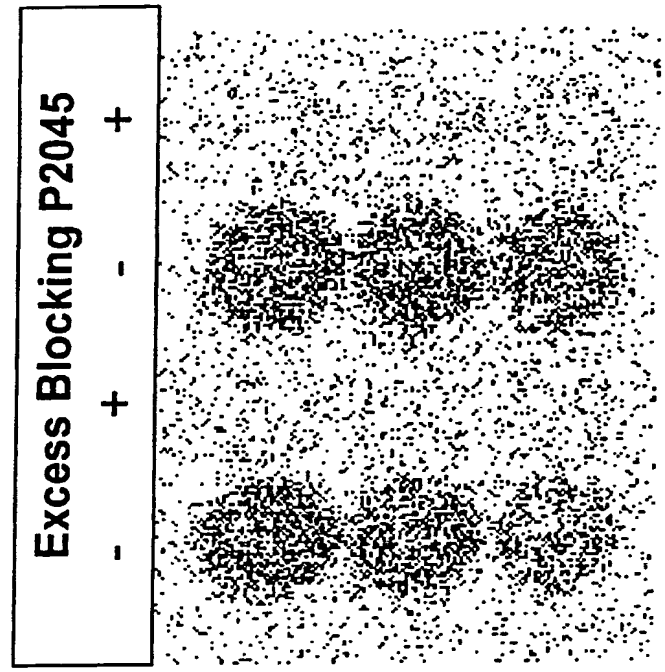

Final Image
(after 1 h incubation)

Fig. 34B

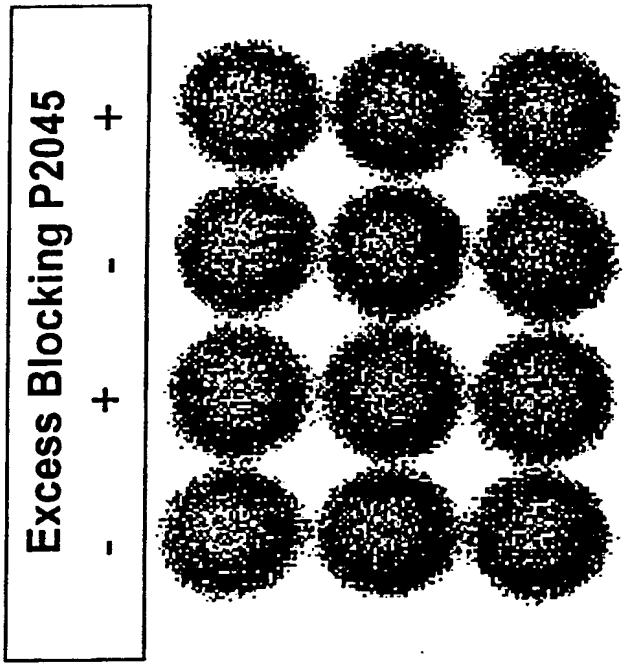

Initial Image

Fig. 34A

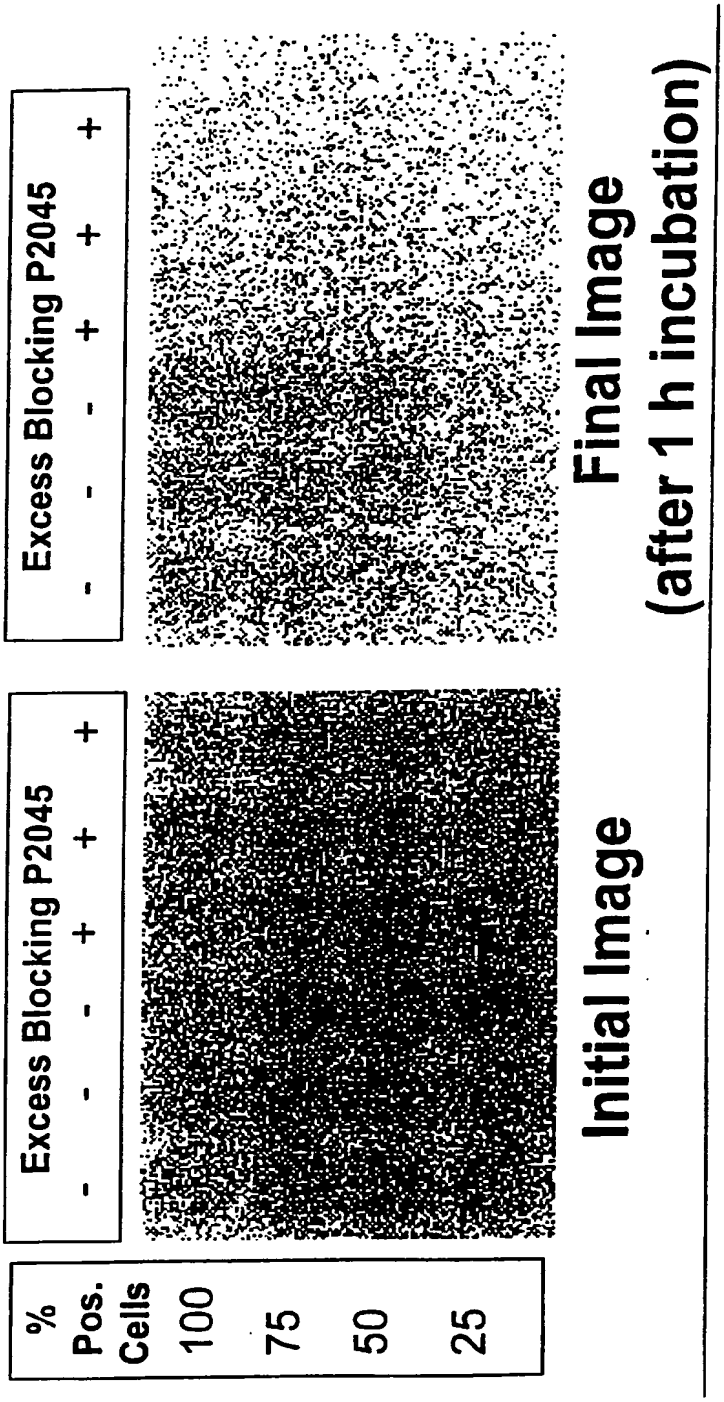

Fig. 35A

Fig. 35B

SEQUENCE LISTING

<110> Donald J. Buchsbaum
Buck E. Rogers
Kurt R. Zinn
David T. Curiel
<120> Gene Transfer Imaging and Uses Thereof
<130> D5836CIPPCT
<141> 2000-08-16
<150> 09/374,972
<151> 1999-08-16
<160> 6

<210> 1
<211> 9
<212> PRT
<213> Artificial sequence
<220>
<223> amino acid sequence of "HA" tag
<400> 1
Tyr Pro Tyr Asp Val Pro Asp Tyr Ala
5

<210> 2
<211> 18
<212> DNA
<213> Artificial sequence
<220>
<221> primer_bind
<223> PCR forward primer for hSSTR2
<400> 2
tggatccttg gcctccag 18

<210> 3
<211> 21
<212> DNA
<213> Artificial sequence
<220>

<221> primer_bind
<223> PCR reverse primer for hSSTR2
<400> 3
attctagaag ccaggtgtga g 21

<210> 4
<211> 20
<212> DNA
<213> Artificial sequence
<220>
<221> primer_bind
<223> PCR forward primer for Ad5
<400> 4
tgtcgtttct cagcagctgt 20

<210> 5
<211> 20
<212> DNA
<213> Artificial sequence
<220>
<221> primer_bind
<223> PCR reverse primer for Ad5
<400> 5
tctgaactca aagcgtggga 20

<210> 6
<211> 8
<212> PRT
<213> Artificial sequence
<220>
<223> HYNIC-modified BBN analogue
<400> 6
Gln Trp Ala Val Gly His Leu Met
5

INTERNATIONAL SEARCH REPORT

International application No.
PCT/US00/22456

A. CLASSIFICATION OF SUBJECT MATTER

IPC(7) :*A61K 48/00, 35/00, 49/00, 51/00*

US CL : 514/44; 424/93.1, 1.41, 1.49,9.1

According to International Patent Classification (IPC) or to both national classification and IPC

B. FIELDS SEARCHED

Minimum documentation searched (classification system followed by classification symbols)

U.S. : 514/44; 424/93.1, 1.41, 1.49,9.1

Documentation searched other than minimum documentation to the extent that such documents are included in the fields searched

Electronic data base consulted during the international search (name of data base and, where practicable, search terms used)

MEDLINE,CAPLUS,WEST2.0,USPATFUL

C. DOCUMENTS CONSIDERED TO BE RELEVANT

Category*	Citation of document, with indication, where appropriate, of the relevant passages	Relevant to claim No.
X,P	US 5,981,504 A (BUCHSBAUM et al.) 09 November 1999, see the entire document.	1-24
X	US 5,902,583 A (BUCHSBAUM et al.) 11 MAY 1999, see the entire document.	1-24
Y	US 5,756,685 A (FRITZBERG et al) 26 MAY 1998, see the entire document.	1-12
X --P Y	US 5,998,205 A (HALLENBECK et al.) 07 December 1999, see the entire document.	21 -- 21-24, 8-12
O, A	US 6,110,702 A (PANG et al.) 29 August 2000, see the entire document.	8-12

☐ Further documents are listed in the continuation of Box C. ☐ See patent family annex.

*	Special categories of cited documents:	"T"	later document published after the international filing date or priority date and not in conflict with the application but cited to understand the principle or theory underlying the invention
"A"	document defining the general state of the art which is not considered to be of particular relevance	"X"	document of particular relevance; the claimed invention cannot be considered novel or cannot be considered to involve an inventive step when the document is taken alone
"E"	earlier document published on or after the international filing date	"Y"	document of particular relevance; the claimed invention cannot be considered to involve an inventive step when the document is combined with one or more other such documents, such combination being obvious to a person skilled in the art
"L"	document which may throw doubts on priority claim(s) or which is cited to establish the publication date of another citation or other special reason (as specified)	"&"	document member of the same patent family
"O"	document referring to an oral disclosure, use, exhibition or other means		
"P"	document published prior to the international filing date but later than the priority date claimed		

Date of the actual completion of the international search 06 NOVEMBER 2000	Date of mailing of the international search report 28 DEC 2000
Name and mailing address of the ISA/US Commissioner of Patents and Trademarks Box PCT Washington, D.C. 20231 Facsimile No. (703) 305-3230	Authorized officer RAM R. SHUKLA Telephone No. (703) 305-1677

Form PCT/ISA/210 (second sheet) (July 1998)*

This Page is Inserted by IFW Indexing and Scanning Operations and is not part of the Official Record

BEST AVAILABLE IMAGES

Defective images within this document are accurate representations of the original documents submitted by the applicant.

Defects in the images include but are not limited to the items checked:

- ☐ BLACK BORDERS
- ☐ IMAGE CUT OFF AT TOP, BOTTOM OR SIDES
- ☐ FADED TEXT OR DRAWING
- ☐ BLURRED OR ILLEGIBLE TEXT OR DRAWING
- ☐ SKEWED/SLANTED IMAGES
- ☐ COLOR OR BLACK AND WHITE PHOTOGRAPHS
- ☐ GRAY SCALE DOCUMENTS
- ☐ LINES OR MARKS ON ORIGINAL DOCUMENT
- ☐ REFERENCE(S) OR EXHIBIT(S) SUBMITTED ARE POOR QUALITY
- ☐ OTHER: _____

IMAGES ARE BEST AVAILABLE COPY.

As rescanning these documents will not correct the image problems checked, please do not report these problems to the IFW Image Problem Mailbox.